

FEASIBILITY STUDY OF SOLAR DOME ENCAPSULATION OF PHOTOVOLTAIC ARRAYS

JPL CONTRACT NO. 954833

LOW COST SOLAR ARRAY PROJECT
ENGINEERING AREA

PHASE I FINAL REPORT

December 1978

Donald Zimmerman
Program Manager

The JPL Low Cost Solar Array Project is sponsored by the U.S. Department of Energy and forms part of the Solar Photovoltaic Conversion Program to initiate a major effort toward the development of low-cost solar arrays. This work was performed for the Jet Propulsion Laboratory, California Institute of Technology by agreement between NASA and DOE.

Prepared for
Jet Propulsion Laboratory
4800 Oak Grove Drive
Pasadena, California 91103

By the
Boeing Engineering and Construction Company
(A Division of The Boeing Company)
Seattle, Washington



(NASA-CR-158368) FEASIBILITY STUDY OF SOLAR DOME ENCAPSULATION OF PHOTOVOLTAIC ARRAYS
Final Report (Boeing Engineering and Construction) : 175 p HC A08/NE A01 . CSCL 10A
N79-21545
Unclas
G3/44 16665

Feasibility Study of Solar Dome
Encapsulation of Photovoltaic Arrays

JPL Contract No. 954833

Low-Cost Solar Array Project
Engineering Area

Phase I Final Report

December 1978

Donald K. Zimmerman
Program Manager

"The JPL Low-Cost Solar Array Project is sponsored by the U.S. Department of Energy and forms part of the Solar Photovoltaic Conversion Program to initiate a major effort toward the development of low-cost solar arrays. This work was performed for the Jet Propulsion Laboratory, California Institute of Technology by agreement between NASA and DOE."

Prepared For

Jet Propulsion Laboratory
4800 Oak Grove Drive
Pasadena, California 91103

By The

Boeing Engineering and Construction Company
(A Division of The Boeing Company)
Seattle, Washington

"This report was prepared as an account of work sponsored by the United States Government. Neither the United States nor the United States Department of Energy, nor any of their employees, nor any of their contractors, subcontractors, or their employees makes any warranty, express or implied, or assumes any legal liability or responsibility for the accuracy, completeness or usefulness of any information, apparatus, product or process disclosed, or represents that its use would not infringe privately owned rights."

ACKNOWLEDGEMENTS

This study was performed as part of the Engineering Area effort of the Low-Cost Solar Array project at JPL. The Engineering Area, headed by Dr. R. G. Ross Jr., provided very helpful comments and data, particularly thermal testing of a module within a plastic film enclosure. The technical monitor for JPL was Paul Sutton; his support and advice throughout the contract were appreciated.

The Solar Energy Systems organization within Boeing Engineering and Construction Company (a Division of The Boeing Company) directed and performed the work described in this report with support from many people in Boeing Engineering and Construction Company and the Boeing Aerospace Company. The participants were too numerous to list here. However, Miss Cheryl Warner deserves special mention as a major contributor for her thermal and performance analyses of the enclosed arrays. The contributions of all the participants are gratefully acknowledged.

ABSTRACT

This report describes a study which investigated the potential technical and economic advantages of using air-supported plastic enclosures to protect flat plate photovoltaic arrays. Conceptual designs for a fixed, latitude-tilt array and a fully tracking array were defined. Another program provided much of the design and supporting analyses for the tracking array. Detailed wind loads and strength analyses were performed for the fixed array. Detailed thermal and power output analyses provided array performance for typical seasonal and extreme temperature conditions. Costs of each design as used in a 200 MWe central power station were defined from manufacturing and material cost estimates. The capital cost and cost of energy for the enclosed fixed-tilt array were lower than for the enclosed tracking array. The enclosed fixed-tilt array capital investment was 38% less, and the levelized bus bar energy cost was 26% less than costs for a conventional, glass-encapsulated array design. The predicted energy cost for the enclosed fixed array was 79 mills/kW·h for direct current delivered to the power conditioning units.

TABLE OF CONTENTS

	PAGE
1.0 Summary of Results	1
1.1 Design Concepts	1
1.1.1 Fixed Latitude Tilt Array	1
1.1.2 Tracking Array	4
1.2 Performance Evaluation	5
1.3 Life Cycle Costs	9
1.4 Comparison of Conventional Arrays	9
1.5 Summary and Conclusions	12
2.0 Introduction	13
2.1 Study Objectives	13
2.2 Study Groundrules	15
2.3 Report Organization	16
3.0 Design Requirements	17
3.1 System Application and Definition	17
3.1.1 Application	17
3.1.2 Definitions	17
3.2 Array Design Characteristics	17
3.2.1 Performance	20
3.2.1.1 Solar Cell Performance	20
3.2.1.2 Subsystem Life	20
3.2.2 Environmental Conditions	20
4.0 Fixed Array Design Concept	22
4.1 Concept Description	22
4.1.1 Protective Enclosure	26
4.1.2 Array Support Structure	31
4.1.3 Foundation	31
4.1.4 Photovoltaic Modules and Panels	34
4.2 Design Analysis	40
4.2.1 Environmental Loads	40
4.2.1.1 Enclosure	40
4.2.1.2 Foundation	50
4.2.1.3 Support Structure	50
4.2.1.4 Module/Panel	51
4.2.2 Electrical Design	53
4.2.2.1 Cell Characteristics	54

	PAGE
4.2.2.2 Shadowing	54
4.2.2.3 Cell Failures	57
4.2.2.4 Module Failures	60
4.2.2.5 Rationale for Selected Configuration	62
4.3 Thermal Performance Analysis	62
4.3.1 Ambient Environment	63
4.3.1.1 Seasonal and Extreme Environments	63
4.3.1.2 Nominal Environment	63
4.3.2 Cooling System Evaluation	64
4.3.2.1 Cooling Concepts	64
4.3.2.2 Cooling System Thermal Performance	64
4.3.2.3 Conclusions	69
4.3.3 Thermal Performance Model Description	69
4.3.3.1 Analysis Model	69
4.3.3.2 Material Radiative Properties	71
4.3.3.3 Convective Heat Transfer Model	71
4.3.4 Thermal Model Verification	75
4.3.5 Temperature Predictions	77
4.3.5.1 Extreme Temperature Analyses	77
4.3.5.2 NOCT Analyses	77
4.3.6 Performance Predictions	77
4.3.6.1 Cell Characteristics	77
4.3.6.2 Seasonal Analysis	82
4.3.6.3 NOCT Analyses	82
4.4 Manufacturing and Installation	86
4.4.1 Production Scenario	86
4.4.2 Module Fabrication	88
4.4.3 Structure Fabrication	88
4.4.4 Installation	93
4.5 Maintenance	95
4.6 Life Cycle Costs	96
4.6.1 Costing Assumptions	96
4.6.2 Costing Analysis Results	99
4.6.3 Energy Cost Analysis	111

	PAGE
5.0 Tracking Array Design Concept	113
5.1 Concept Description	115
5.1.1 Protective Enclosure	115
5.1.2 Base/Foundation	116
5.1.3 Array Support Structure	117
5.1.4 Tracking System	117
5.1.5 Photovoltaic Modules	124
5.1.6 Power Collection	129
5.2 Design Analysis	129
5.2.1 Environmental Loads	129
5.2.1.1 Enclosure Wind Load Analysis	129
5.2.2 Electrical Design	131
5.2.3 Tracking System	131
5.3 Thermal/Performance Analysis	133
5.3.1 Ground Rules and Assumptions	133
5.3.2 Ambient Environment	133
5.3.3 Thermal Performance Model Description	133
5.3.4 Temperature Predictions	134
5.3.4.1 Seasonal Analyses	134
5.3.4.2 Extreme Temperature Analysis	134
5.3.4.3 NOCT Analysis	138
5.3.5 Performance Predictions	139
5.3.5.1 Seasonal Analysis	139
5.3.5.2 NOCT Analyses	139
5.4 Manufacturing and Installation	139
5.5 Maintenance	143
5.6 Life Cycle Costs	145
5.6.1 Costing Analysis Results	145
5.6.2 Energy Cost Analysis	145
6.0 Evaluation of Results	155
6.1 Summary of Results	155
6.2 Comparison to Conventional Array	156
7.0 Conclusions	161
8.0 Recommendations	162
9.0 New Technology	164
10.0 References	

1.0 SUMMARY OF RESULTS

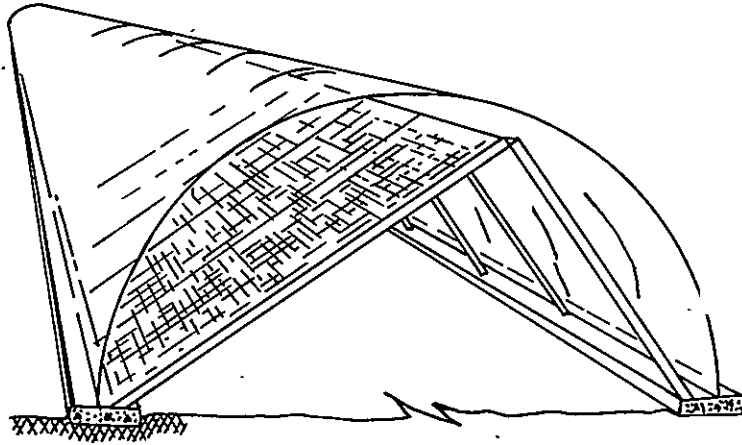
This study shows that air-supported enclosures can reduce costs of photovoltaic arrays and produce less expensive energy than conventional arrays. The concepts are technically feasible and require no technical breakthroughs. Costs, based on highly automated production and anticipated high volume materials useage, indicate that central power stations using these concepts can be economically viable. This section briefly describes the two concepts evaluated - a tracking array in a spherical enclosure and a fixed-tilt array in a cylindrical enclosure - summarizes their performance and life cycle costs, and compares the results to a conventional array.

1.1 Design Concepts

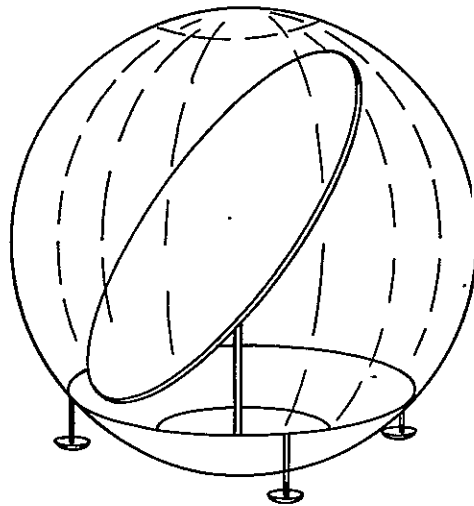
The overall configurations of the two enclosed array concepts are shown in Figure 1-1. The tracking array, contained within a 9.7 meter (31.8 foot) diameter spherical enclosure, is supported on a central pedestal. A two-axis tracking system keeps the array normal to the sun. The fixed-tilt array is tilted 33.4 degrees toward the south with the rectangular photovoltaic modules supported from a wood A-frame structure. The design concepts are described further below.

1.1.1 Fixed Latitude Tilt Array

The fixed latitude tilt array, Figure 1-1a, consists of a long series of approximately 2.4 by 7.3 meters (8 by 24 feet) photovoltaic panels supported by a wood A-frame structure and contained in a 9.1 meter (30 foot) diameter half-circle cross-section cylindrical protective enclosure. The panels are connected in series between ground and the power collection wiring at +600 volts dc. Each panel is assembled from six identical modules of approximately 1.2 by 2.4 meters (4 by 8 feet) in dimension, which are connected in parallel to power collection busses along each of the 7.3 meters (24 foot) panel sides. Each module contains 1200 4.5 by 4.6 cm (1.77 by 1.81 inch)



a) Fixed - tilt array



b) Tracking array

Figure1-1. Solar Dome Concepts for Photovoltaic Arrays

silicon solar cells electrically connected with eight cells in parallel and 150 in series. Each module produces approximately 294 watts at 63 volts when operating at the Nominal Operating Cell Temperature (NOCT) of 60°C. Physically the modules and panels have a flexible plastic film substrate with cells and interconnects bonded in place. The cells do not require a protective front surface cover.

The flexible panels are supported at top and bottom by a wood A-frame and the south foundation. The connections between panel and support are made with U-shaped hooks along each edge. The panel is suspended as a catenary, and the catenary tension maintains the connection. The tension in the film is controlled by the amount of sag in the catenary, and is well below the creep limit of the film.

The A-frame supporting the panels is made from lumber. Connections to make the A-frame, beams, and cross-bracing are made with barbed connector plates commonly used in wood roof truss construction. The A-frame also serves as a support for the power collection wiring. The tunnel formed by the A-frames and panels permits access with mechanical equipment and personnel for installation and replacement of the panels. The A-frame rests on linear-concrete foundation strips which also anchor the inflated enclosure. The concrete foundations are emplaced in a continuous process using a curb-laying machine. Attachment plates for the enclosure are embedded in the concrete as part of the concrete emplacement.

The enclosure is made from a weatherized 0.18 millimeter (0.007 inch) thick polyester film. The weatherizing additives prevent ultraviolet degradation of the polyester and screen out UV radiation from the energy transmitted to the array. Pressure in the enclosure is selected to limit deflections under the wind and snow load design conditions for Phoenix. Although the combined environmental loads and inflation pressure load dictates a polyester film thickness of about 0.10 millimeter (0.004 inch), the design and costs are based on the 0.18 millimeter (0.007 inch) film for greater ruggedness. The selected design also would be suitable in areas with more severe environments than Phoenix.

1.1.2 Tracking Array

The photovoltaic panels selected for the tracking array are also designed for individual panel replacement within the enclosure. With the 9.7 meter (31.8 foot) diameter spherical enclosure used with the tracking array, access constraints dictate a much smaller panel. The module shape permits a single panel design and a convenient arrangement for the support structure. However, it does require staggering the parallel rows of cells within the module, which creates a more difficult cell interconnect design problem. An alternative design, which was not pursued, using a large circular array with horizontal rows of cells, would simplify the design of both the module/panel and the support structure. Unfortunately, a large panel would require removal of the enclosure to replace the panel. The best of the two configurations could be identified with more detailed analysis of failure modes and their detection, failure rates, and maintenance and repair procedures. However, the first design was selected for detailed analysis and costing.

Each of the modules in the selected tracking array design produces 109 watts at 13 volts when operating at the NOCT of 52°C. When connected in series, the entire array of 63 modules would produce about 830 volts dc.

The panels are supported by lightweight hexagonal frames which are in turn supported by six arms radiating from the central hub. The array is mounted on an azimuth-elevation gimbal to permit two-axis sun tracking. The tracking control and actuation system is designed to provide less than 5° error between the array normal and the sun vector. This system is less expensive than the extremely accurate tracking system required for the heliostats. Tracking is controlled with a microprocessor that computes sun position, moves the array in the tracking mode, and carries out operational commands.

The array is gimballed atop a slender pedestal to allow freedom of movement. The array may be rotated nearly 180° in elevation and 360° in azimuth.

The transparent enclosure is a one piece spherical dome fabricated by thermo-forming a circular blank of polyester film. It attaches to an enclosure base made from sheet steel. The enclosure base is supported by three stanchions attached to concrete piles.

1.2 Performance Evaluation

Array performance is evaluated by computing the thermal behavior and then determining the temperature related power output of the modules. Transient thermal analyses, using Phoenix weather data, provided temperature throughout the day for average conditions in each of the four seasons, and for extreme hot and cold sunny day conditions. Temperatures were also computed for the steady-state Nominal Operating Cell Temperature (NOCT) conditions:

- . Insolation: 800 W/m² (thermal), 1000 W/m² (electrical)
- . Ambient Temperature: 20°C (68°F)
- . Wind Speed: 1 m/s

Typical transient analysis results are shown in Figure 1-4 for the fixed-tilt array and in Figure 1-5 for the tracking array. Tracking broadens the cell temperature response curve, although cell peak temperatures in the two figures are the same. This is not always true, as is shown in Table 1-I. The tracking array peak temperatures tend to be higher than the fixed-tilt array, even though the enclosure and inside air temperatures are lower. Higher ambient temperatures in the afternoon, along with the high normal insolation to the array, cause the increased tracking array temperatures. The tracking array enclosure and inside air are cooler than in the fixed-tilt array because the spherical enclosure provides greater convective and radiative cooling for a given solar input.

Electrical output per unit module area and solar cell efficiency variations through a typical day are shown in Figure 1-6 for the fixed-tilt array and in Figure 1-7 for the tracking array. Figure 1-7 shows the total daily output for the four days typical of each season and the extreme hot and cold days. Based on the average seasonal conditions, the annual average output is 810 W·h/m²/day for the fixed-tilt array. The tracking array averages 1149 W·h/m²/day, or 142% of the fixed-tilt array output.

The insolation levels derived from the SOLMET data tape for Phoenix are extremely high, about 1200 W/m² at solar noon including direct and diffuse radiation. The standard desert value of insolation (Ref. 1) is near 1100 W/m². Therefore, the temperatures and electrical output of the arrays

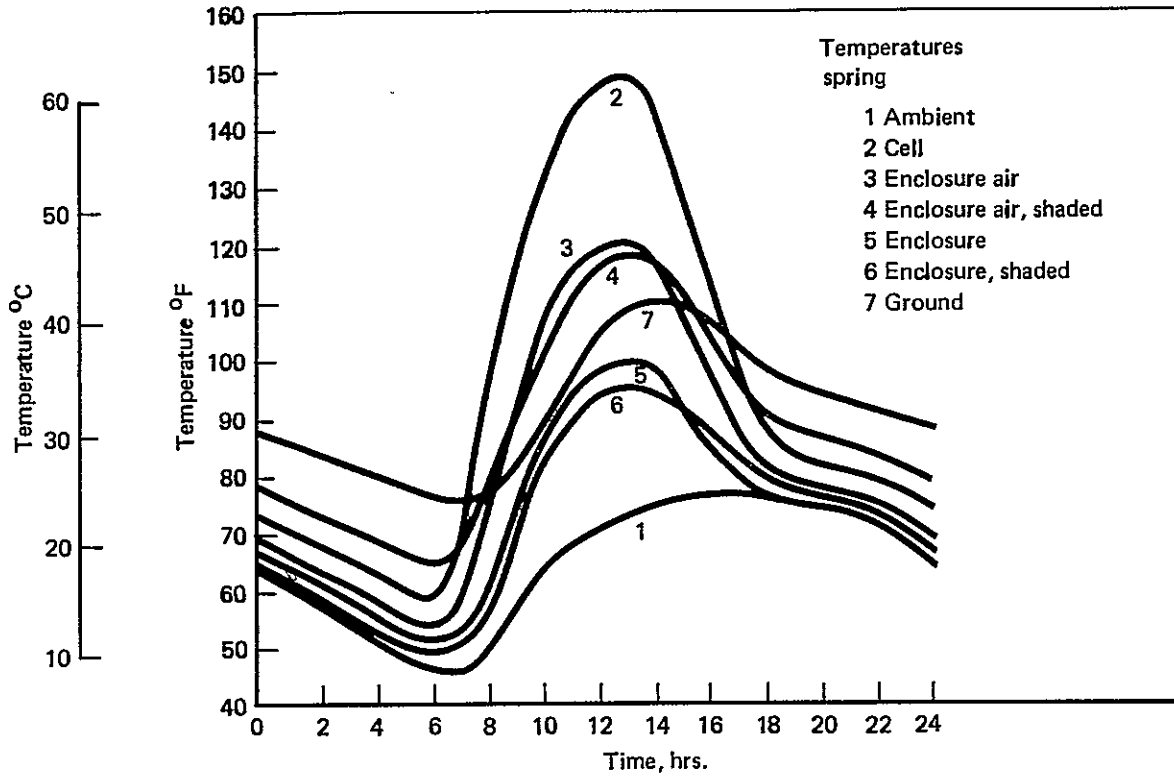


Figure 1-2. Typical Enclosed Fixed - Tilted Array Temperature Response

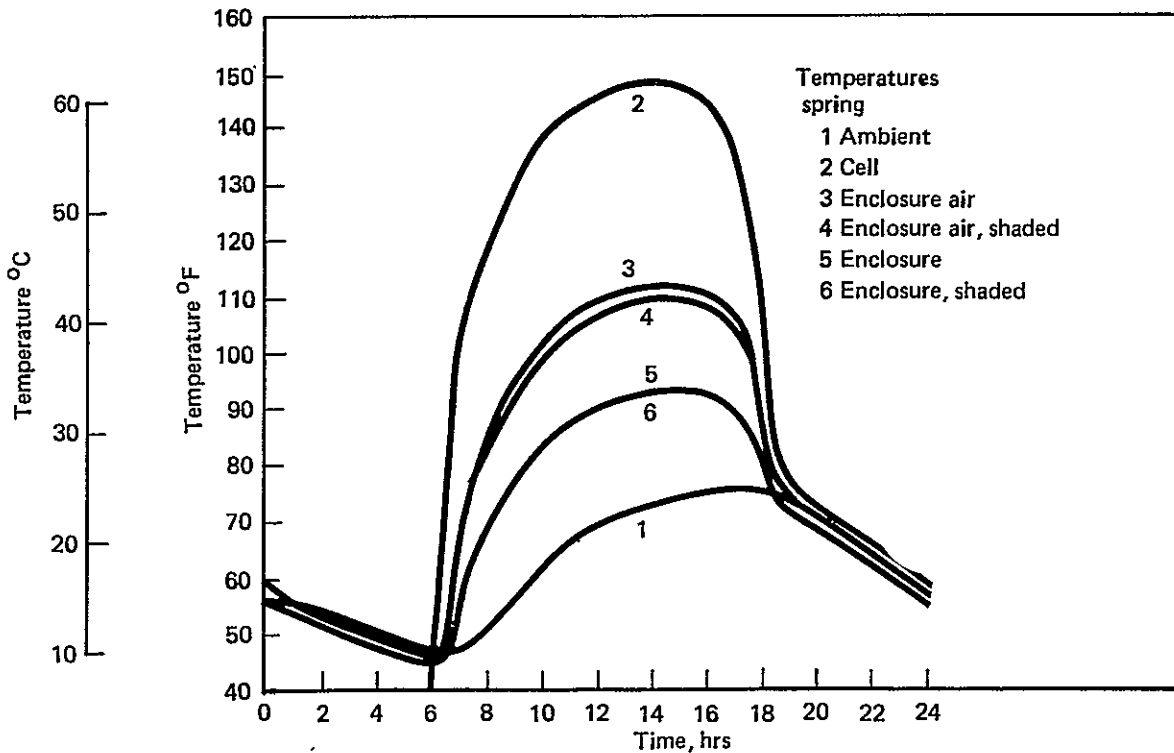


Figure 1-3. Typical Enclosed Tracking Array Temperature Response

TABLE 1 - I PREDICTED PEAK TEMPERATURES FROM TRANSIENT ANALYSIS

AMBIENT CONDITION	PEAK DAILY TEMPERATURE °C (°F)						
	AMBIENT	FIXED ARRAY			TRACKING ARRAY		
		CELL	ENCLOSURE AIR	ENCLOSURE	CELL	ENCLOSURE AIR	ENCLOSURE
Spring Nominal	24 (76)	64 (148)	49 (120)	37 (99)	64 (148)	44 (112)	34 (93)
Summer Nominal	39 (102)	72 (162)	59 (138)	49 (120)	78 (173)	58 (137)	48 (119)
Fall Nominal	29 (85)	67 (152)	52 (126)	42 (107)	67 (153)	48 (119)	39 (102)
Winter Nominal	22 (71)	55 (131)	42 (107)	32 (89)	58 (136)	39 (103)	31 (87)
Summer Extreme Heat	47 (116)	79 (175)	66 (151)	57 (134)	86 (186)	66 (151)	56 (133)
Winter Extreme Cold	8 (46)	42 (108)	29 (84)	18 (65)	45 (113)	26 (79)	17 (63)

7

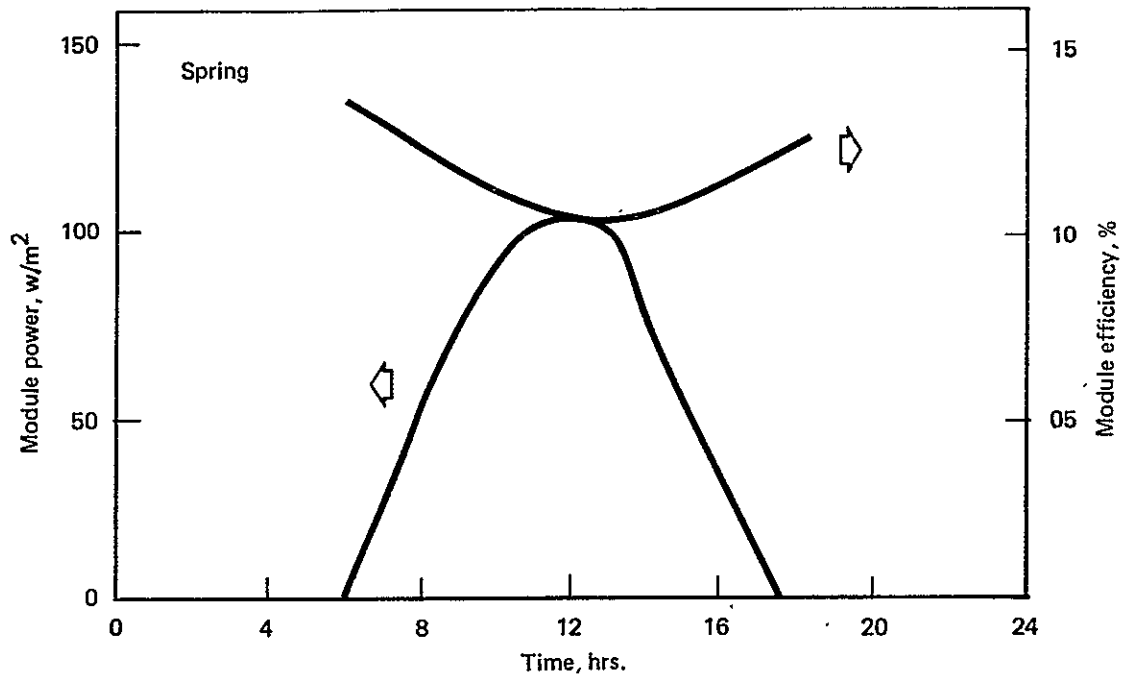


Figure 1-4. Module Power Output and Efficiency for Typical Day: Fixed Tilt Array

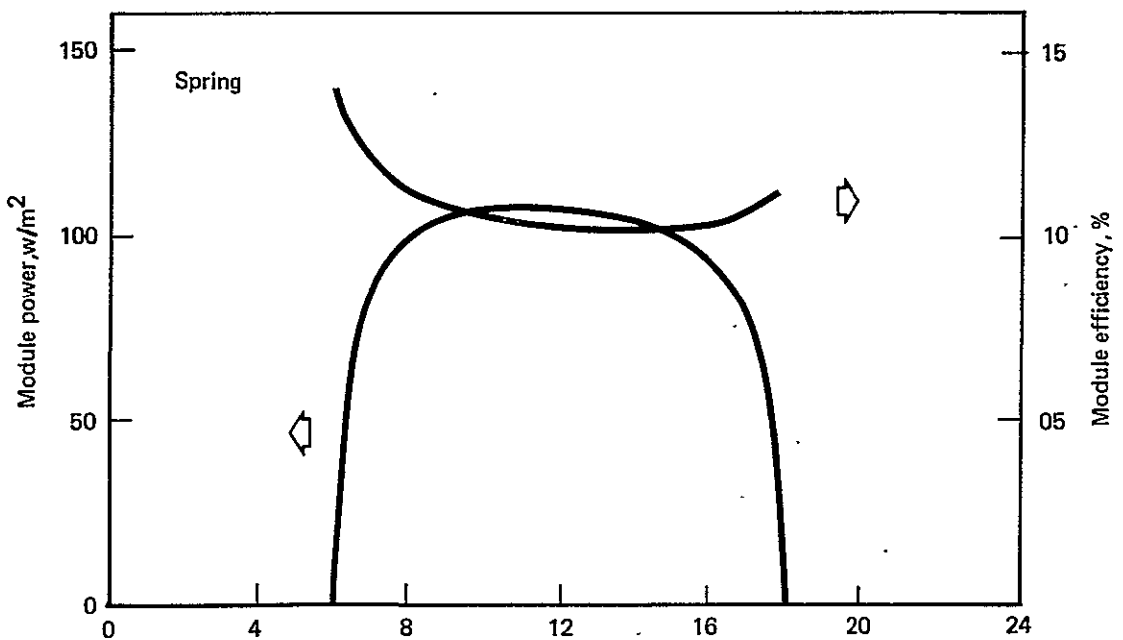


Figure 1-5. Module Power Output and Efficiency for Typical Day: Tracking Array

are higher than would be obtained with standard insolation levels. Analysis of the arrays under NOCT conditions yields the results shown in Table 1-II.

1.3 Life Cycle Costs

The cost analysis includes materials, labor, facilities and equipment for producing, installing, and maintaining the photovoltaic arrays. The structure, including enclosures, must be capable (by periodic replacement, if necessary) of lasting 30 years. Module/panel life is assumed to be 20 years. Energy costs are calculated for both 20 and 30 year power plant economic lifetimes. The costs are summarized in Table 1-III for the two enclosed arrays with 20 year economic life, which has lower costs. The cost of buying and leveling the land required for the arrays is included. These costs differ because the arrays have different land/array area ratios. This additional cost more than offsets the increased energy output of the tracking array, resulting in 20% higher bus bar energy costs than the fixed array.

1.4 Comparison to Conventional Arrays

A direct cost comparison can be made between the enclosed arrays and a conventional array. The conventional array design used for this comparison is described in a recently completed study by Bechtel National, Inc. (Ref. 31). A large number of module sizes, and panel and support structure designs were investigated in this study. The modules, having glass front surface, plastic pottant, and polyester back film, all cost very near $\$60/\text{m}^2$. Costs for the panel frame (which provides structural attachments for the module), the array structure, and the foundation are selected for the least-cost concepts and the smallest wind loading (35 PSF) given in Table 7-I of Ref. 31. The enclosed array costs are compared with the conventional array costs in Table 1-IV. It can be seen that the enclosed fixed-tilt array offers a substantial cost reduction in both the cost per unit area and cost per peak watt. This comparison does not include the power collection wiring, where some additional savings might be achieved with the enclosed fixed-tilt array, because most of the wiring is protected from the weather.

TABLE 1-II: POWER OUTPUT FOR NOCT CONDITIONS

	NOCT °C (°F)	POWER (WATTS/M ²)	
		NOCT	28°C
Fixed Array	59.8 (139.7)	106.0	126.1
Tracking Array	43.5 (125.5)	109.4	124.3

TABLE 1-III: SUMMARY CAPITAL AND MAINTENANCE COSTS
FOR ENCLOSED ARRAYS (1975 DOLLARS)

ITEM	COST - \$/m ² EXCEPT AS NOTED	
	FIXED ARRAY	TRACKING ARRAY
Land and Fence	2.03	4.84
Field to PCU Wiring	5.51	7.79
Foundations	4.52	5.56
Enclosures	4.60	4.01
Support Structure	1.33	22.99
Module/Panels	49.21	48.74
Tracking System	--	9.19
Array Field Total	<u>67.20</u>	<u>103.21</u>
Distributables and Indirect	1.65	4.18
Capital Cost (Cost at NOCT Output, \$/W)	68.85 (.65)	107.38 (.98)
Maintenance Cost	14.97	21.42
Total Cost (Total Cost, at NOCT Output, \$/W)	83.82 (.79)	128.80 (1.18)
Direct Current Bus Bar Energy Cost, Mills/kW-H(dc) (1975 Dollars)	51.5	56.3

TABLE 1-IV: NORMALIZED COST SUMMARY
(1975 DOLLARS)

ITEM	\$/m ²		\$/w _p AT NOCT	
	AIR ENCLOSURE	CONVENTIONAL* ARRAY (BECHTEL)	AIR ENCLOSURE (10.6% AT NOCT)	CONVENTIONAL ARRAY (BECHTEL) (12.7% AT NOCT)
Modules	49.21	60.00	0.46	0.47
Structures				
• Air-Enclosure	4.60	--	0.04 +	--
• Panel Structure	--	14.70	--	0.11
• Support Structure	1.33	7.40	0.01	0.06
• Foundations	<u>4.52</u>	<u>14.90</u>	<u>0.04+</u>	<u>0.12</u>
Structure Total	10.45	37.00	0.10	0.29
Array Total	59.66	97.00	0.56	0.76

*Ref. 31, Table 7-1 (page 154), Array Case 7, Panel Type J

1.5 Summary and Conclusions

This evaluation has shown that a fixed-tilt photovoltaic array design which uses an air-supported, transparent enclosure costs less and produces lower cost energy than a comparable conventional design. While the energy costs for the enclosed tracking array are much higher than for the enclosed fixed-tilt array, and slightly higher than for the conventional array, this approach offers a more uniform power production profile through the day. Accordingly, tracking may be of value to applications requiring a more uniform power production profile, rather than the strongly peaked profile characteristic of fixed-tilt arrays.

2.0 INTRODUCTION

This report describes a study which investigated the potential advantages of using air-supported plastic enclosures to environmentally protect flat plate photovoltaic arrays. The study was performed under contract to the Jet Propulsion Laboratory as part of the Engineering Area analyses for the Low-Cost Solar Array (LSA) Project. This project is being managed by JPL for the Department of Energy, Division of Solar Technology.

2.1 Study Objectives

The Department of Energy (DOE) photovoltaic program (Ref. 2) has the overall objective to ensure that photovoltaic conversion systems will contribute significantly (50 GWe) to the nation's energy supply by the year 2000. The DOE has established specific price goals which are deemed necessary to achieve the desired industry growth and market penetration. These goals, i.e., flat-plate modules costing \$0.50 per peak watt and producing energy at 50-80 mills/kW·h by 1986 (expressed in constant 1975 dollars), are recognized as very challenging, since to meet them, industry must reduce cell and module costs by more than an order of magnitude. Less dramatic but, nonetheless, large cost reductions are needed for system components other than the photovoltaic modules.

The study reported herein evaluates the use of an air-supported enclosure for environmental protection of the photovoltaic arrays. The objective of the study was to determine the potential technical and economic benefits obtained by using the enclosure. Similar transparent plastic protective enclosures are being developed by Boeing Engineering and Construction Company as part of the DOE solar-thermal electric program, where the intended use is to protect heliostat mirrors. Figure 2-1 shows a research experiment heliostat with 5.18 meter (17 foot) diameter enclosure, and Figure 2-2 shows an artist's rendering of the current (preliminary) design for commercial production. The major advantage of the air supported enclosure is the protection from the

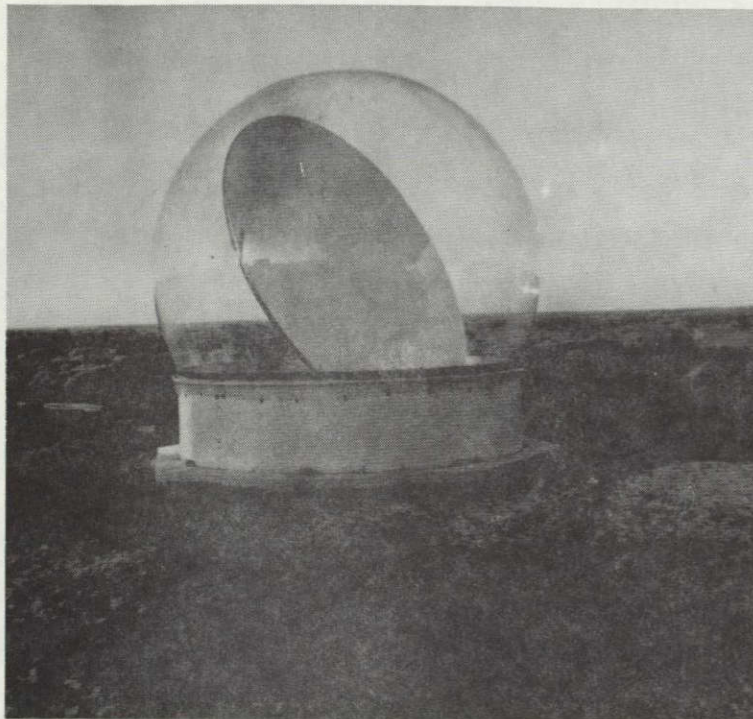


Figure 2-1. Research Experiments Heliostat

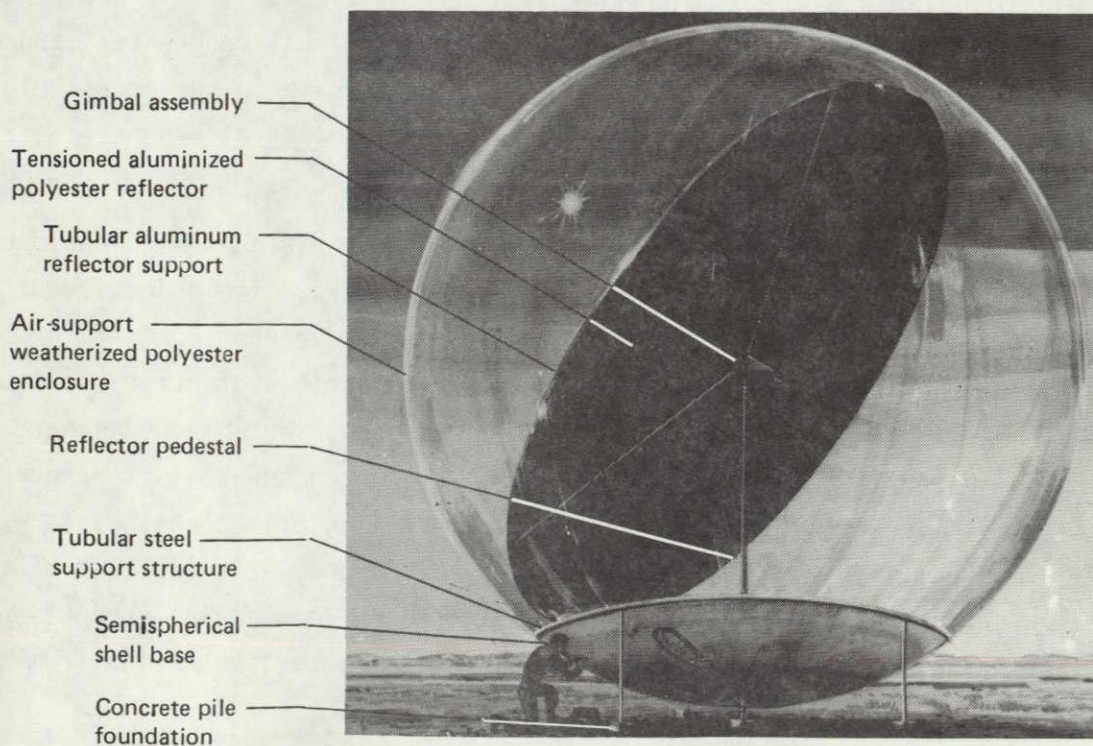


Figure 2-2. Baseline Heliostat Design

environment provided to the modules and support structure. Wind loads, dust, hail and other precipitation will not interfere with the operation of the photovoltaic modules or degrade their performance with time. The supporting structure must resist only the small gravity and earthquake loads; the enclosure resists the much higher wind and snow loads.

2.1 Study Groundrules

The basic approach to the study was to evaluate enclosed photovoltaic array designs and to compare the results to comparable conventional arrays. Conventional arrays are assumed to be arrays composed of photovoltaic modules having a glass front surface, plastic pottant and polyester film back cover, and plastic back surface (i.e., encapsulant), with the modules mounted at latitude tilt on a structural steel framework. The selected system application is a 200 MWe (peak) central power station located in the Phoenix, Arizona area. While the study did not encompass the complete power station design, the overall power station concept was briefly investigated to provide the basis for the array conceptual design. Many of the detailed assumptions necessary in the study were defined by JPL. All of the groundrules used in the study are given in Section 3.1 Design Requirements. The most significant assumptions, in addition to the application noted above, include the following:

- 20 year array design life, 30 year structure design life.
- Environment from Phoenix "SOLMET" weather data tape.
- Unencapsulated (bare) cell efficiency of 16% at 28°C, 1000 W/m² insolation, air mass of one (AM1).
- Interconnected cell cost of \$40/m².

The original plan was based on studying only a tracking array using the enclosure and other common elements from the design shown in Figure 2-2. Early in the study an additional concept with fixed latitude-tilt arrays enclosed in a half circle cross-section cylindrical enclosure was formulated. This concept was equally attractive, with the possibility of substantially reduced costs (compared to the tracking array) to overcome the lower power production

of the fixed array. A choice between the two approaches could not be made, so both have been evaluated in this study and compared to the conventional array.

2.3 Report Organization

This section is preceded by a summary of the program evaluations and results in Section 1.0. Section 3.0 lists the detail design requirements used in the study. Sections 4.0 and 5.0 give a description of the conceptual designs, discussions of the design and performance analyses, and a summary of the cost analyses for the fixed-tilt and tracking arrays, respectively. The fixed-tilt array is discussed first because more design definition and analysis was required for this new concept. Comparisons of these designs to the conventional array concept are made in Section 6.0. Conclusions are given in Section 7.0, Recommendations in Section 8.0, New Technology in Section 9.0, and References are in Section 10.0.

3.0 DESIGN REQUIREMENTS

3.1 System Application and Definition

3.1.1 Application

The photovoltaic array subsystem is conceived to be part of a power station providing power to an electrical transmission/distribution grid. The power plant is considered to be sited in the Southwest United States, specifically at Phoenix, Arizona, and would produce power to meet peak and intermediate demands.

This study does not address the complete central power station design. Only the photovoltaic array design and costs related to array area (power collection wiring and land) are considered.

3.1.2 Definitions

Terms describing elements of the photovoltaic power plant as used in this report are described in Figure 3-1 for the fixed-tilt array concept and in Figure 3-2 for the tracking array concept. This terminology is consistent with that used by the Engineering Area of JPL's LSA Program at the time of this report.

3.2 Array Design Characteristics

The photovoltaic array converts incident solar radiation into dc electrical energy, which is collected by the dc power collection wiring. Design and performance characteristics required of the array are covered in the following sections.

SOLAR CELL -- The basic photovoltaic device which generates electricity when exposed to sunlight.

MODULE -- The smallest complete, environmentally protected assembly of solar cells and other components (including electrical connectors) designed to generate dc power when under unconcentrated terrestrial sunlight.

PANEL -- A collection of one or more modules fastened together, factory preassembled and wired, forming a field installable unit.

ARRAY -- A mechanically integrated assembly of panels together with support structure (including foundations) tracking and other components, as required, to form a free-standing field installed unit that produces dc power.

BRANCH CIRCUIT -- A group of modules or paralleled modules connected in series to provide dc power at the dc voltage level of the power conditioning unit (PCU). A branch circuit may involve the interconnection of modules located in several arrays.

ARRAY SUBFIELD -- A group of solar photovoltaic arrays associated by the collection of branch circuits that achieves the rated dc power level of the power conditioning unit.

ARRAY FIELD -- The aggregate of all array subfields that generate power within the photovoltaic central power station.

PHOTOVOLTAIC CENTRAL POWER STATION -- The array field together with auxiliary systems (power conditioning, wiring, switchyard, protection, control) and facilities required to convert terrestrial sunlight into ac electrical energy suitable for connection to an electric power grid.

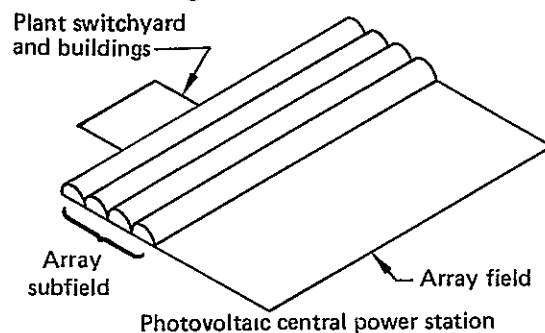
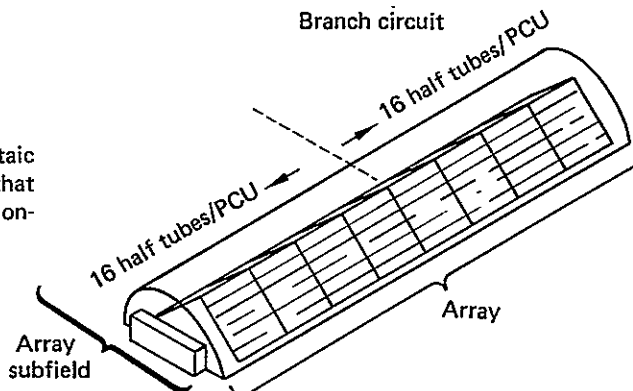
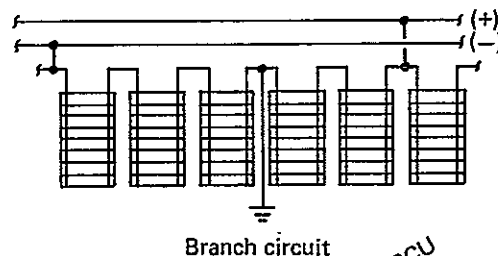
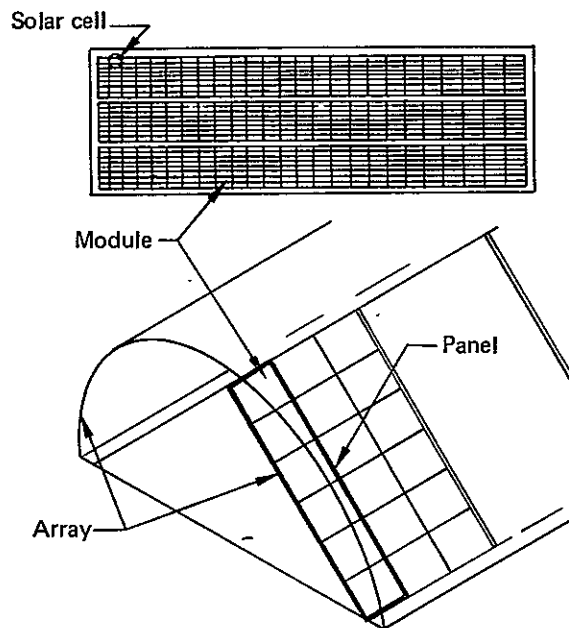


Figure 3-1. Delineation of Terminology , Fixed tilted array

SOLAR CELL — The basic photovoltaic device which generates electricity when exposed to sunlight.

MODULE — The smallest complete, environmentally protected assembly of solar cells and other components (including electrical connectors) designed to generate dc power when under unconcentrated terrestrial sunlight.

PANEL — A collection of one or more modules fastened together, factory preassembled and wired, forming a field installable unit.

ARRAY — A mechanically integrated assembly of panels together with support structure (including foundations) tracking and other components, as required, to form a free-standing field installed unit that produces dc power.

BRANCH CIRCUIT — A group of modules or paralleled modules connected in series to provide dc power at the dc voltage level of the power conditioning unit (PCU). A branch circuit may involve the interconnection of modules located in several arrays.

ARRAY SUBFIELD — A group of solar photovoltaic arrays associated by the collection of branch circuits that achieves the rated dc power level of the power conditioning unit.

ARRAY FIELD — The aggregate of all array subfields that generate power within the photovoltaic central power station.

PHOTOVOLTAIC CENTRAL POWER STATION — The array field together with auxiliary systems (power conditioning, wiring, switchyard, protection, control) and facilities required to convert terrestrial sunlight into ac electrical energy suitable for connection to an electric power grid.

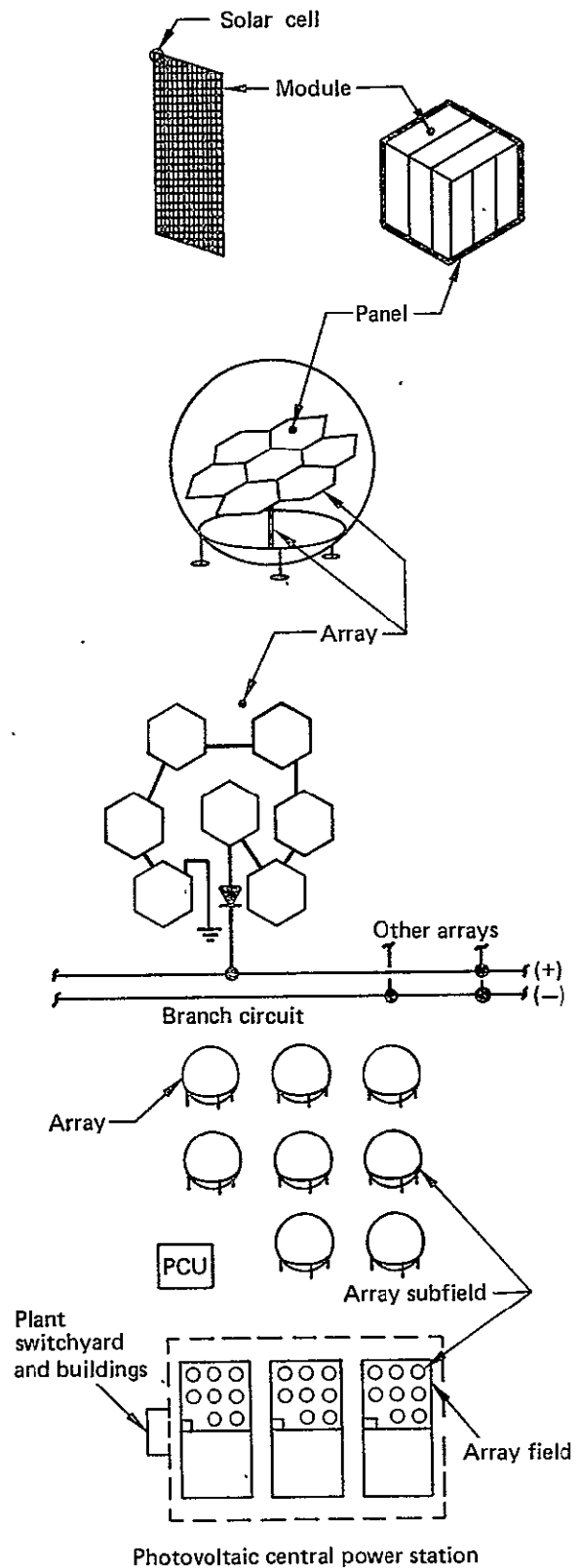


Figure 3-2. Delineation of Terminology, Tracking Array

3.2.1 Performance

3.2.1.1 Solar Cell Performance

Electrical energy output of a photovoltaic module is based on the following:

- . Unencapsulated (bare) cell efficiency: 16% at 28°C
- . Encapsulated cell efficiency: 15%
- . Nominal Operating Cell Temperature (NOCT): 44°C (non-enclosed arrays only)
- . Power measured at NOCT, 100 mW/cm², AM1
- . Nesting efficiency: 93% (square cells)
- . Temperature sensitivities:
 - . Maximum Power
$$(P_{28C}-P)/P_{28C}/(T-28C) = 0.005 \text{ Watts/Watt/}^{\circ}\text{C}$$
 - . Open Circuit Voltage
$$(V_{28C}-V)/V_{28C}/(T-28C) = 0.0038 \text{ Volts/Volt/}^{\circ}\text{C}$$
 - . Short Circuit Current
$$(I-I_{28C})/I_{28C}/(T-28C) = 0.0002 \text{ Amps/Amp/}^{\circ}\text{C}$$

3.2.1.2 Subsystem Life

The array subsystem is designed for 30 year useful life, except the modules and panels for which a 20 year life is assumed. Scheduled component replacement may be employed to achieve the required life, but replacement costs must be included in the economic evaluation.

3.2.2 Environmental Conditions

The arrays are designed for the environmental conditions defined in the following subparagraphs.

Environmental Variations and Extreme Conditions -- Arrays must operate in the nominal and extreme insolation and temperature conditions defined below. Tracking arrays must be capable of going to a non-operating status when insolation is not available.

Temperature -- Ambient temperature environment is defined by the SOLMET data tape for Phoenix, Arizona available from the National Climatic Center. Arrays and control systems shall be capable of surviving without degradation in performance 50 thermal cycles between -40°C and $+90^{\circ}\text{C}$, as a qualification test.

Precipitation -- Quantities shall be consistent with the Phoenix environment.

Hail -- The array subsystem shall survive 3.8 centimeter (1-1/2 inch) diameter hail with a terminal velocity of 27.4 meter/second (90 feet/second).

Insolation -- Yearly insolation shall be defined by SOLMET data tape for Phoenix, Arizona.

Winds -- The array shall survive winds of 35.8 meters/second (80 mph) at 10 meters (30 foot) height, including gusts. This is the annual extreme fastest-mile speed for a 100 year mean recurrence interval for Phoenix as defined in Ref. 3. The wind profile upstream of the power station boundary may be considered exponential with height to the 1/7th power. The cumulative effect of upwind structures within the power station on wind profile, with its attendant reduction in design pressures, may be accounted for in the design. However, any increases in pressures or suction and buffeting resulting from surrounding structures also must be allowed for in the design.

Seismology - Earthquake forces are based on Seismic zone 3, with horizontal and vertical accelerations of 0.25g based on Ref. 3.

Nominal Operating Conditions -- Environmental conditions for use in conceptual design, nominal performance comparisons, and initial economic analyses are as follows:

- . Insolation = 800 W/m^2 (thermal analysis) 1000 W/m^2 (power output)
- . Air Temperature = 20°C
- . Wind Average Velocity = 1 m/s
- . Array Location at 33.4° North Latitude (Phoenix, Arizona)

Design and Construction -- The array electrical circuit shall be capable of maintaining electrical integrity with 5000 VDC potential between the cell string and module ground.

4.0 FIXED ARRAY DESIGN CONCEPT

Configuration of the fixed array, Figure 4-1, is in many respects similar to the concept for a conventional array. Rectangular photovoltaic panels tilted at the site latitude rest on a support structure of beam and column members. A concrete foundation anchors the array and distributes applied loads into the soil. Modules are electrically connected to introduce power at the desired voltage into the power collector wiring. Beyond this brief description, the enclosed array concept and the conventional concept are very different, as summarized in Table 4-I.

The following subsection describes the enclosed fixed array design concept. Section 4.2 describes analyses supporting the choice of the selected concept and provides the rationale for the geometry, thicknesses, and materials used in the design. Section 4.3 presents the related thermal and electrical performance predictions, including an evaluation of several cooling concepts. The preliminary manufacturing and installation plan are discussed in Section 4.4. Section 4.5 presents maintenance assumptions, and Section 4.6 summarizes the life cycle costs for this concept.

4.1 Concept Description

The length of each array is dependent on total array area required in the power station, module dimensions, dimensions of the available land, and other factors. An overview description of the central power station, Figure 4-2, provided the basis for the selected array dimensions. Each array feeds power from its center toward both ends of the array. Power conditioning units receive the output from sixteen half-arrays, which comprise an array subfield. The array field consists of eighteen subfields with nine power conditioning units located along the east side and nine units on the west side. Power output from the power conditioning units is bussed around the array field perimeter to a switchyard on the north side of the plant.

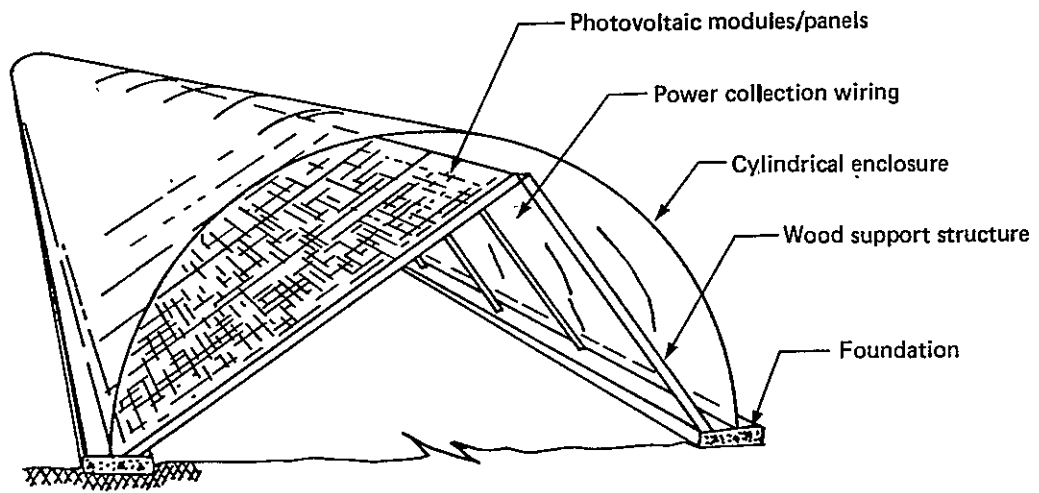


Figure 4-1. Fixed Tilt Array Concept

TABLE 4-I: COMPARISON OF ENCLOSED AND CONVENTIONAL ARRAY CONCEPTS

FEATURE	CONVENTIONAL ARRAY	ENCLOSED ARRAY
Modules	Fully encapsulated, glass front surface, glass or plastic back, electrical isolation under wet conditions. Loads carried by plate bending.	Not encapsulated, plastic film substrate. Electrical isolation for dry conditions.
Panels	Welded steel frames containing one or more modules and with provisions for attaching to the support structure.	Module substrates joined to form panel. Gravity loads only, carried in tension.
Support Structure	Painted or galvanized structural steel members, bolted or welded assembly.	Wood roof-truss type construction, press-on connector plates, no preservatives necessary.
Foundation	Auger-cast concrete piles or shallow-based spread concrete footings.	Linear concrete "curbs".
Enclosure	None.	Half-circle cylinder of plastic film; carries wind loads in tension.
Power Collection Wiring	Fully insulated, weatherproof connectors and wiring.	Weather protection provided by the enclosure.

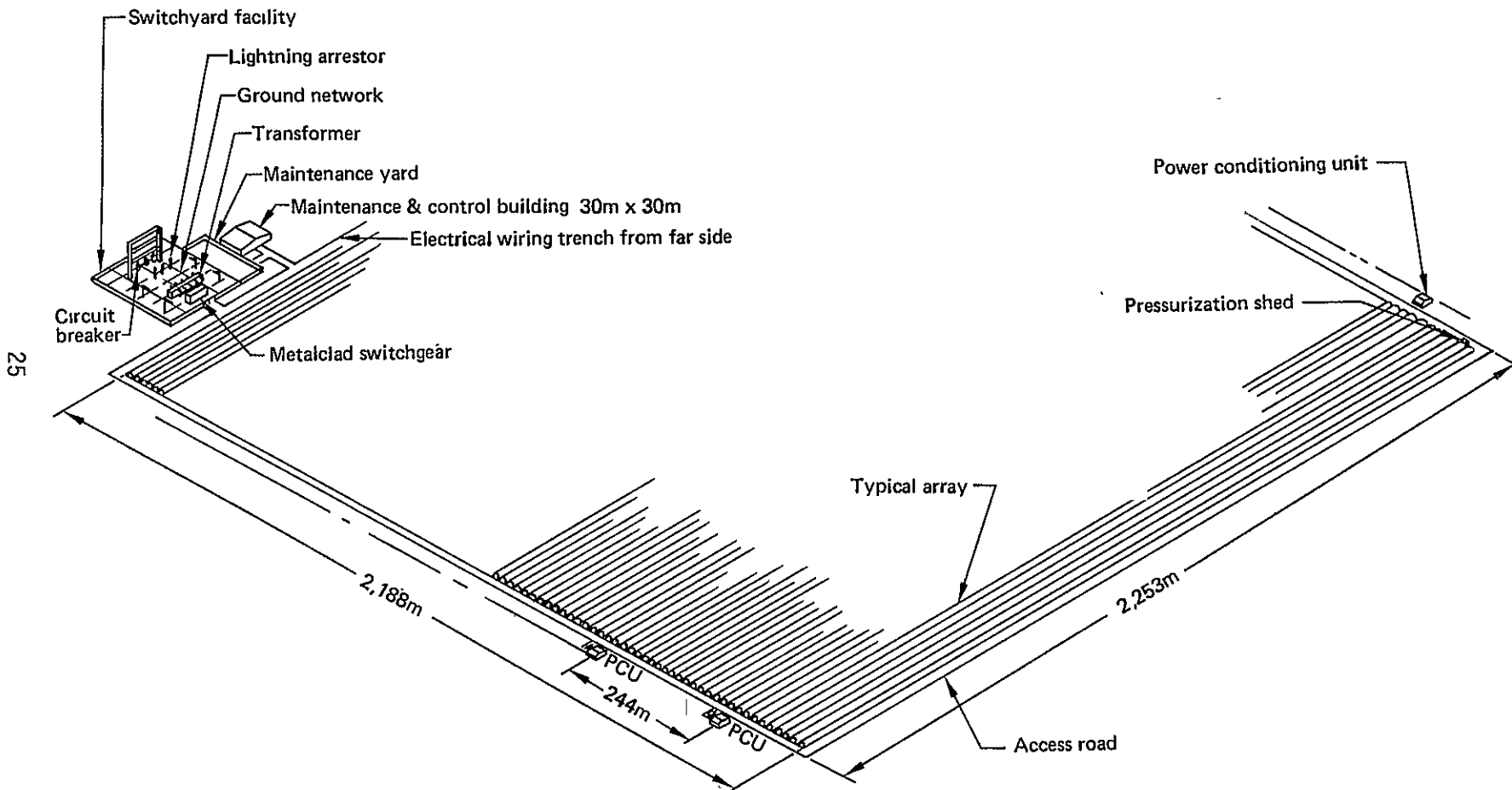


Figure 4-2. Overview of 200 MW Photovoltaic Power Station - Fixed Tilt Array

Size of the array field includes the effect of losses from the array interface with the power collection wiring to the distribution system interface. The total estimated losses shown in Table 4-II are 15.3% of the 200 MW peak power output of the plant. The arrays must produce a total power output of 232.2 MW when each of the subsystem efficiencies are applied sequentially. With an array temperature of 67°C (153°F), estimated in a preliminary thermal analysis, and with preliminary values for the array packing density and enclosure transmittance, 144 arrays which are 2253 meters (7392 feet) in length are required. The number and length of arrays are adjusted to produce a nearly square array field.

The major elements of the fixed array concept are discussed in the following subsections.

4.1.1 Protective Enclosure

The selected enclosure configuration, shown in Figure 4-3, is a cylindrical shell with a half-circle cross section. The simple dimension evaluation shown in Figure 4-4 indicates that the half-circle (beta of 90 degrees) should be near optimum to minimize non-module costs. The polyester film used for the enclosure is purchased in the largest available width (currently 152 centimeters (60 inches) and is bonded using a heat setting polyester adhesive to form a continuous cylinder. A rope bonded into the bottom edges of the enclosure provides a positive restraint and evenly distributes the enclosure loads when clamped to the foundation. Internal air pressure of 320 Pa (0.047 psi or 6.77 psf) supports the enclosure in the circular cylindrical shape and resists wind and snow loads. A simple concept for the pressurization system, employing a centrifugal blower, is shown in Figure 4-5.

A closure, shown in Figure 4-6, at each end of the cylinder provides access for either vehicles and equipment or personnel; a portable air lock would be used when use of the large equipment access doors is required. Such access should be infrequent after installation and checkout of the modules is

TABLE 4-II: POWER STATION PERFORMANCE GATHERING NETWORK
LOSSES AT PEAK POWER OUTPUT

ITEM	RATING, MW	LOSS, PERCENT	LOSS, MW	POWER INPUT, MW
High Voltage Transformer	200.0	3.0	6.0	206.0
Switchgear	106.0	0.5	1.0	207.0
Cable From Power Conditioners	207.0	0.7	1.5	208.5
Power Conditions	208.5	7.0	14.6	223.1
End Connections, Enclosures	223.1	0.3	0.6	223.7
Within Enclosures (67°C Cells)	~223.7	3.8	8.5	232.2
Enclosures Required = $\frac{232.2 \times 10^6 \text{ W}}{720 \text{ W/m} \times 2253 \text{ m/Tube}} = 144$				

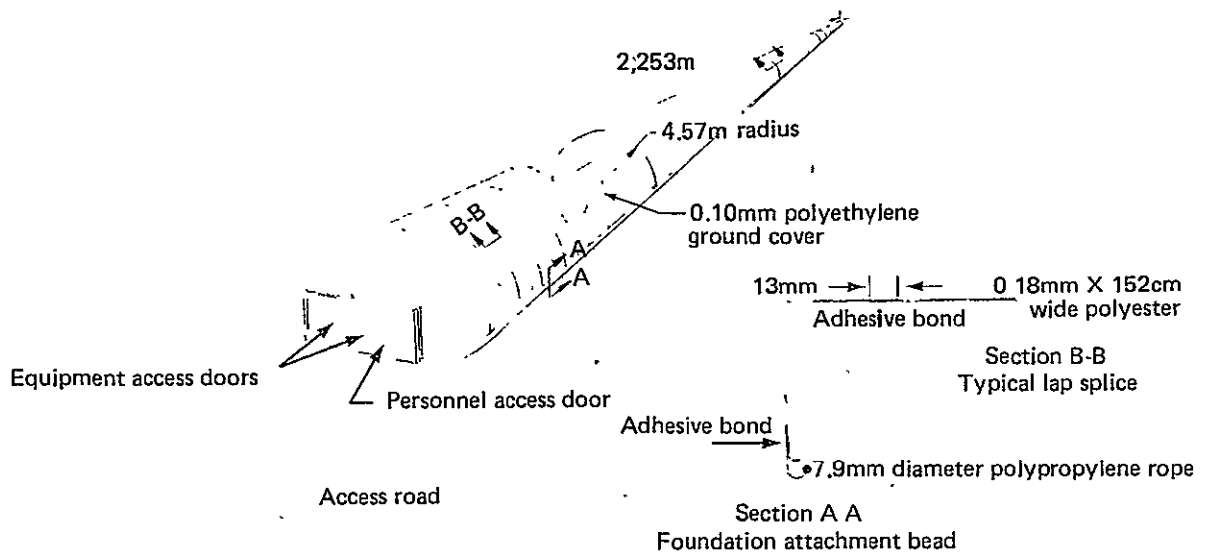


Figure 4-3. Overview of Enclosure Configuration - Fixed Tilt Array

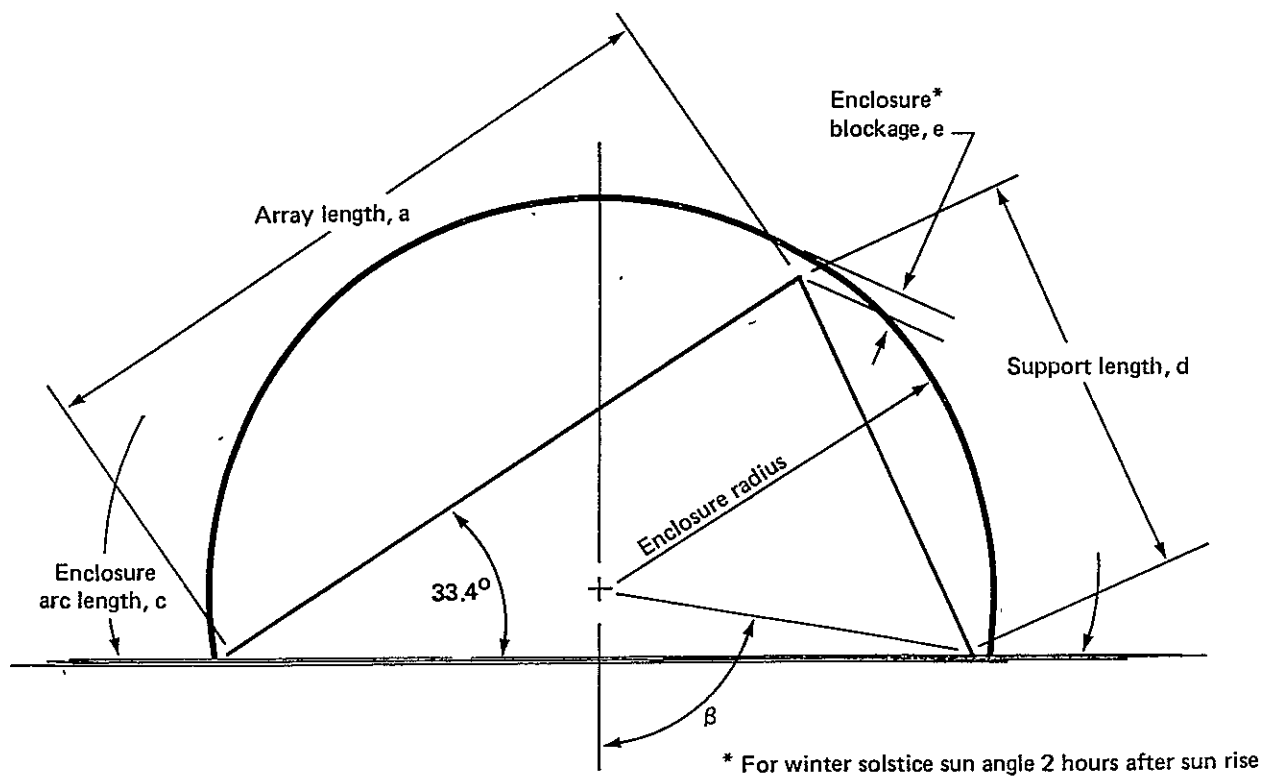
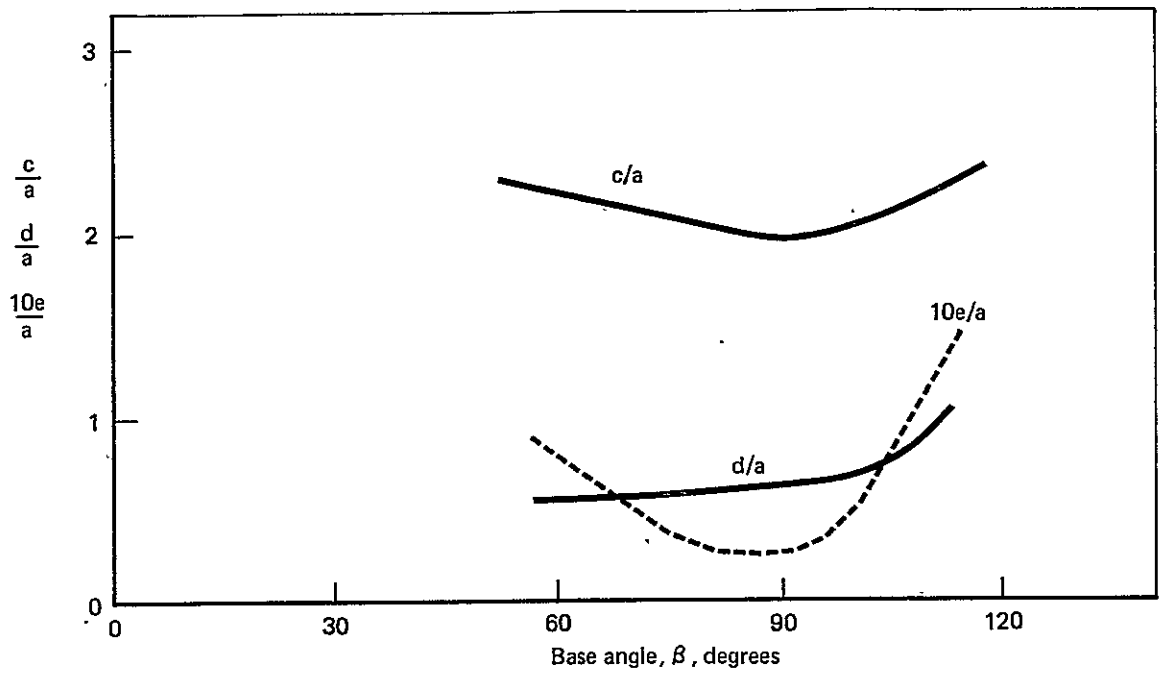


Figure 4-4. Parametric Dimensional Evaluation of Cylindrical Enclosure

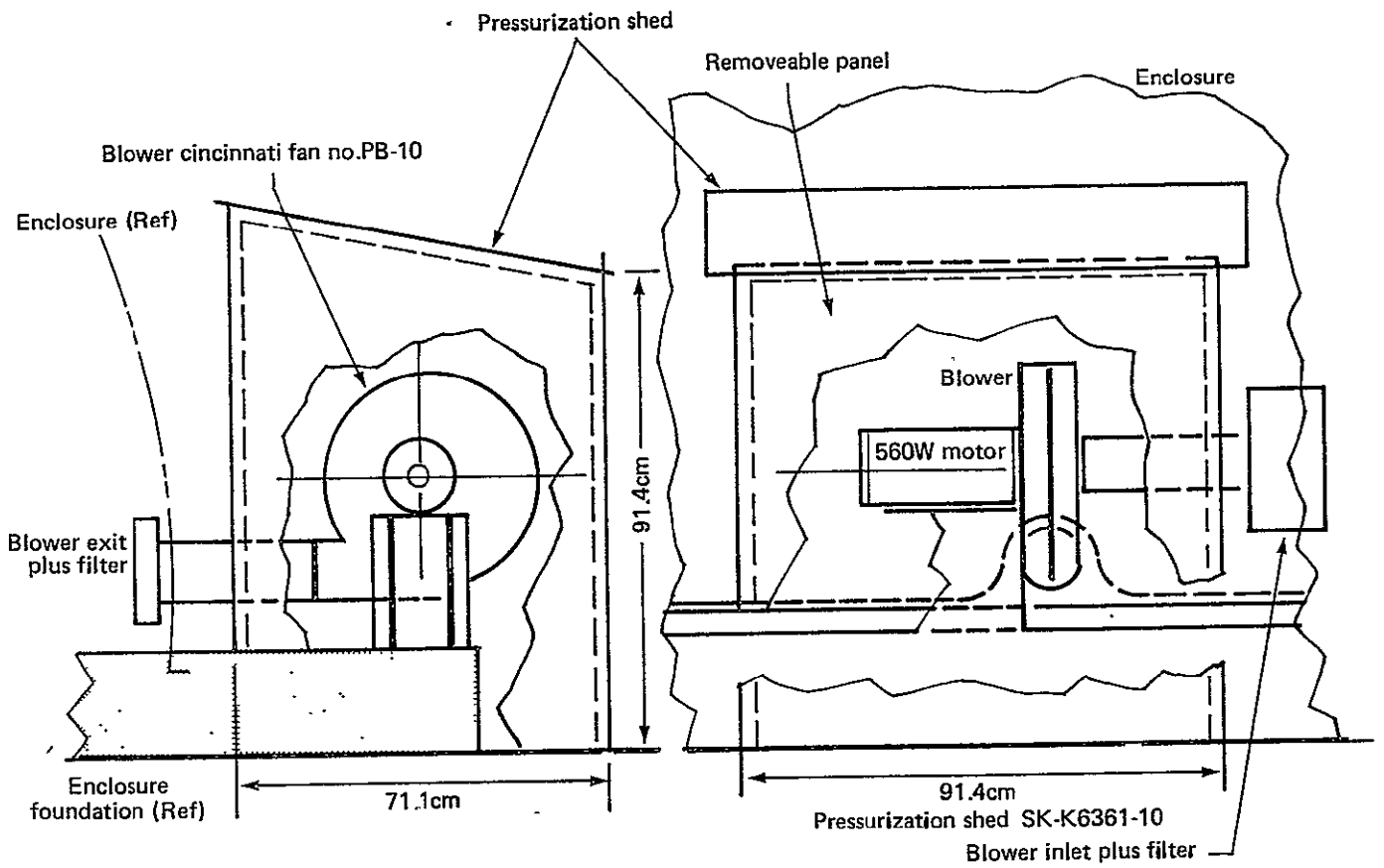


Figure 4-5. Pressurization System

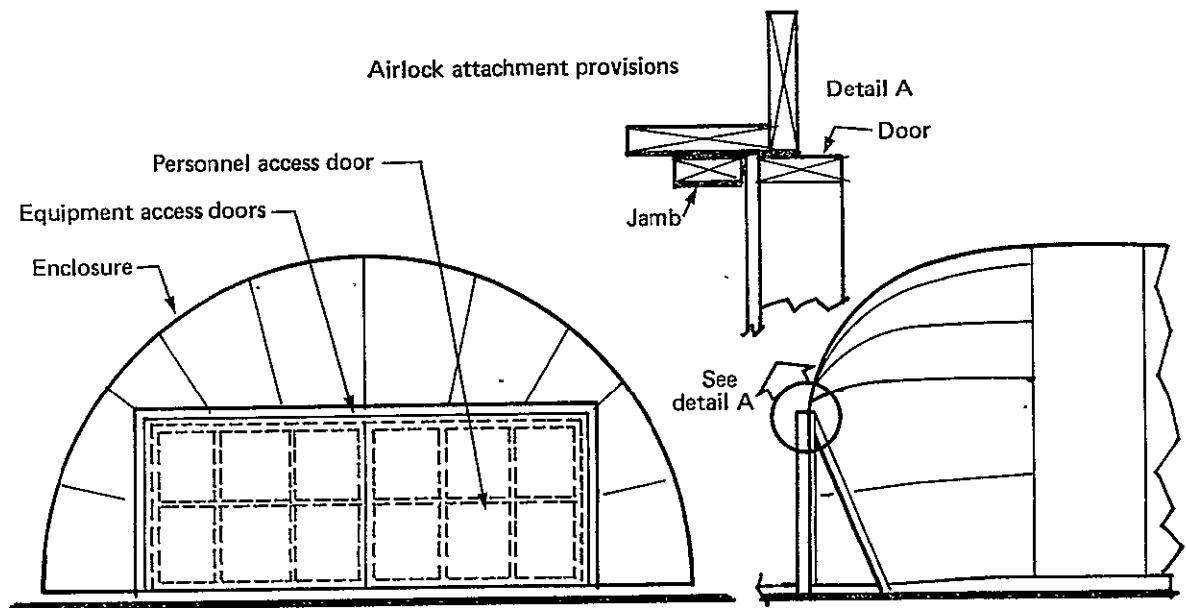


Figure 4-6. Enclosure End Configuration

complete, so a permanent air lock is not mandatory. The doors are inward opening and bear against pressure seals in the closed position to minimize air leakage.

4.1.2 Array Support Structure

The support structure for the photovoltaic modules and power collection wiring is a wood A-frame structure with geometry and construction techniques similar to those used in wood-frame building construction. Figure 4-7 shows the geometry of the structure and the lumber dimensions. Splices in the module support beam, which runs along the peak of the frame, are placed at the one-fourth points of each span, where bending moments are minimal. Shear bracing is placed in every fifth bay to resist earthquake forces and stabilize the structure in the long direction of the array. The lumber lengths are compatible with current lumber finishing practices.

A detail of the upper portion of the A-frame, Figure 4-8, shows the connector plates used for assembling the structure. These are commercially available and commonly used to fabricate roof trusses. The connector plates have barbed teeth punched from the plate material. Hydraulically actuated clamps are used to embed the teeth in the wood.

4.1.3 Foundation

The foundation of both the enclosure and the support structure is a concrete strip along each side of the cylinder. These strips are shown in Figure 4-7, for example. A detail of the cross section of the foundation is shown in Figure 4-9. The cross section is designed to interface most conveniently with the enclosure and support structure and to provide sufficient weight to prevent uplift under wind and internal pressures. The concrete is partially buried to prevent sliding under wind drag loads. A steel plate provides the interface with the enclosure attachment. Figure 4-9 shows the roll formed attachment fitting which connects the enclosure to the steel plate. The fitting on the south footing shown in Figure 4-9 also provides a support for

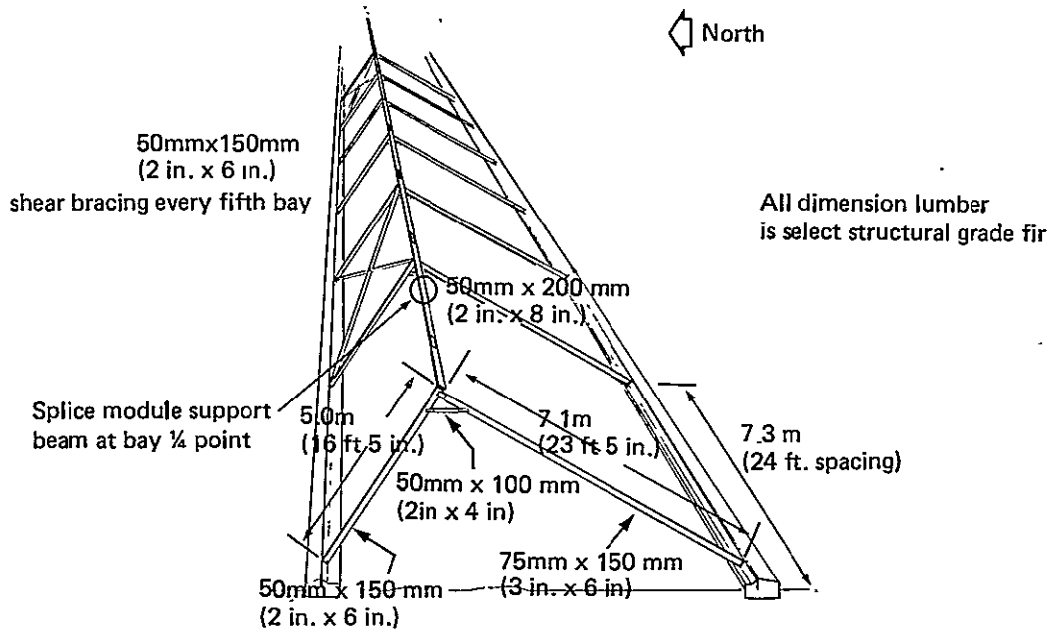


Figure 4-7. Overview of Array Support Structure - Fixed Tilt Array

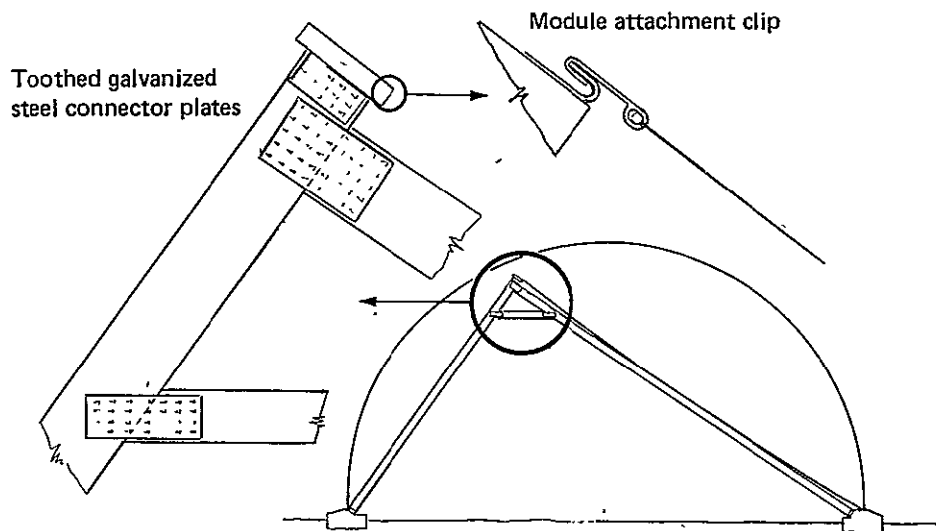


Figure 4-8. Array Support Structure Details - Fixed Tilt Array

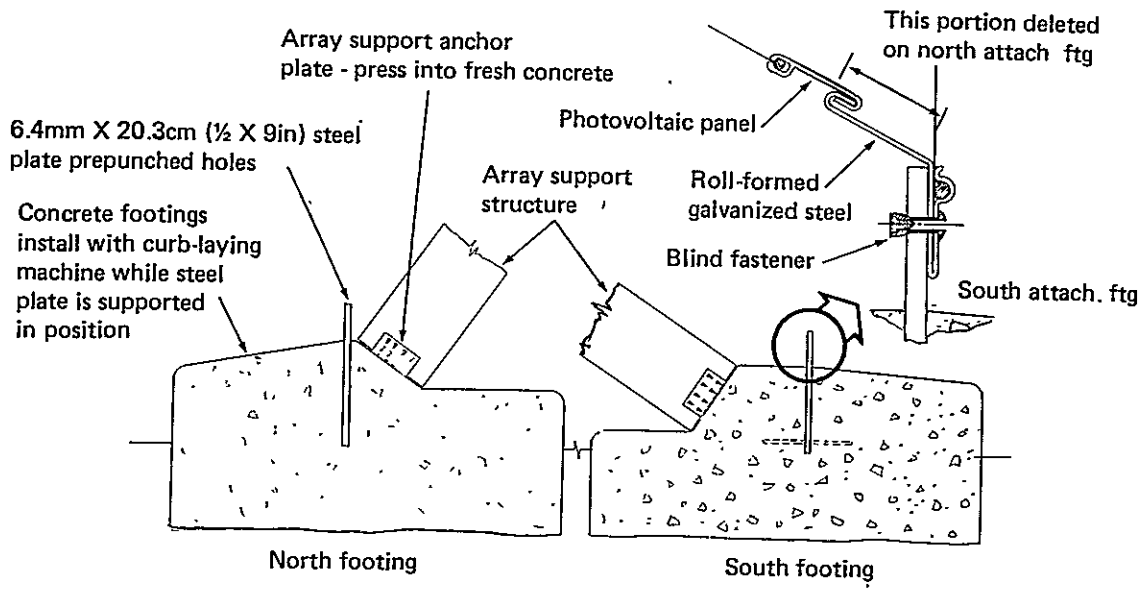


Figure 4-9. Enclosure Foundation & Attachment - Fixed Tilt Array

the lower end of the photovoltaic panel, as discussed later. A curb-laying machine would be used to install the concrete foundations, as discussed in Section 4.4.

4.1.4 Photovoltaic Modules and Panels

Three photovoltaic panels, each approximately 2.4 meters wide by 7.3 meters long (8 feet wide by 24 feet long) fit within each bay of the support structure as shown in Figure 4-10. The upper and lower edges of the panels have beads (similar to those on the enclosure) contained by extruded clips as shown in Figures 4-8 and 4-9. The clips interlock with a clip mounted on the panel support beam and the roll formed attach fitting at the south foundation. The panel is flexible and is retained in the clips by the tensile catenary stresses in the panel substrate.

Each panel is assembled from six identical modules shown in Figure 4-11. The modules are about 1.2 by 2.4 meters (4 by 8 foot) and contain 1200 solar cells. The substrate is a polyester film with weatherizing agents added to prevent UV degradation, and fire retardants to prevent fires from possible electrical arcing. The modules are joined using the same lap joint process used for the enclosure. Solar cells on the module are arranged in three groups each with eight cells in parallel and with a total of 150 cells in series. Current flow directions are shown in Figure 4-11.

Cells are interconnected both in series and in parallel, as indicated in Figures 4-12 and 4-13, to provide tolerance to individual cell failures and shadows. The cell size selected, 4.48 by 4.61 centimeters (1.77 by 1.81 inch), is slightly smaller than the five centimeter square cell originally selected as a baseline. The overall geometry of the array and modules (which were selected first) and the optional electrical circuit dictated these dimensions. The larger cells could be used if the design were built up from the basic cell dimensions.

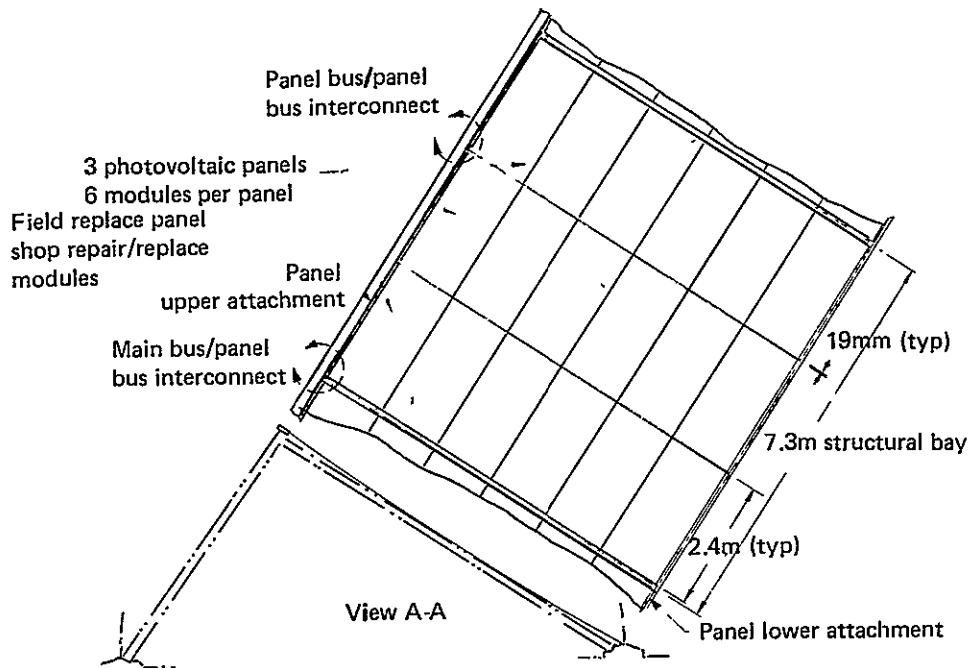


Figure 4-10. Overall Panel Geometry

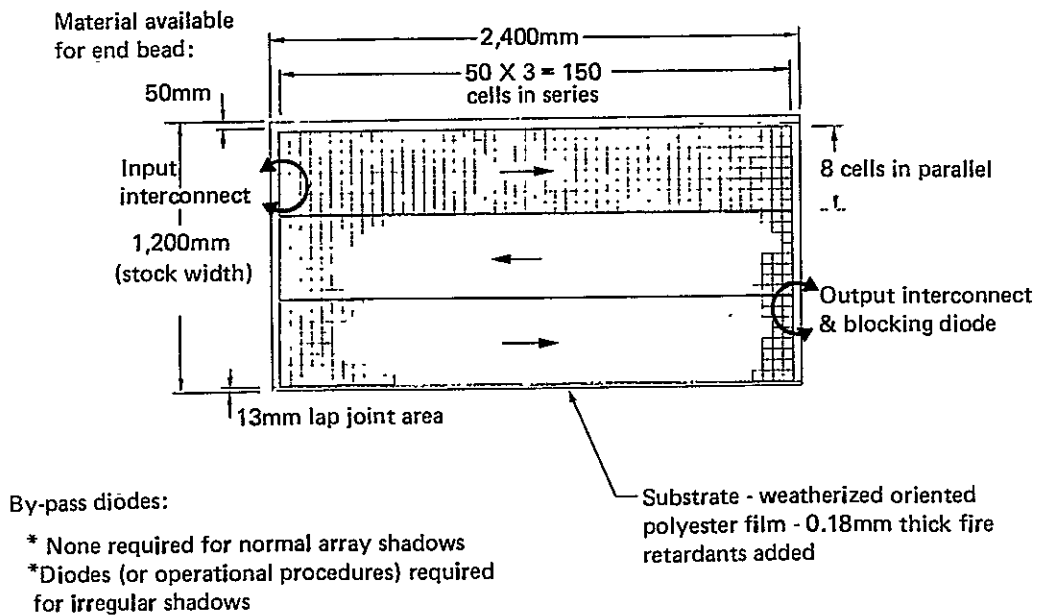


Figure 4-11. Module Configuration

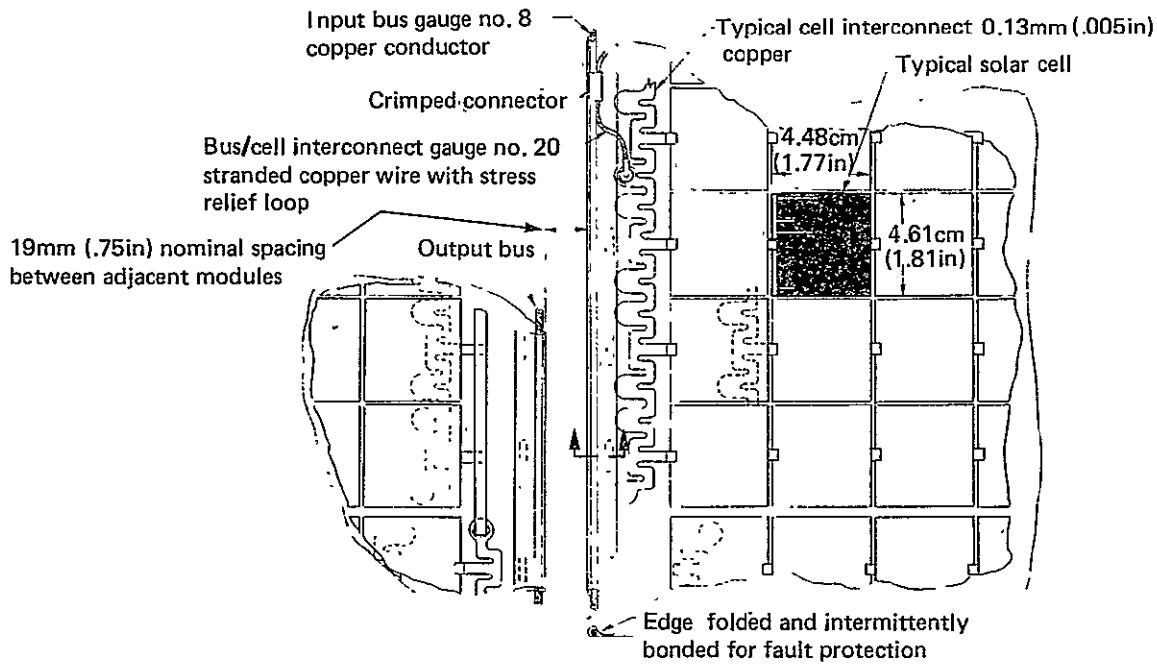


Figure 4-12. Detail of Module/Panel Input Interface

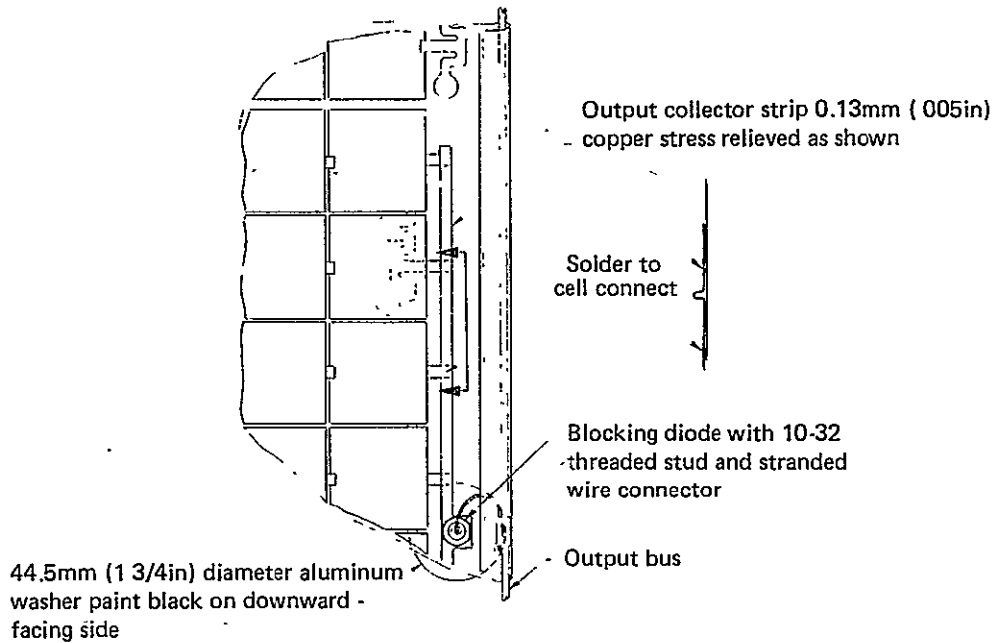


Figure 4-13. Detail of Module/Panel Output Interface

Conductors mounted along each side of the panel collect the power generated by each of the modules. Details of the conductors and the connections to the module circuit are shown in Figures 4-12 and 4-13. The edge of the panel substrate is wrapped around the bare connectors and bonded into place to insulate them from adjacent wiring.

Circuits within each panel are arranged in two forms as shown in Figure 4-14. The two orientations of the panels permit the panel interconnection scheme shown at the bottom of Figure 4-14. This minimizes the pigtailed connections between the panels and the power collection wiring and avoids large potentials between adjacent panels. The panel orientation is changed by inverting the modules; all components and assembly methods are identical. Terminal blocks as shown in Figure 4-15 provide the means of connecting adjacent panels and the pigtail to the power collection wiring.

The cell/module/panel/power collection wiring circuit described above has been selected to limit maximum array subfield voltage to 600 volts. The design is based on a maximum output of 16% efficiency at 28⁰C and a maximum of 0.5 volts per cell. Thus each module (and panel) produces power at 75 volts maximum and eight panels in series produce 600 volts dc maximum. The performance analysis discussed in Section 4.3.6 shows that maximum power output is about 124 watts per m² of module area or $124/.893 = 139$ watts per m² of cell area (module packing efficiency is .893). Cells will produce power between 0.4 and 0.5 volts depending on cell temperature.

4.1.5 Power Collection Wiring

The power is collected in conductors which are routed from the center to the end of the array, then through a trench to the array subfield power conditioning unit. The wiring installation concept within the array is shown in Figure 4-16. The number of conductors in each side of the circuit varies from one at the center of the array to three at the end of the array.

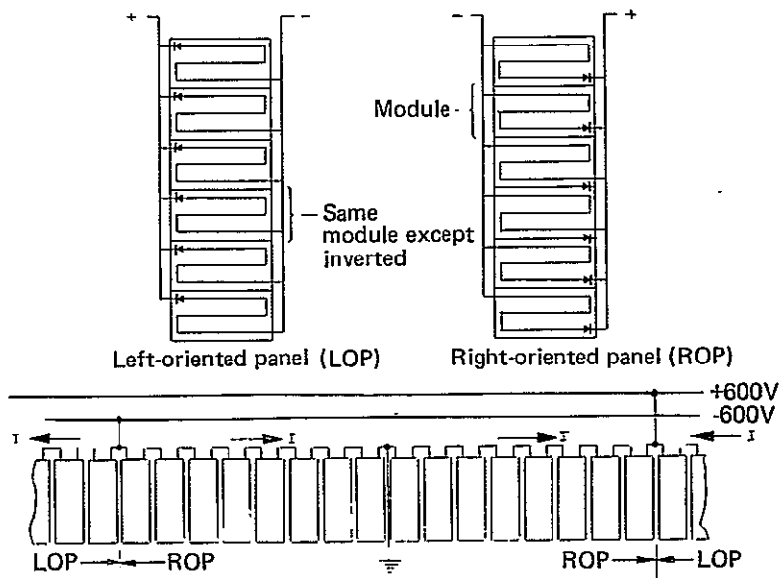


Figure 4-14. Selected Circuit Arrangement

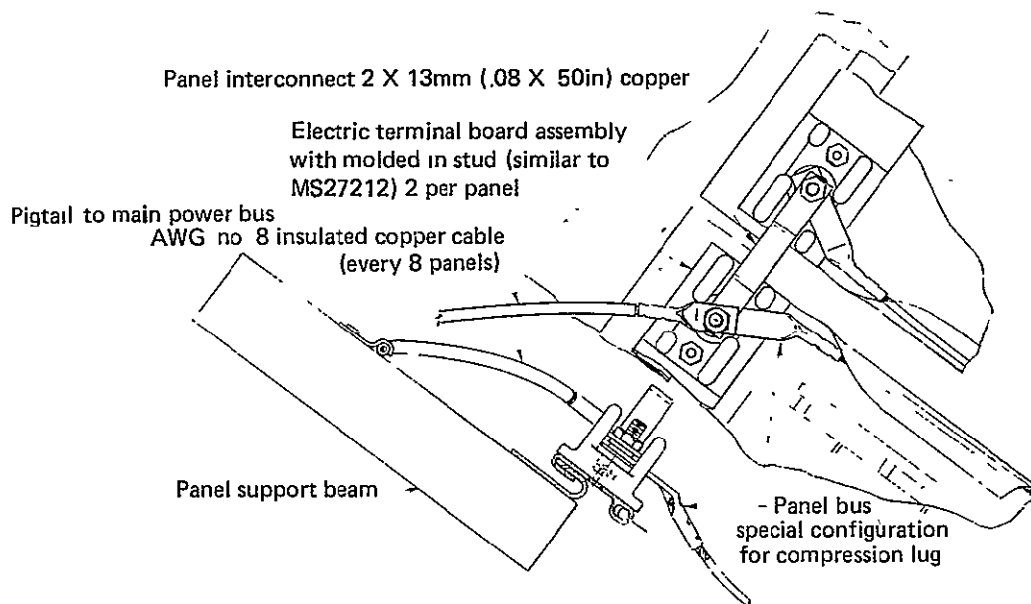


Figure 4-15. Panel Terminal Concept

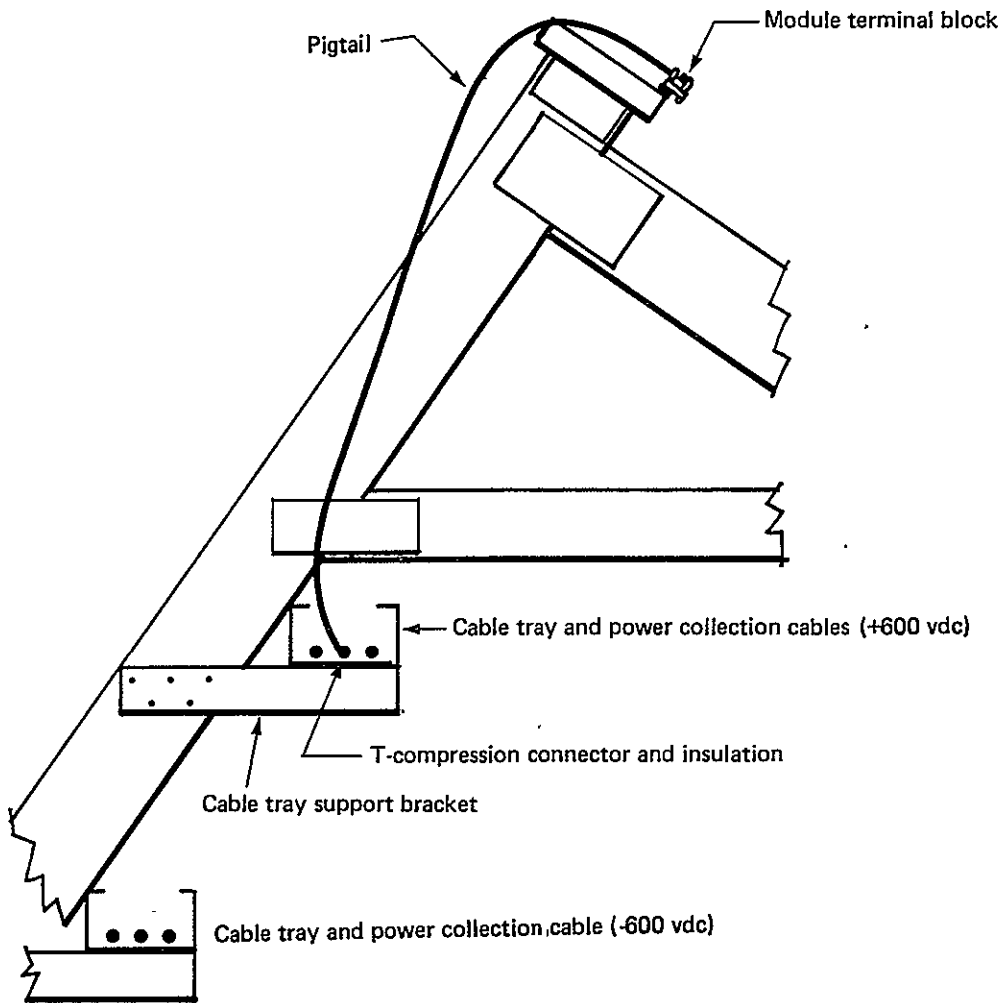


Figure 4-16. Module to Power Collection Wiring Pigtail

4.2 Design Analysis

This section describes the analyses and data that together were used to size and define the selected configuration, including the choice of materials.

4.2.1 Environmental Loads

The major environmental loads of concern in photovoltaic array design are wind, snow and ice, hail, gravity, earthquake, and thermally induced stresses. Limited analyses have been performed in each of these areas for elements of the array where the loading effects might be significant. Environmental effects on each element are summarized in Table 4-III, which suggests the benign environment that the enclosure provides to the support structure and modules. The asterisks indicate areas where analyses were conducted. Stress relief was allowed for in the conceptual design of the panel interconnects. However, thermal stress analysis of the interconnects was not performed, since this is a detailed design problem common to most panel designs. More than one environmental load may contribute to the element sizing so the following discussion is organized around the array elements rather than the individual environments.

4.2.1.1 Enclosure

Wind and Snow Loads

The primary loads on the enclosure are combined wind and internal pressure and combined snow and internal pressure. Enclosure membrane stresses and deflections under the wind condition may be determined as a function of the internal pressure level. Similarly, the deflections under the snow load versus pressure can be found. Specifying maximum deflection under these loading conditions defines the required inflation pressure and the membrane stress.

TABLE 4-III: ENVIRONMENTAL EFFECTS ON ARRAY ELEMENTS

Array Element Environmental Load	Enclosure	Foundation	Support Structure	Module/Panel
Wind	Combines with inflation pressure * to produce maximum stress.	Uplift and drag loads. *	None	None
Snow and Ice	Determines minimum * inflation pressure.	Negligible	None	None
Hail	Impact resistance minimum thickness.	None	None	None
Gravity	Negligible *	Resists wind uplift * loads.	Module reactions, * self weight.	Catenary stresses. *
Earthquake	Negligible	Negligible	Side loads. *	Negligible.
Thermal Stress	None	Sealed expansion joints if needed.	Negligible	Stress relief required in interconnects and wiring.
Dust	Reduced transmittance. * Periodic washing. Filtered inflation air.	None	None	None
Humidity	Occasional external condensation. *	None	None	Possible need to * dehumidify inflation air, prevent condensation.

* Areas where analyses were conducted.

Wind loads for structures are normally computed in compliance with American National Standard ANSI A58.1 (Ref. 3). Paragraph 6.3.5 of this standard states that:

- . No reductions are allowed for direct shielding, and
- . Increases in pressure or suction due to other obstructions must be allowed for.

These very restrictive requirements apparently reflect the reductions already included in the three exposure levels used in the standard: A - centers of large cities, B - suburbs, and C - flat, open country. In the standard, appendix paragraph A6.3.5 allows the following exceptions to the above requirements:

- . The cumulative effect of upwind structures on wind profile transition is permitted.
- . Shielding may reduce loads for some wind directions, but channeling and buffeting may increase pressures. Wind tunnel testing is recommended.
- . Paragraph 6.3.5 does not disallow shielding if increases are also allowed for.

The approach used in this study takes advantage of these exceptions and determines modified wind profiles and enclosure wind loads from test data and analyses. Wind loads for the spherical enclosure, discussed in Section 5.2.1.1, are based on wind tunnel tests performed in another program (Ref. 4). Such directly applicable data is not available for the cylindrical enclosures. However, a reasonably accurate analysis is made possible by the spherical enclosure analysis/test correlations and limited wind tunnel test data on cylinders. A comparison of results of this analysis with a direct application of the ANSI standard is illustrated in Figure 4-17 and shows that enclosure membrane loading, with deformations not accounted for, is larger when using the results of the analysis. For the ANSI standard analysis, the wind profile with the protective fence is assumed to be the Enclosure B (suburban) wind. Large deflections of the enclosure greatly affect the loading. The large difference in load reduction due to deflections for unprotected and protected enclosures is caused by the nonlinear response of the enclosure. Further detail of the wind loads analysis is covered in the following paragraphs.

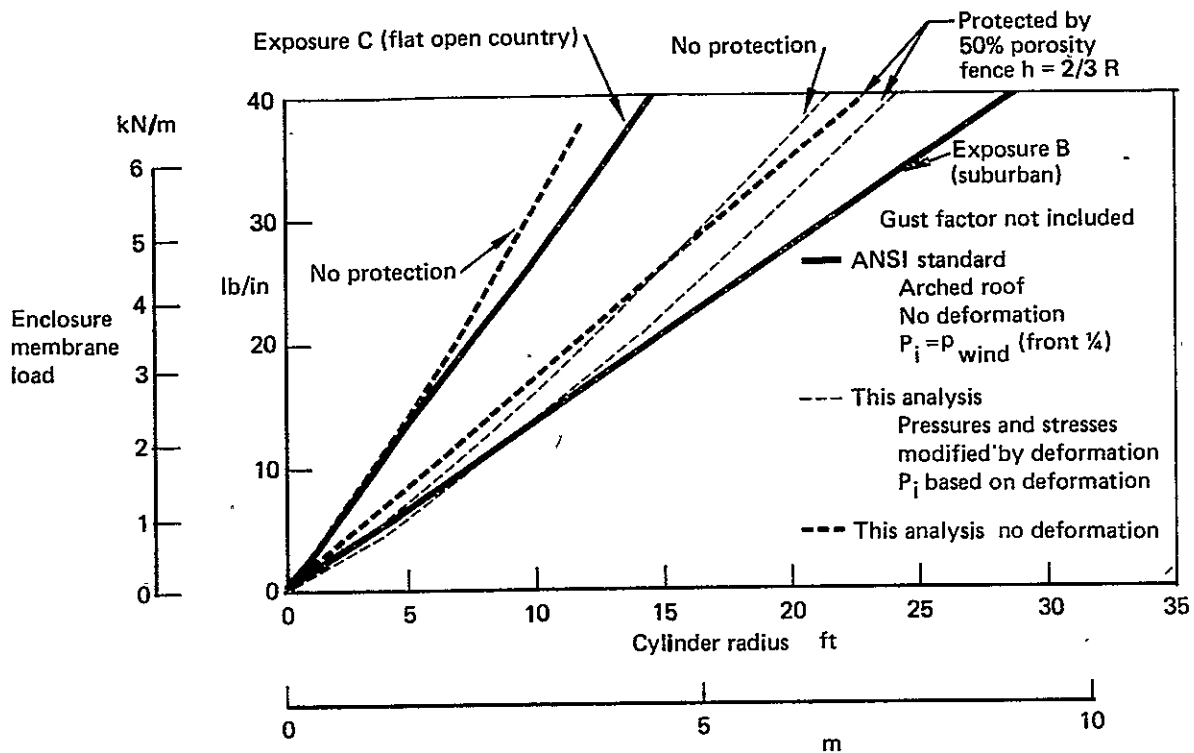


Figure 4-17. Cylindrical Enclosure Loads Comparison - Present Method versus ANSI

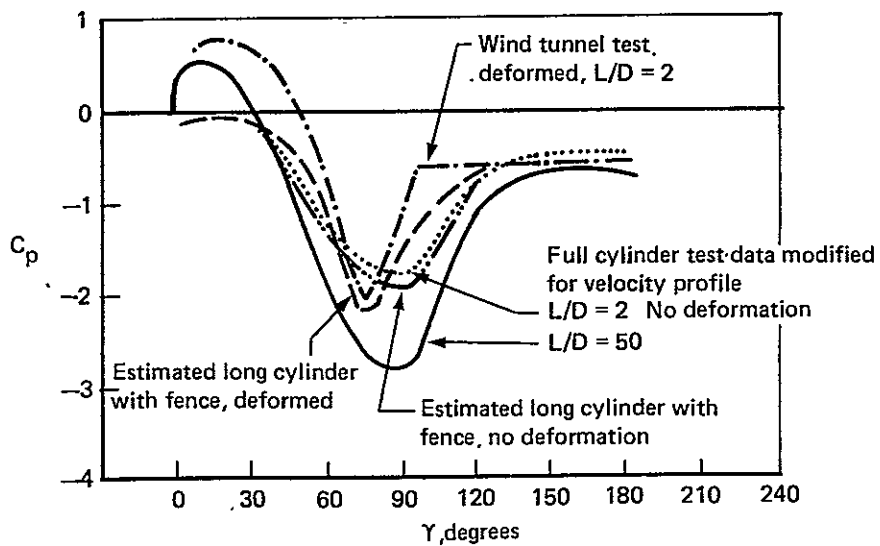


Figure 4-18. Available and Estimated Wind Pressure Distributions for Half-Cylinder Enclosure

Wind Pressure Distributions: Wind pressures on the enclosure surface are defined by:

$$p_w = c_p q_h$$

where c_p is the pressure coefficient and q_h is the dynamic pressure, $1/2\rho V^2$, of the wind at an elevation equal to the height of the enclosure. Figure 4-18 shows c_p around the cylinder surface under various conditions. Limited wind tunnel tests on an inflated half-cylinder, with a length to diameter (L/D) ratio of 2, were reported in Ref. 5. The pressure coefficient values are influenced by the cylinder length to diameter ratio. Wind tunnel test data from Ref. 6 on free standing, complete cylinders, shows that longer cylinders have higher pressure coefficients. These data adapted to the wind velocity profile near the ground are shown in Figure 4-18. The effect of the protective fence on pressure coefficients in Figure 4-18 is estimated from test data on spherical enclosures. Based on all of these considerations, a final estimate of the pressure coefficient for a long deformable cylinder protected by a fence is shown in Figure 4-18. This can be considered only approximate because of the several factors involved and large uncertainties in the absence of directly applicable test data. However, this same approach with the spherical enclosures yielded results in reasonable agreement with subsequent test data.

Enclosure Deflections and Loads: Distortions in the cylindrical enclosure due to wind or snow loads far exceed the limits that would permit use of small deflection shell theory. In one respect, these distortions are beneficial; the radius on the upper portion, where the wind loading is highest, is substantially reduced which decreases the membrane stress. A large deflection solution is available (Ref. 7) but requires more analysis effort than was considered warranted for this study. Instead, an "experimental" analysis was done using a weighted string model as shown in Figure 4-19. A check of predictions using this model compares very favorably (Figure 4-20) with measured deflections from Ref. 5.

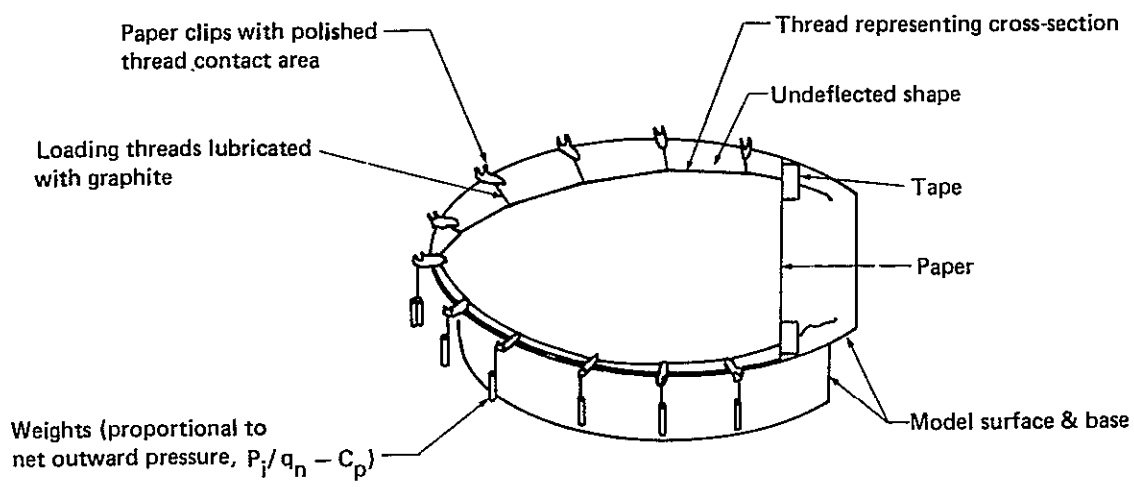
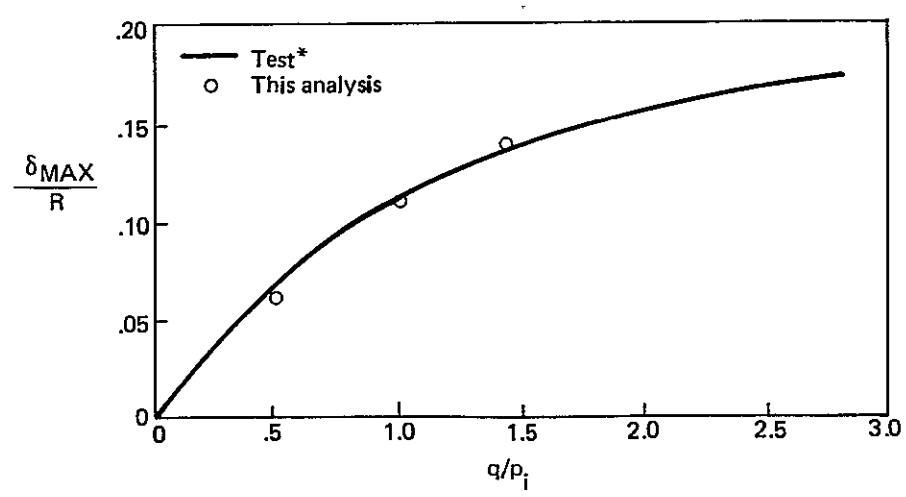


Figure 4-19. Model for Determining Large Deflections of Cylindrical Heliostat Enclosures



*"Zur Windbelastung von Tragluftbauten", Konstruktiver Ingenieurbau Berichte, Nov. 13, 1972

Figure 4-20. Comparison of Maximum Deflections with Test Data

Results of this analysis are given in Figure 4-21 for the wind loads and in Figure 4-22 for snow load. The wind loads analysis shows that the internal pressure controls the relative magnitude of the deflection and membrane loading and that requiring the deflections to be small results in high loading. The snow load does not significantly stress the enclosure, but can cause collapse if the snow load exceeds the internal pressure. By limiting the snow load/internal pressure ratio to 0.75, for Phoenix, with a 240 Pa (5 psf) snow load, P_s , the internal pressure is $P_s/0.75$ or 320 Pa (6.67 psf). The enclosure membrane load with the peak wind condition and this internal pressure is shown in Figure 4-23.

Thickness requirements for two different plastic films are indicated on Figure 4-23. To achieve the desired 4.57 meter (15 foot) radius, it is necessary to use a high strength film like the polyester. Although 0.10 millimeter (0.004 inch) thickness would be sufficient for the wind loads, 0.13 millimeter (0.007 inch) has been selected for added ruggedness.

Hail

The inflated polyester film enclosure is highly resistant to hail damage as was verified by a BEC test program (Ref. 8). The specification in that program required survival without damage of impact by 25 millimeter (1 inch) hailstones at a velocity of 23 meters per second (75 fps). Hailstones at the specification conditions did not penetrate any of the films tested, including a 0.05 millimeter (0.002 inch) thick weatherized polyester. Penetration of this film occurred at a velocity of 34.4 m/s (113 fps). The large hailstones did cause some indentations. Analysis of the environment (Ref. 9) and the effect of the indentations show a specular transmittance loss after 15 years of 0.1 to 1.6% for the average and maximum areal densities of hailstones, respectively. Effect on total transmittance through the thicker polyester enclosures should be negligible, based on these results.

Dust

MIT Lincoln Laboratories (Ref. 10) has measured photovoltaic array performance degradation of 5-10% in five months at Mead, Nebraska and much more in polluted urban areas. The arrays measured are silicone rubber encapsulated

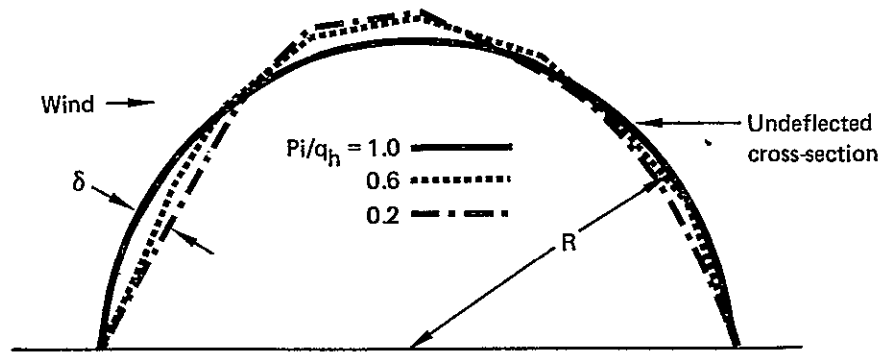
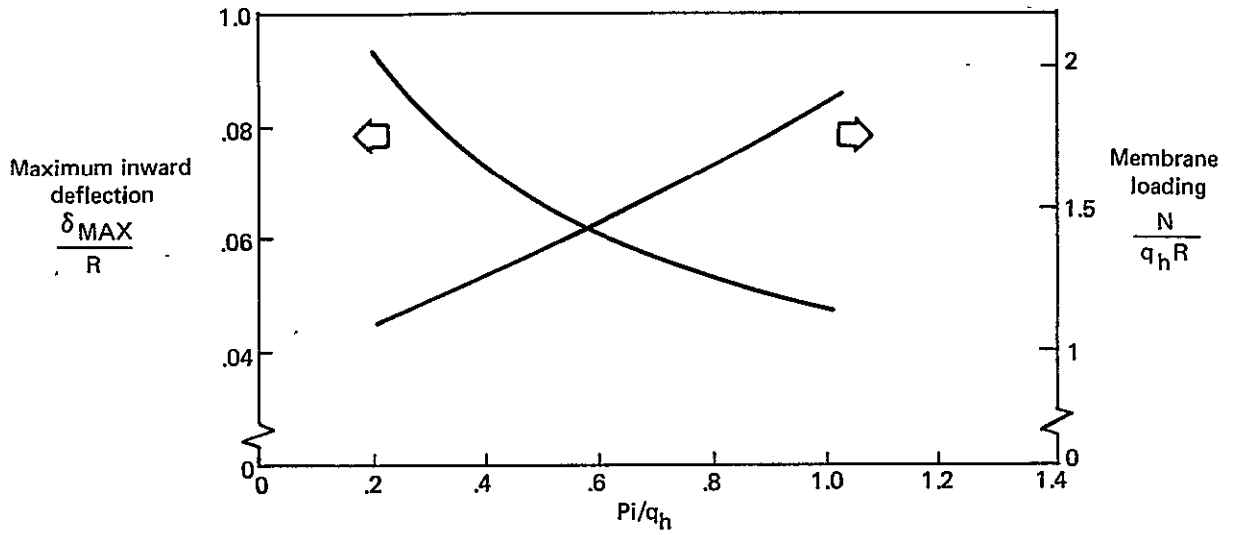


Figure 4-21. Cylindrical Enclosure Deflections and Loads Due to Wind

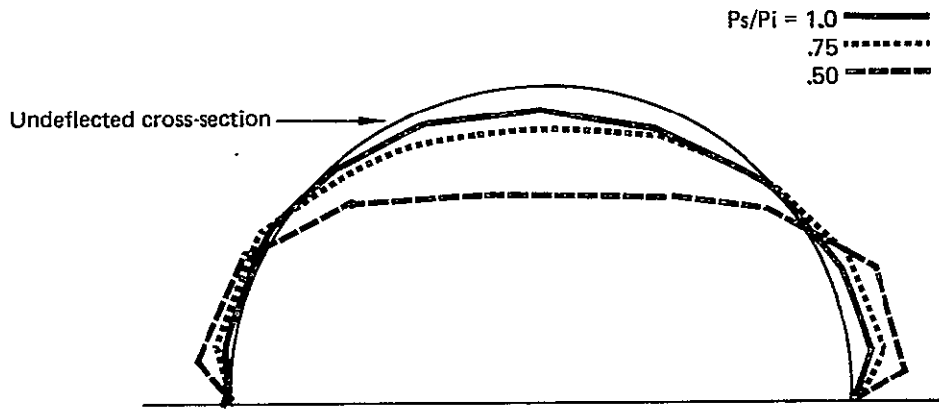
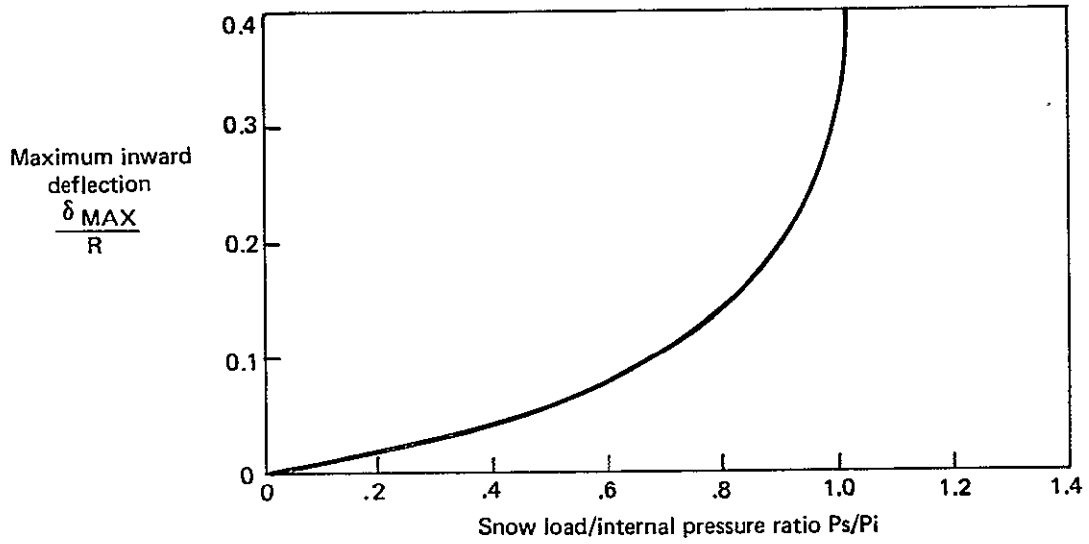


Figure 4-22. Cylindrical Enclosure Deflections and Loads Due to Snow

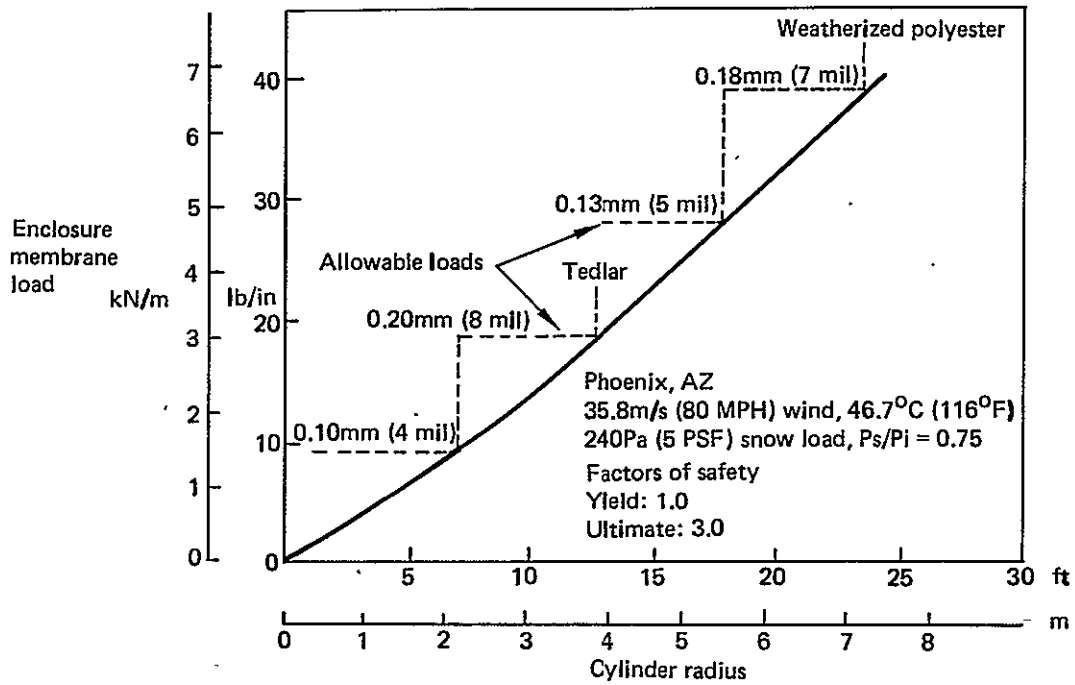


Figure 4-23. Cylindrical Enclosure Sizing

modules. For the air-enclosure concept, dust and dirt will accumulate on the enclosure rather than the modules. The most directly applicable data (Ref. 11) indicates the normal transmittance of Tedlar film is reduced by 5% after one month and 12% after four months of exposure in the Albuquerque area. However, total hemispherical transmittance values for the soiled samples were identical to the values obtained for unexposed material. It was concluded that the dirt scatters, but still transmits the radiation. The scattered light contributes to the effective radiation intensity on the modules, so the performance will not degrade as rapidly as the normal transmittance would indicate. However, it is optimistic to assume zero degradation over long time periods. In this study, frequent enclosure rinsing and occasional washing has been included in maintenance costs, and the transmittance is based on a clean film.

4.2.1.2 Foundation

Uplift on the foundation due to wind and inflation pressure, and drag due to wind are the primary foundation loads. The uplift force is approximately equal to the enclosure membrane force, or 3.94 kilonewton per meter (270 lb/ft) for the 9.1 meter (30 foot) diameter enclosure. Hence, the cross section area of the footings must be about 0.18 m² (1.9 ft²) for 2320 kilogram per cubic meter (145 pcf) concrete. The selected cross section is approximately 0.186 m² (2.0 ft²). Partially burying the footings prevents sliding under drag loads.

In the design concept presented here, it is assumed that the tension strength of the steel attachment plate will prevent major cracks and separation of the concrete under thermal cycling. If the plate is not sufficient for this purpose, expansion joints can be added.

4.2.1.3 Support Structure

The panel support beam reacts to the catenary tension in the flexible panel substrate then transmits the load to the A-frame. The south frame member

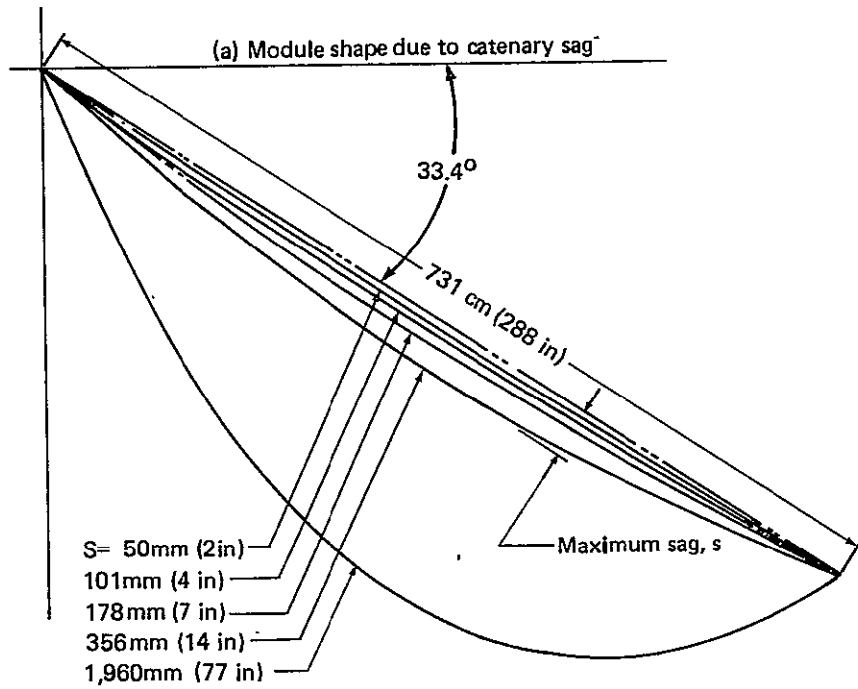
carries most of the load as a compressively loaded column. The amount of load from the catenary tension depends on the sag permitted in the panel, as shown in Figure 4-24. The column-loaded member is the most critical element of the support structure. Critical column loads for this analysis were determined using the method in Ref. 12, with a factor of safety of 2.74 and a column eccentricity of 25 millimeters (1 inch). Permissible catenary forces for three column cross sections are indicated on Figure 4-24. Selecting a 75 by 150 millimeter (3 by 6 inch) wood beam (i.e., a beam that has a 64 by 140 millimeter (2.5 by 5.5 inch dressed section) requires a sag in the panel of at least 16.0 centimeters (6.3 inches).

The catenary force for the 16.0 centimeters (6.3 inch) sag is 298 newtons per meter (1.7 lb/in), which with the dead weight gives a beam stress of 3.45 megapascals (500 psi). This is well below the 11.0 megapascals (1600 psi) permitted for Douglas Fir under long term loading. Deflection of the 50 by 200 millimeter (2 by 8 inch) panel support beam due to the 16.0 centimeter (6.3 inch) sag is 0.81 centimeters (0.32 inch).

Bracing in every fifth bay provides shear stiffness along the array structure. With crossed diagonals made from 50 by 150 millimeters (2 by 6 inch) wood, the structure will carry a 0.25 g lateral acceleration.

4.2.1.4 Module/Panel

Stress in the plastic film substrate for the module/panel may be found by dividing the catenary force by the film thickness: i.e., 298 N/m divided by 0.13 mm or 1.68 MPa (243 psi). Since this is well below the creep limit for polyester, long term stresses should not be a problem. Strain in the film at this stress is only about 5×10^{-4} cm/cm (inches/inch) which should be accommodated easily by stress-relieved interconnects and a pliable adhesive for cell attachment.



b) Catenary force versus module sag

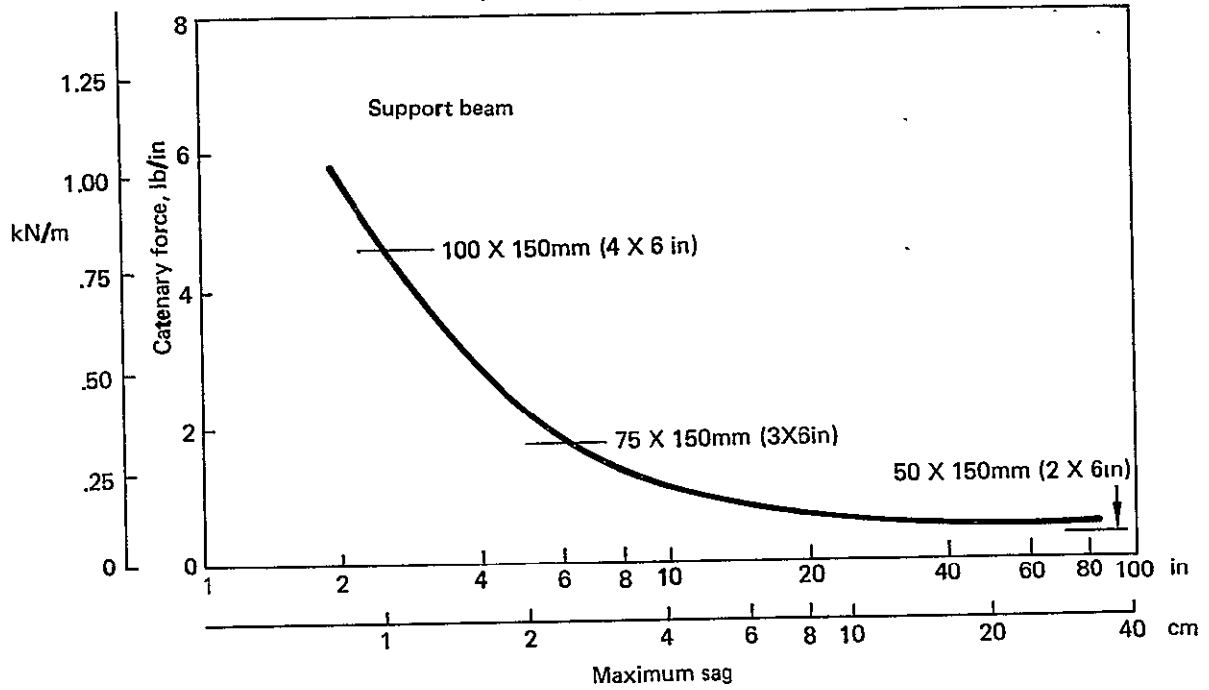


Figure 4-24. Module Catenary Geometry and Forces

With the solar cells bare inside the air-enclosure, the humidity within the enclosure must be controlled to prevent condensation and, perhaps, prevent exceeding an upper limit relative humidity of 50-90%. Moisture control is needed to limit corrosion of solar cell coatings, contacts and interconnects. Engineering data available is not sufficient to specify a humidity limit. However, in our judgement (and of others based on statements expressed at the Ninth Low-Cost Solar Array Project Integration Meeting, April 1978), a well designed module using materials that are not susceptible to moisture should survive indefinitely as long as water does not condense on it.

Review of the SOLMET data for Phoenix reveals that 100% humidity will occur occasionally on winter mornings. To maintain a constant pressure in the enclosure, heated air will vent out during the sunlit morning hours. As the air cools during the afternoon and night, the pressurization system will pump air into the enclosure. Most of the returning air will enter during the afternoon when humidity is low, but a steady flow of air is required throughout the night. Thus, it is possible that some air at 100% relative humidity (based on external ambient temperature) will enter the enclosure. If thoroughly mixed with warmer, dryer air in the enclosure, this should be no problem. However, with discrete pressurization locations, local areas of condensation are possible. A dehumidifier in line with the pressurization system would prevent this from occurring. Cost of this equipment is not included, but previous studies show the effect on overall costs is negligible.

4.2.2 Electrical Design

Goals in the electrical portion of the array conceptual design included (1) selection of electrical parameters that give efficient power output; and (2) a module and array configuration which would be both fault- and shadow-tolerant. The design analyses were simple hand calculations. A representative I-V curve was constructed to match the JPL supplied solar cell characteristics (see Section 3.2.1.1). Using this curve, the response of the power output to shadowing was determined for various module circuit

designs. The effect of failed cells, modules, and panels were examined also. The final module configuration is based on a compromise of the efficiency, shadowing and failure effects.

4.2.2.1 Cell Characteristics

The assumed solar cell I-V curve is shown in Figure 4-25. The maximum power point at 28°C was defined by the specified efficiency and an arbitrarily selected voltage of 0.5 volts. A fill factor of 0.75 was used to help define the curve shape. The curves as modified by the JPL temperature sensitivity equations are shown in Figure 4-25 for a NOCT of 28°C and for 67°C, which is representative of enclosed array temperatures.

4.2.2.2 Shadowing

Shadows may be cast on the arrays by adjacent arrays, snow, personnel, enclosure cleaning equipment, etc. Except for the adjacent array shadowing, these will be infrequent and irregular. The modules must survive, but need not perform as efficiently as possible with this type of shadowing. However, the adjacent array shadowing will occur twice daily during fall and winter months and can have a significant impact on total energy production.

Module shadowing by the adjacent array was determined for the winter solstice as a function of spacing between arrays. Figure 4-26 shows that a spacing less than 15.2 meters (50 feet), i.e., 6.1 meters (20 feet) clear plus 9.1 meters (30 feet) diameter enclosure, quickly increases shadowing. The 15.2 meter (50 foot) spacing was selected as a compromise between land and wiring requirements and moderate winter shadowing. Figure 4-27 shows the seasonal variation of the module shadowing for this spacing. Shadowing is no longer present at the equinoxes.

The effect of shadows on module electrical output was determined with the approximate analysis method described in Ref. 13. For solar cell strings connected both in parallel and series, this method reduces current in proportion to the maximum extent of shadowing across the array. If the

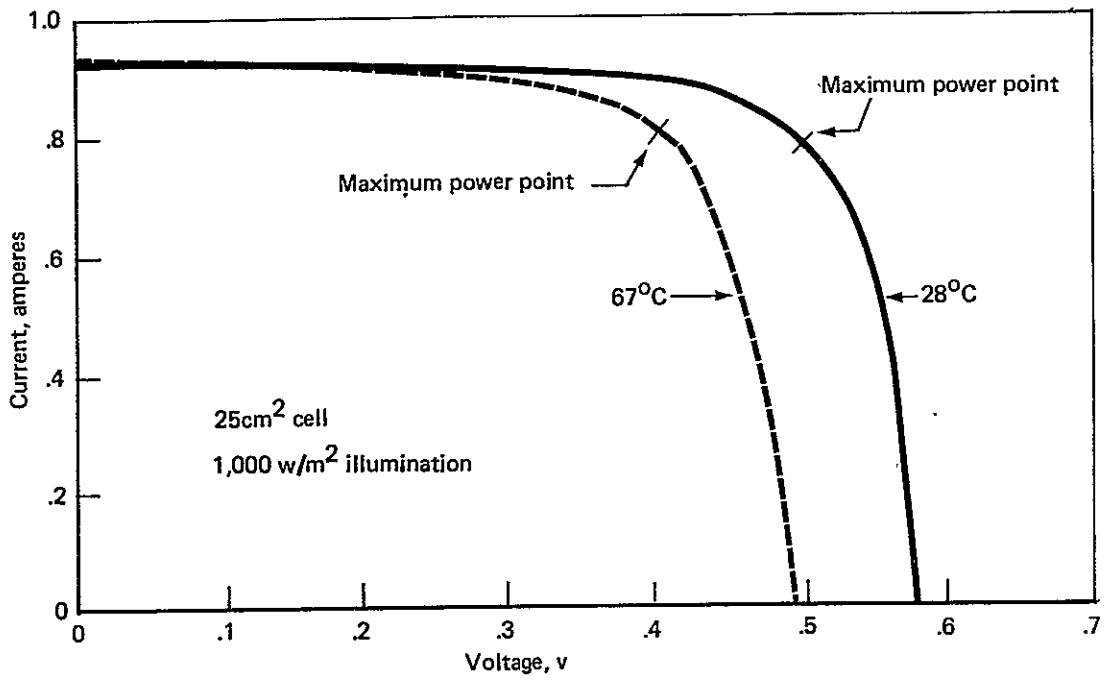


Figure 4-25. Assumed Solar Cell Characteristics

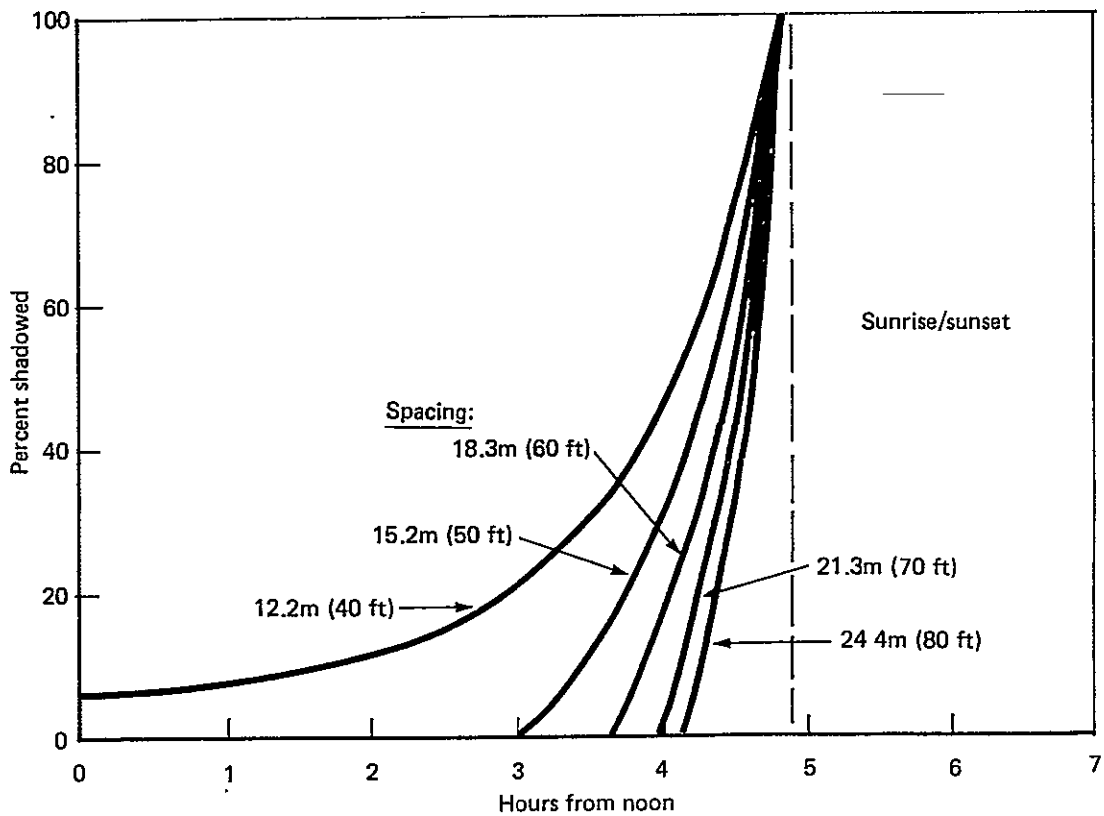


Figure 4-26. Effect of Spacing on Shadowing at Winter Solstice

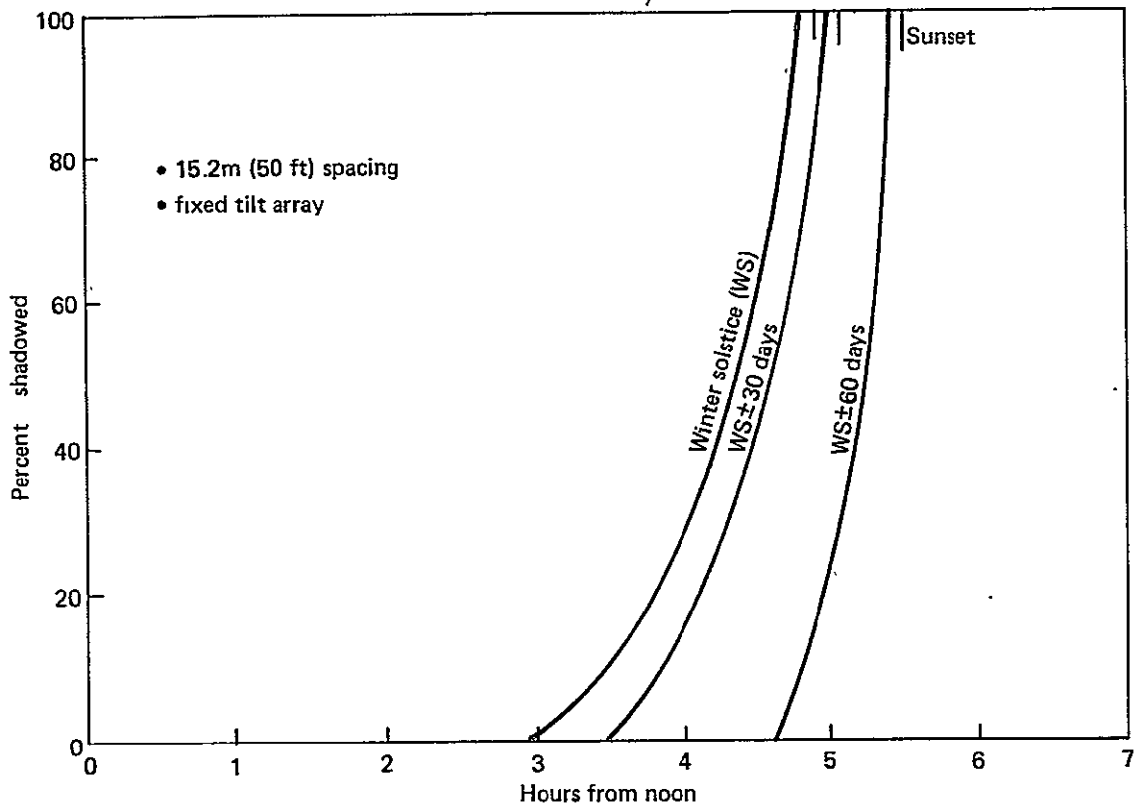


Figure 4-27. Seasonal Effect on Shadowing

shadow extends completely across, the current drops to zero; with a shunt diode around the shadowed portion, the voltage drops proportional to the amount of the string bypassed.

Solar cell string layouts analyzed included single-pass and multiple-pass vertical and horizontal rows, and a varying number of modules per panel. A Winter Solstice Shadow Factor (ratio of total daily energy output with and without shadowing) was calculated for each string layout. Figure 4-28 shows a typical power output curve as affected by shadowing. Results for horizontal and vertical strings are shown in Figure 4-29. The vertical string shadow factor is based on using a large number of bypass diodes. Otherwise, the effects of the series shadowing would be much worse. Single horizontal strings are subjected to parallel shadowing; bypass diodes are not required, but blocking diodes are needed to prevent reverse biasing of shadowed cells. Parallel shadowing of multiple pass horizontal strings becomes series shadowing when the unshadowed remainder of the lowest pass of the string can no longer carry the current. Bypass diodes around each pass are required unless the entire module is already removed from the circuit by the blocking diode. While the vertical string is most convenient for the selected panel dimensions, the horizontal layout is selected to minimize the bypass diode requirements.

Figure 4-29 implies a large number of modules per panel is desirable. However, power losses due to the blocking diode on each module must be considered. Figure 4-30 shows a rough approximation of annual energy output reduction, including the blocking diodes losses. The curve including both shadow and diode losses is quite flat and shows that two to eight three-pass modules per panel would be acceptable.

4.2.2.3 Cell Failures

While the reliability of the cells and interconnects is not defined, failures are likely to be frequent enough to require a design tolerant to a small percentage of faulty components. Figure 4-31 shows the panel power

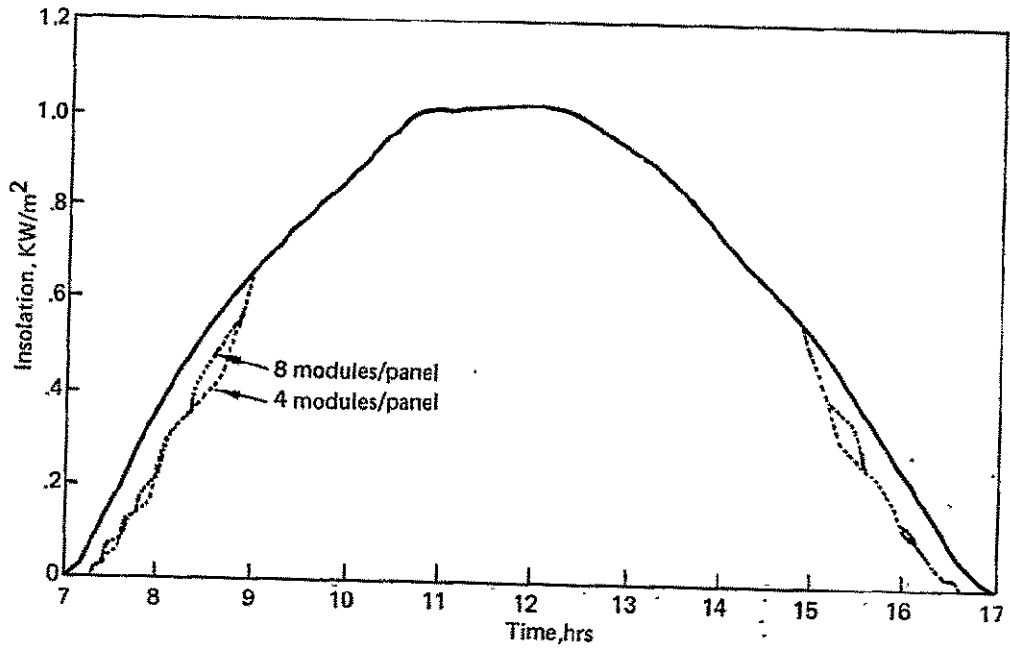


Figure 4-28. Hourly Insolation

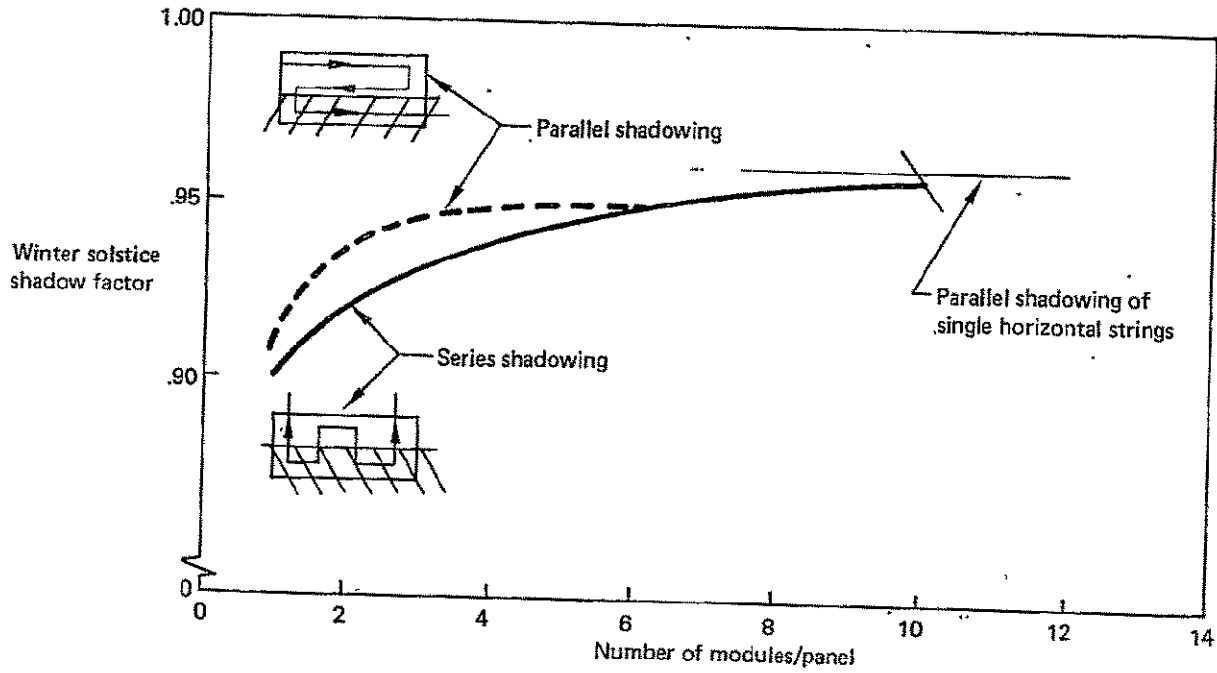


Figure 4-29. Effect of Number of Modules on Shadowing Losses

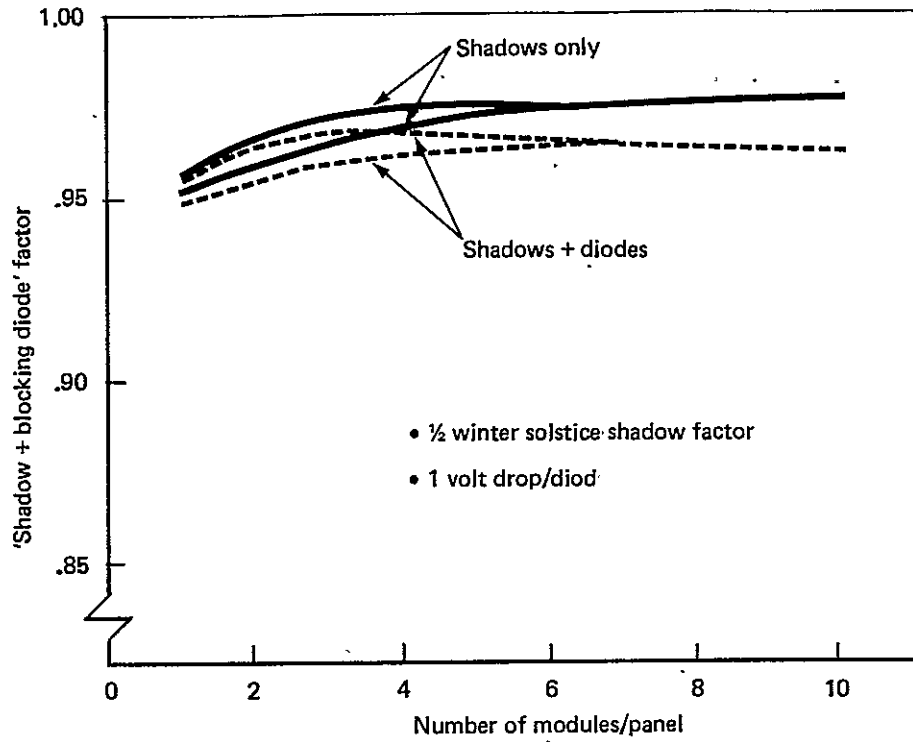


Figure 4-30. Approximate Effect of Shadowing & Blocking Diode Losses

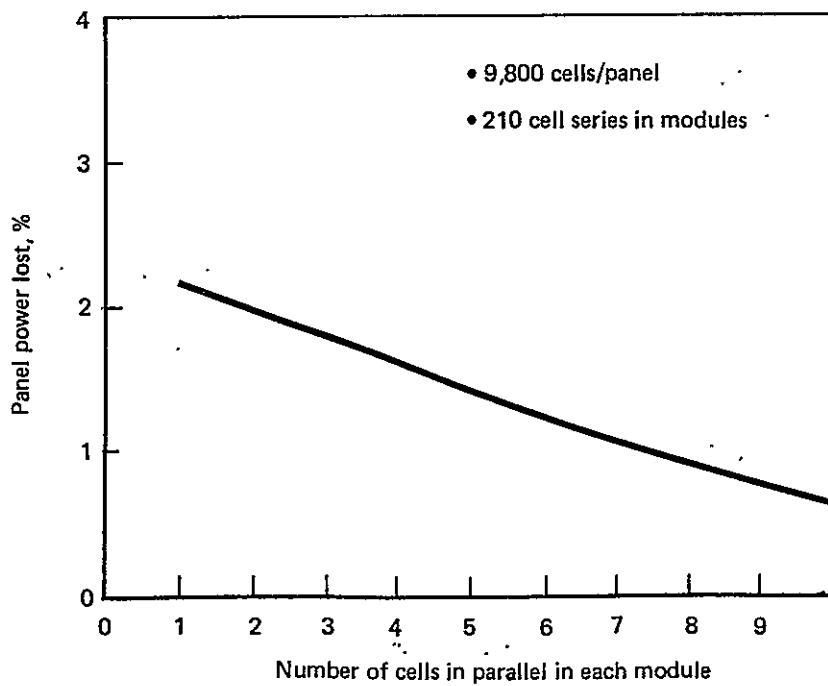


Figure 4-31. Effect of Number of Parallel Cells on Power Loss Due to a Cell Fail

lost due to a single failed cell as a function of the number of cells in parallel. Constraints in this analysis are shown on the figure. The curve shows that the number of cells in parallel should be large enough to minimize the effect of failed cells. However, a large number of cells in parallel results in high current and I^2R losses, or heavy busses on the panel. The latter is inconvenient for the selected lightweight panel concept.

4.2.2.4 Panel Failures

Panels are connected in series to supply power at the system voltage. Panels in the series that have inactive modules will be forced to carry the current through a reduced number of modules. Module blocking diodes will shut down the remainder of the panel if module current becomes too high. In turn, this will terminate power output of the entire series string of panels. Other problems, such as disconnected bus wires or shorts to ground, could cause the same result.

If the bypass diode is provided for each panel, blocking of the entire panel series by overloaded modules of a single panel is prevented.—The remaining panels of the series that are operating must be capable of producing power at the system voltage. That is, the open circuit voltage of this operating panel string must exceed the system voltage. Otherwise, the string will act as a series of rectifier diodes draining power from the system. The amount of power lost (neglecting the power drain) as a function of the number of panels in series is shown in Figure 4-32. For the assumed solar cell I-V characteristics, at least six panels must be in the series for the series to continue producing power when one panel fails. As more panels are added, the voltage shift of each operating panel off the maximum power point becomes less pronounced and the power loss decreases. From Figure 4-32, it appears desirable to have either one panel per series or perhaps eight or more panels per series.

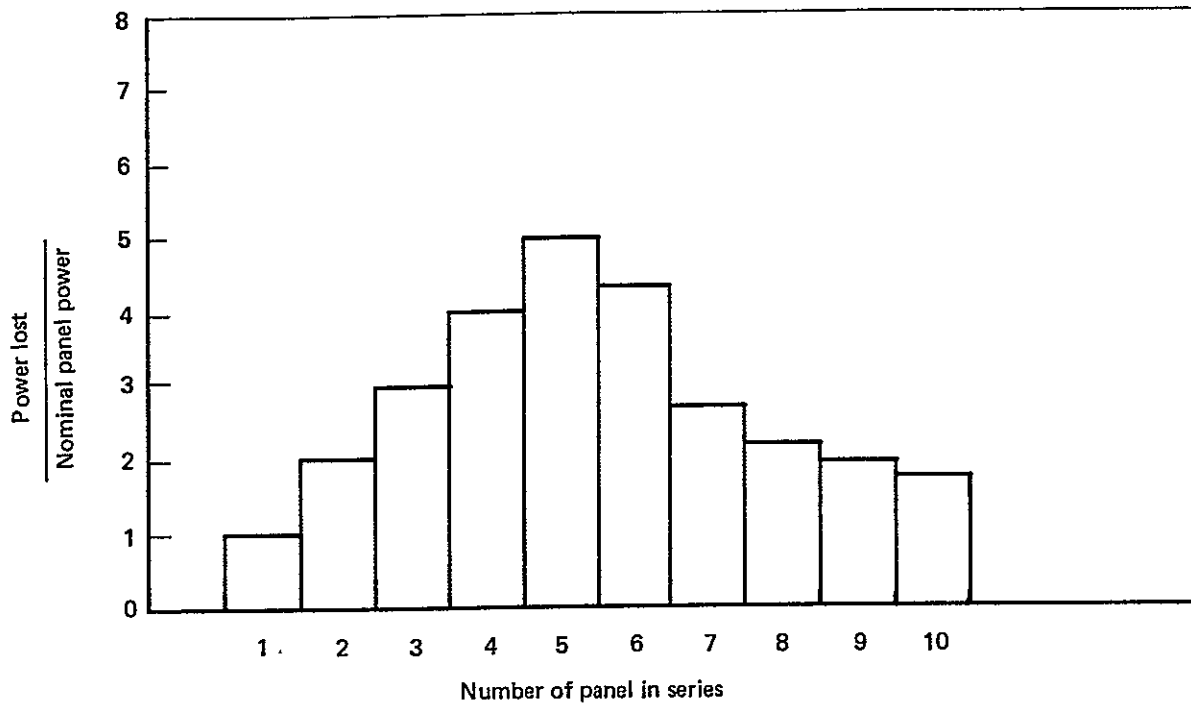


Figure 4-32. Effect of a Panel Failure on System Power Loss

4.2.2.5 Rationale for Selected Configuration

In summary, based on the preceding, these factors must be considered in the design:

- 1) Horizontal string layout to avoid large numbers of bypass diodes,
- 2) Two to eight modules per panel to minimize shadowing and blocking diode losses,
- 3) Several cells in parallel to minimize cell failure effects,
- 4) Either one or eight or more panels in series to produce system voltage, and
- 5) Panels in series should have bypass diodes.

In the design concept being evaluated, a single panel having enough cells in parallel to satisfy 3) above is large enough to produce the system voltage. The approximate shadow factor analysis, Figure 4-30, indicated roughly one percent lower output for the one module per panel configuration, but the analysis is probably not accurate enough for this to be a major consideration. However, other factors tend to favor a configuration with multiple modules per panel and multiple panels in series. Among these are the reduced number of pigtails connected to the power collection wiring, reduced voltage gradients in the panel, and greater fabrication convenience with the smaller modules. From these considerations, a design with eight cells in parallel, six modules per panel, and eight panels in series was selected.

4.3 Thermal/Performance Analysis

Enclosing the photovoltaic arrays leads to higher module temperatures. The increase in temperature decreases the module efficiency. Extremely high temperature might damage the modules, or require special materials and processes. This analysis investigates the array temperature response by modeling the array, enclosure and surrounding environment. The model provides thermal as well as performance data. Cooling concepts are investigated as possible means of reducing array temperatures.

4.3.1 Ambient Environment

4.3.1.1 Seasonal and Extreme Environments

Insolation data for Phoenix, Arizona on a SOLMET tape provided the solar inputs to the thermal and performance analysis. The SOLMET tape for Phoenix provides insolation and weather data from 1952. Due to the expense of reading and printing the information on the SOLMET tape, data for the first year on the tape was extracted and adjusted to represent average and extreme temperature conditions.

The hourly insolation values for the solstices and equinoxes served as the seasonal insolation profiles. If the solstice or equinox day wasn't clear, insolation data from a clear day near the solstice or equinox day was used. The horizontal hourly total insolation values were converted to hourly insolation values on a tilted surface using the method in Ref. 14.

A seasonal temperature profile was determined by averaging the mid-month clear day hourly temperature values for the three months of the season. Hot and cold day temperature/time curves were determined by adjusting the average temperature curve to provide the extreme maximum and minimum temperatures for a 20 year period at Phoenix, as given in Ref. 15.

The analysis was performed using a wind velocity of 2 meters/second. The ground temperature was assumed to be ambient temperature. From Ref. 16, the sky temperature was 6.1°C (11°F) lower than ambient, an average value given in Ref. 16.

4.3.1.2 Nominal Environment

The nominal operating cell temperature (NOCT) was determined by performing a steady-state thermal analysis with the NOCT environmental conditions defined by JPL. These conditions, as given in Ref. 17, are:

- Insolation = 800 W/m^2
- Air Temperature = 20°C
- Wind Average Velocity = 1 m/s

For this analysis, the ground temperature is assumed equal to the air temperature, and the sky temperature is assumed to be 6.1°C (11°F) lower than the air temperature. Wind velocity was varied between zero and 2 m/s.

4.3.2 Cooling System Evaluation

4.3.2.1 Cooling Concepts

After a thorough examination of cooling systems for the enclosure, three candidate cooling concepts emerged. Two passive and one conventional active cooling systems were selected for further evaluation. Although the two passive systems cool without the burden of parasitic power losses, the conventional active cooling system, which has parasitic losses, ensures adequate cooling.

4.3.2.2 Cooling System Thermal Performance

Externally Vented Duct

The passive cooling concept shown in Figure 4-33 consists of an externally vented duct running along the array. The array is cooled by air flowing through the duct due to a natural draft of the heated air and a forced draft due to the wind suction over the top of the enclosure. Fins were placed on the array to aid in heat pickup by the forced draft. The duct is not tall enough to create a natural draft as in a cooling tower. The forced draft cooling due to wind is the primary driving force. Figure 4-34 shows the array temperatures for a range of wind speeds.

For the winds experienced in the Phoenix, Arizona area, cooling by the externally vented duct doesn't provide enough reduction in array temperature or increase in array efficiency to justify the addition of the duct. A preliminary estimate of uncooled array cost was \$1530/linear meter (\$465/linear foot). Assuming ducts with fins at 75 mm (3 inch) spacing, the array

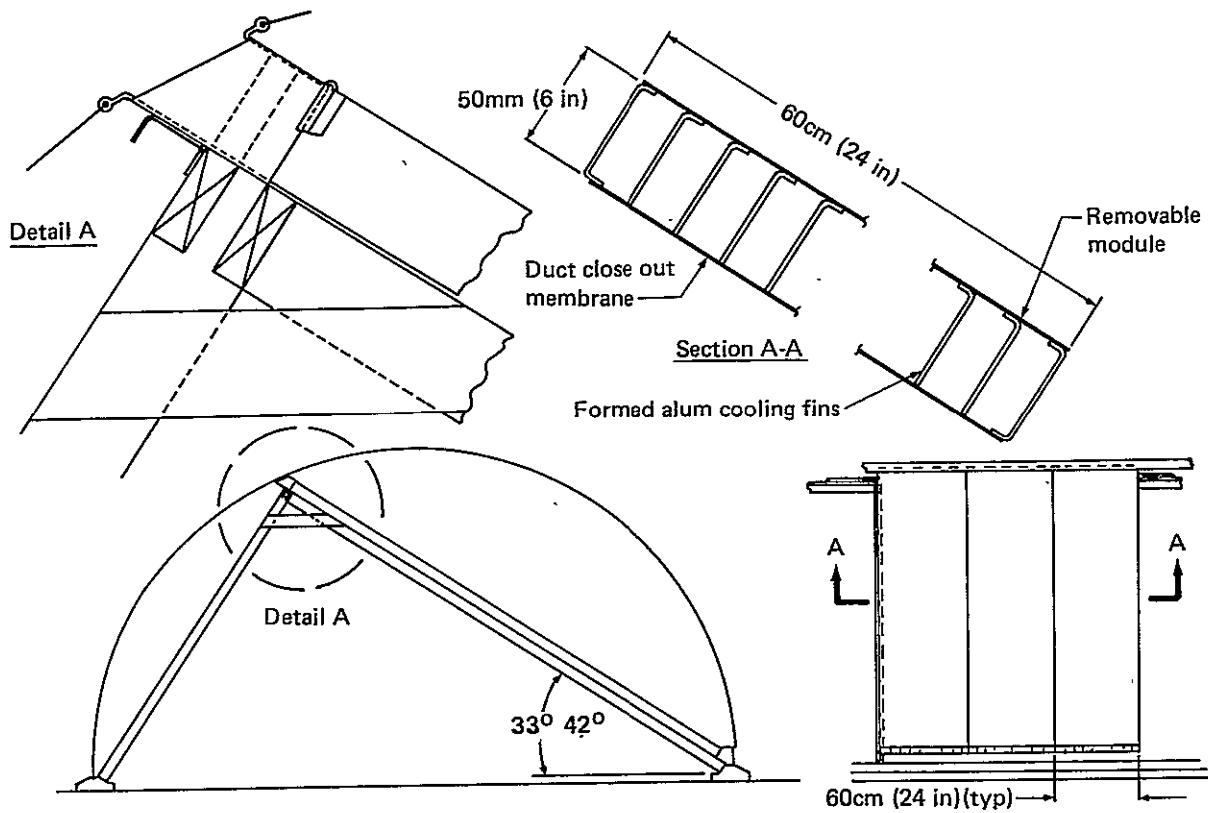


Figure 4-33. Externally Vented Duct Configuration

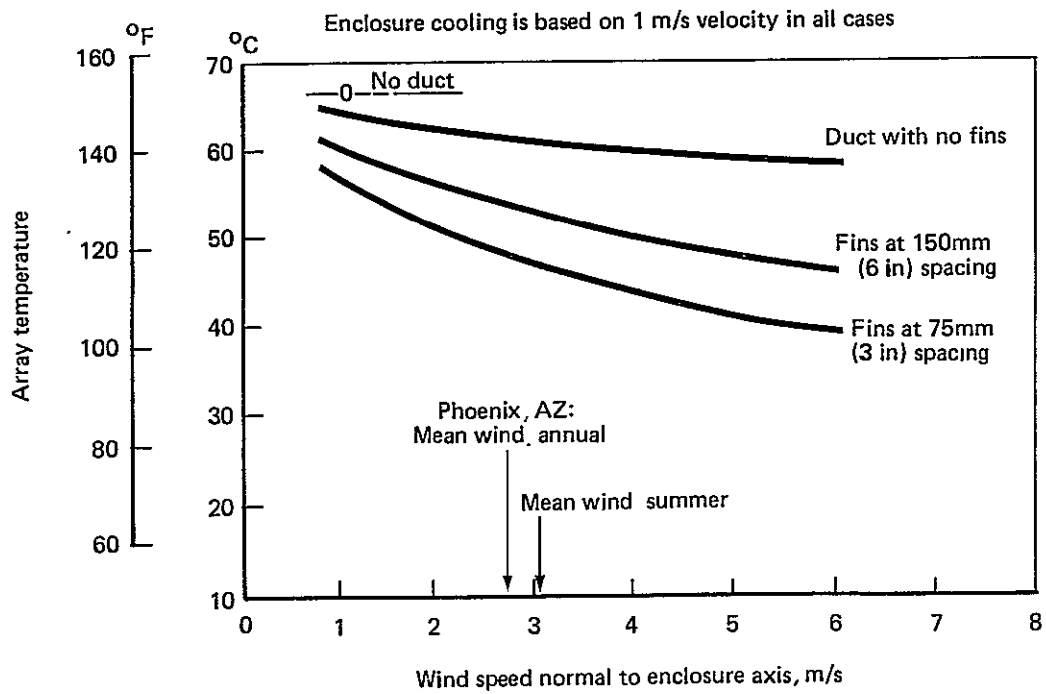


Figure 4-34. Effect of an Externally Vented Duct on Array Temperatures

is cooled from 67°C (152°F) to 49°C (120°F). The increased efficiency gives a savings of \$130/linear meter (\$39.50/linear foot) in reduced array area, but the additional cost of the externally vented duct is \$144/linear meter (\$43.90/linear foot). Hence, there is no net cost reduction with duct cooling.

Thermosyphon

A hand analysis described in the following paragraphs determined the feasibility of a thermosyphon cooling system. Heat absorbing tubes on the back of the array, an external finned tube heat exchanger, and an insulated return loop constitute the thermosyphon system. Buoyancy of the heated water provides the driving force to circulate the coolant.

Three main equations were generated to describe the cooling system. The first accounts for the thermosyphon and natural convection effects, the second takes into account the heat transfer between the tube wall and water, and the last equation describes the heat transfer of the heat exchanger on top of the array.

The basic solution procedure is to solve the first two equations for T_m and m , for given values of T_{array} and $Q_{removed}$. These values are then used in the last equation to determine the length of the heat exchanger.

Assumptions were made to simplify the analysis. There is little thermal resistance between the tube wall and the array, so the temperature of the tube wall is assumed to be the array temperature. (The majority of the resistance is the water in the tube.) When evaluating the friction effects inside the tube, it was assumed the effects due to elbows and bends are negligible.

The first equation was derived from the analysis in Ref. 18. Basically, the thermosyphon head is set equal to the friction head. The flow rate is

then:

$$m^2 = \frac{Q_{removed} d^4 (2AT_m + B)(h_2 - h_1)}{5.65 \times 10^{-6} L v_m (2C_p)} \quad (A)$$

where:

$$A = 2.5 \times 10^{-6}$$

$$B = 5.83 \times 10^{-5}$$

d = tube diameter, feet

Q_{removed} = heat removed from array, BTU/h

T_m = mean water temperature

h_2-h_1 = vertical height of array, feet

L = length of tube being tested, feet

ν_m = mean kinematic viscosity, ft^2

C_p = specific heat, $\text{BTU}/\text{lb}_m \text{ } ^\circ\text{F}$

m = water mass flow rate, lb/h

The heat transfer coefficient in the second equation uses a Nusselt number from Ref. 19.

$$Q_{\text{removed}} = A_{\text{tube}} (1.75) \left(\frac{\mu_B}{\mu_w} \right)^{0.14} \left(\frac{K}{d} \right) \left[\text{Gz} + 0.0083 (\text{GrPr})^{0.75} \right]^{1/3} \cdot (T_{\text{tube}} - T_m) \quad (\text{B})$$

where:

K = thermal conductivity $\text{BTU}/\text{h}\cdot\text{ft}\cdot^\circ\text{F}$

μ_B, μ_w = absolute viscosity, bulk or wall, $\text{lb}/\text{ft}\cdot\text{sec}$

Gz = Graetz number

Gr = Grashof number

Pr = Prandtl number

Free and forced convection are combined, and a total heat exchanger surface area is calculated for the last equation:

$$T_{\text{tube}} = \frac{Q_{\text{removed}}}{\phi_{\text{fin}} h_{\text{total}} A_{\text{total}}} + T_{\text{ambient}} \quad (\text{C})$$

where:

ϕ_{fin} = fin efficiency

For a given T_{array} and Q_{removed} , m and T_m fall out of equations A and B. The length of the heat exchanger required for heat rejection outside the enclosure is found from equation C. Figure 4-35 shows the amount of heat that must be removed to reduce array temperature. With the thermosyphon tubes running up and down the panels, spaced every 30.5 centimeters (1 foot) along the array width (horizontal direction), the required length of

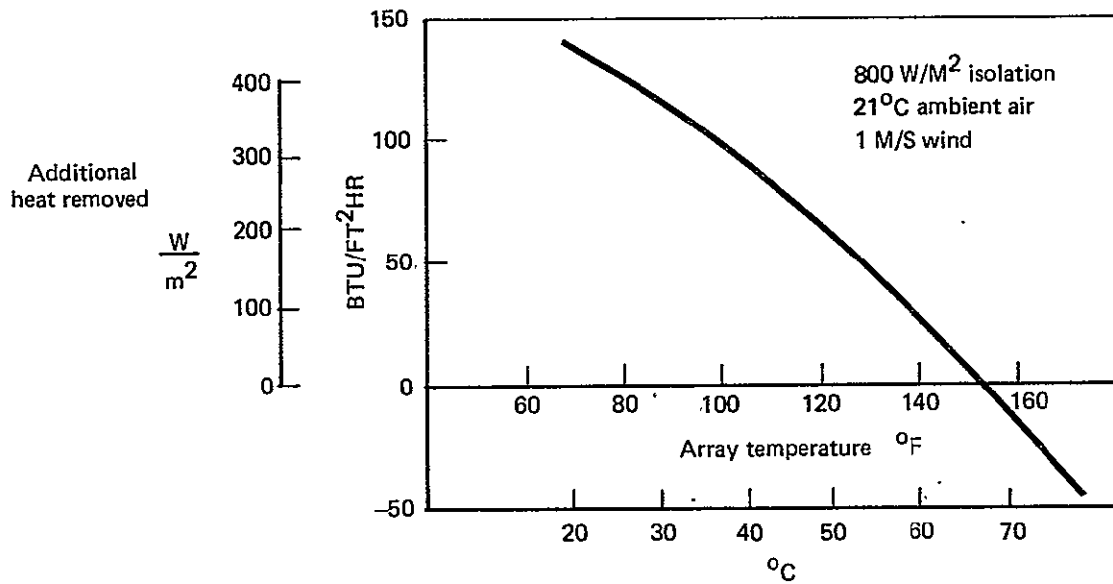


Figure 4-35. Cooling Required for Reduced Array Temperatures

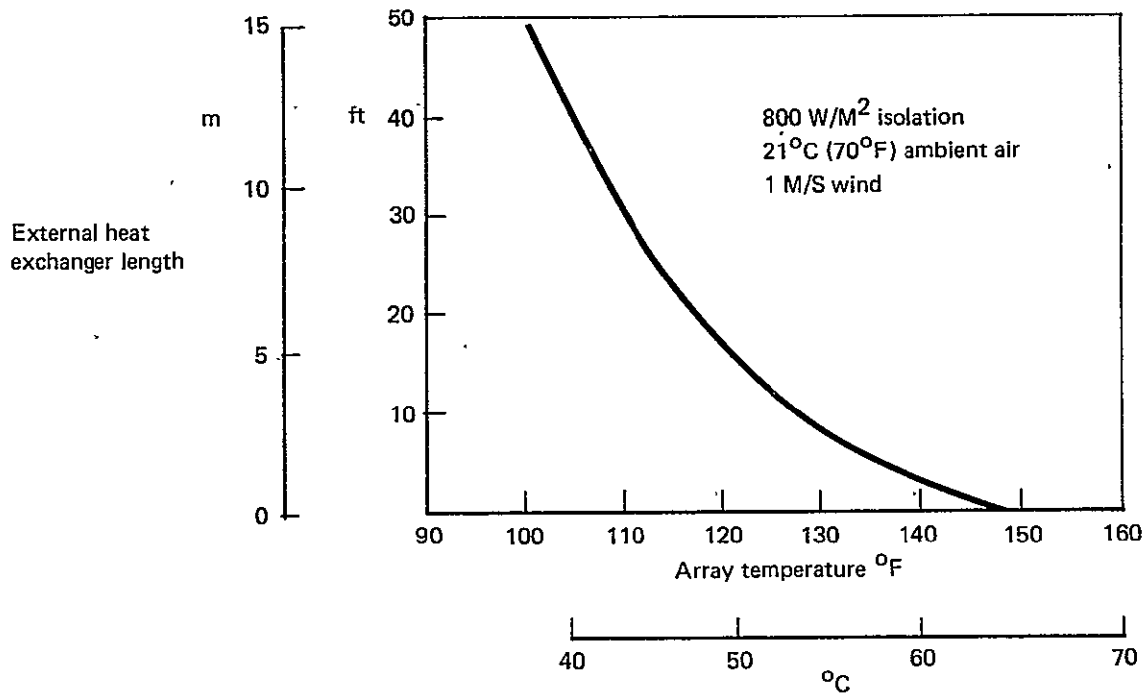


Figure 4-36. Effect of Heat Exchanger Length on Array Temperature - Thermosyphon Cooling

external finned tube heat exchanger is defined in Figure 4-36. The external heat exchanger tube must be 4.8 meters (16 feet) long to cool the array to 49°C (120°F). This amount of heat exchanger located at every foot along the array does not appear to be a practical design.

Active Cooling System

The active cooling system comprises a compressor, condenser, and expansion valve. A cooling fluid heated by the array would run through the compressor and on to the condenser. The fluid then proceeds through an expansion valve before returning to the array. The condenser is located outside the enclosure so it can exchange heat with the ambient air.

The major concern with an active cooling system is the parasitic power losses, principally the compressor. Figure 4-37 shows the compressor power loss for array cooling. As is seen from that figure, cooling the array with an active cooling system requires more power than is gained from the higher efficiency of cooler solar cells.

4.3.2.3 Conclusions

The passive cooling systems add complexity while displaying only modest cooling capacities. The cost analysis for the most inexpensive of the three cooling concepts, the externally vented duct, yielded no net cost reduction. The thermosyphon requires more extensive equipment for the same amount of cooling, so it will not yield a net cost reduction either. The active cooling uses more power than is gained by the cooling and, hence, it has no cost benefit. On the basis of this analysis, it is not cost effective to cool the array.

4.3.3 Thermal Performance Model Description

4.3.3.1 Analysis Model

The thermal/performance model represents the heat transfer and temperature-related electrical output of the array. Temperatures are calculated for

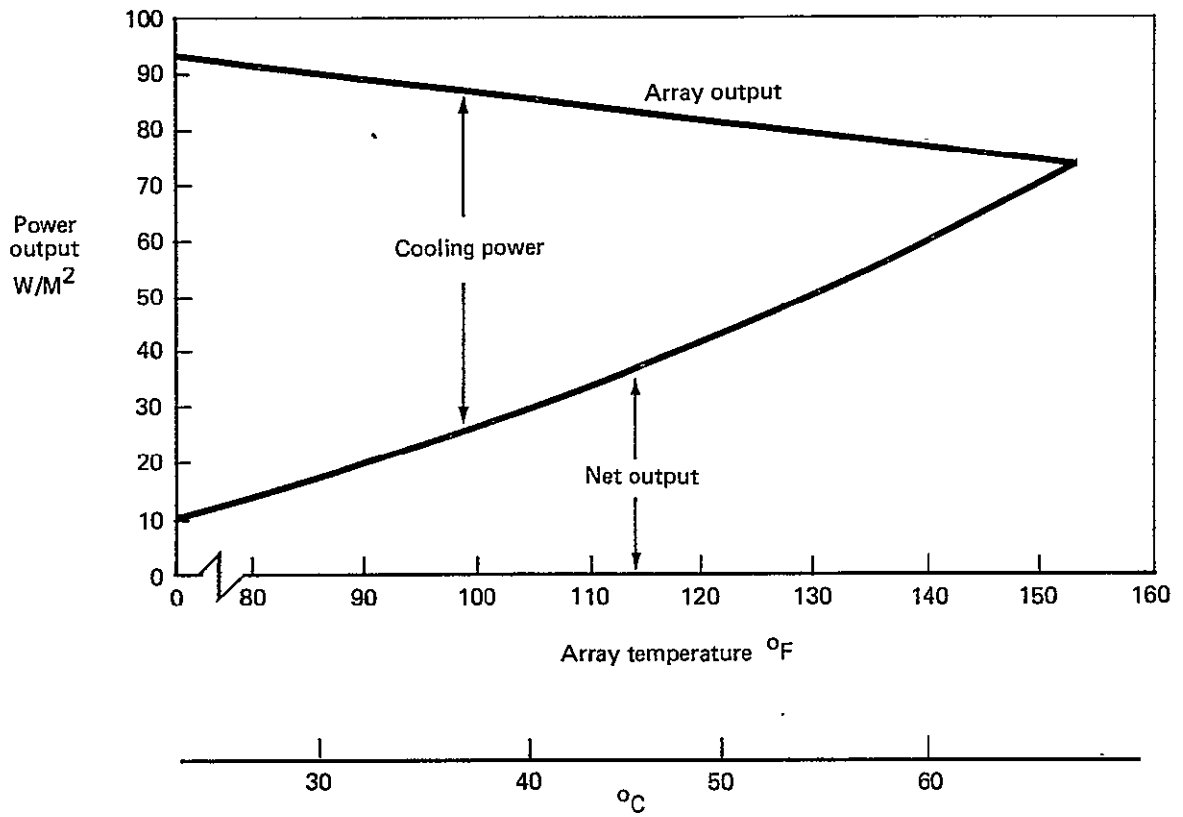


Figure 4-37. Effect of Active Array Cooling on Power Output

steady state and transient conditions using convective, conductive and radiative heat transfer equations. The model reflects the varying ambient temperature and insolation for different seasons. Module efficiency and electrical output are found using the temperature and insolation from the thermal analysis. The Boeing Engineering Thermal Analyzer Program (BETA) is used to perform the thermal and performance analyses. BETA provides options of transient or steady state heat transfer analysis. The analysis may include heat generation and heat transfer by conduction, convection, and radiation. Physical properties may vary with temperature, time, or distance.

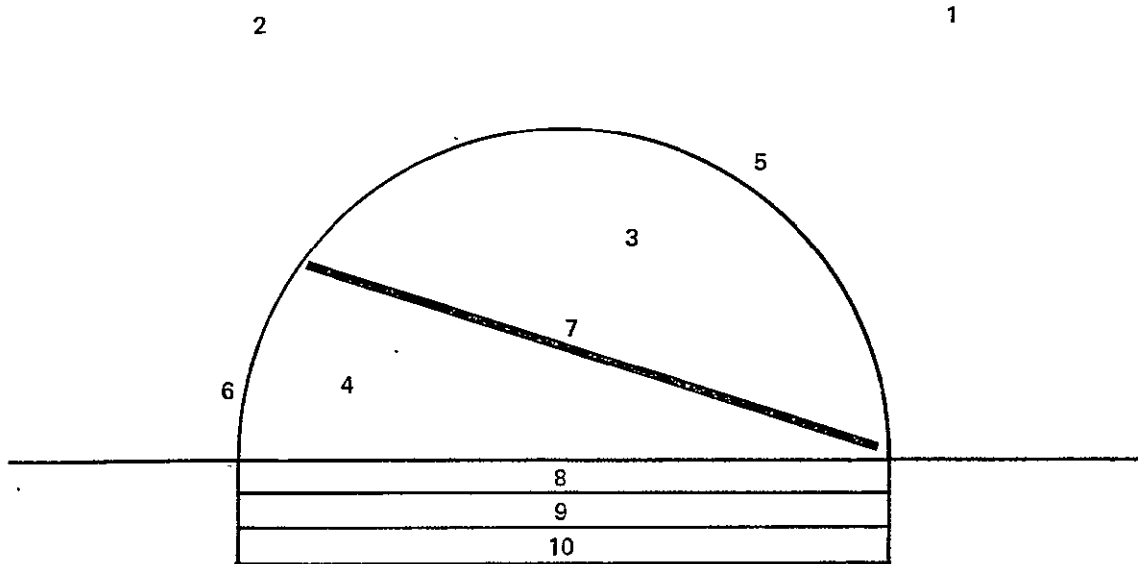
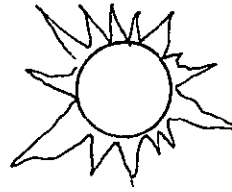
The major inputs to the program are the heat transfer relationships between lumped nodes. Figure 4-38 is a diagram of the nodes for the fixed array analysis. Heat transfer equations must be specified between all appropriate nodes. Solar insolation is also input. A chart of the heat transfer mechanisms connecting the nodes is shown in Table 4-IV.

4.3.3.2 Material Radiative Properties

Material properties used for the radiation equations are listed in Table 4-V. The enclosure material is a weatherized polyester. View factors were estimated using geometric relationships between the surfaces in the design; a gray body multi-surface view factor determination was not performed.

4.3.3.3 Convective Heat Transfer Model

Free convection transfers heat from the array to the enclosure, where the ambient air removes it by free and forced convection. The inside free convection heat transfer coefficients are taken from Ref. 20. This method was selected based on a comparative evaluation of existing solutions for natural convection in enclosures, Ref. 32. Since the method of Ref. 20 is based on a rectangular enclosure, the present analysis breaks the



Nodes

- 1 Ambient
- 2 Sky
- 3 Enclosure air
- 4 Enclosure air, shaded
- 5 Enclosure

- 6 Enclosure, shaded
- 7 Array
- 8 Ground below enclosure
- 9 Ground
- 10 Ground

Figure 4-38. Fixed Array Nodal Network

Table 4-IV: Heat Transfer Paths in Fixed Array Thermal Model

NODE DESCRIPTION	NODE NO.	1	2	3	4	5	6	7	8	9	10
AMBIENT	1					R*	R*				
SKY	2					R	R	R	R		
ENCLOSURE AIR	3										
ENCLOSURE AIR, SHADED	4										
ENCLOSURE	5	CV		CV			R	R			
ENCLOSURE, SHADED	6	CV			CV			R	R		
ARRAY	7			CV	CV				R		
GROUND	8				CV						
GROUND	9								C		
GROUND	10									C	

C - Conduction CV - Convection R - Radiation
 * Ground outside of enclosure included in ambient node.

Table 4-V: Material Properties

ENCLOSURE EMITTANCE	.851
ENCLOSURE IR TRANSMITTANCE	.071
ENCLOSURE ABSORPTANCE	.077
ENCLOSURE SOLAR TRANSMITTANCE	.843
ARRAY EMITTANCE	.84
ARRAY ABSORPTANCE	.90
GROUND EMITTANCE	.85
GROUND PLASTIC EMITTANCE	.90

volume within the enclosure into two spaces above and below the array. These spaces approximate tilted rectangular enclosures. The heat transfer coefficient of a rectangular enclosure is not very sensitive to tilt angle, according to Ref. 21, unless the heated surface is overhead and horizontal. Convective mixing of the two spaces is ignored in the analysis. The inside Nusselt number is:

$$Nu_{\text{inside}} = 0.155 (Gr_L)^{0.315} (H/L)^{-0.265}$$

where:

Gr_L = the Grashof number based on the length, L , of a rectangular cross section.

The values of height, H , and length, L , of the cross section are determined by estimating the dimensions of a rectangular enclosure approximately the same size as the air space within the enclosure, above or below the array.

Free convection outside the enclosure is determined using Ref. 22. For a large cylinder with fluid flow in the turbulent range,

$$h = 0.18 (\Delta T)^{1/3}$$

The forced convection heat transfer coefficient from the enclosure exterior is estimated by averaging the values for an upward facing horizontal surface and a vertical surface. Ref. 16 gives a heat transfer coefficient for wind on a flat, horizontal plate:

$$h_{\text{wind}} = 5.7 + 3.8V \text{ (watts/m}^2\text{·}^\circ\text{C)}$$

where:

V = wind velocity, m/s

The coefficient for a vertical plane surface from Ref. 22 is:

$$h_{\text{wind}} = 0.99 + 0.21V \text{ (BTU/h·ft}^2\text{·}^\circ\text{F)}$$

where:

V = wind velocity, ft/s

With a wind velocity of 2 meters per second, for the fixed array transient studies, the two wind heat transfer values are similar; their average is assumed to be an overall forced heat transfer coefficient.

Conduction within the enclosure and array components is too small to have much of an effect on the analysis, and is not included. Vertical conduction between the ground nodes is included to obtain a realistic ground surface temperature.

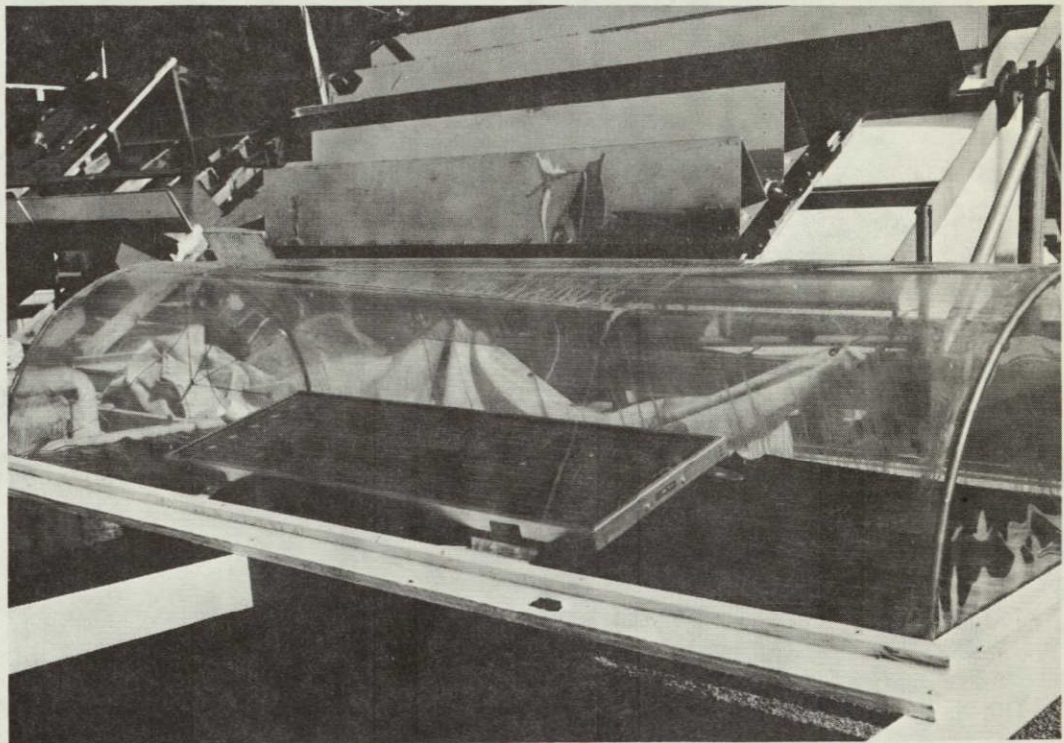
4.3.4 Thermal Model Verification

Simulation of a test performed by JPL in Pasadena, California, Ref. 33, verified the computer modeling procedure. The test setup and conditions are shown in Figure 4-39.

A BETA thermal/performance model was build to simulate the design and environmental conditions of the JPL test. The computer model delivered temperature and power production values for the steady state condition. Heat transfer analysis methods were essentially identical to those used for the design analysis. Wind velocities from 0 to 2 meters per second were simulated. Heat transfer from the plywood platform is evaluated using an equation for flat plates in Ref. 23. Wind heat loss off the ground is modeled by forced convection off a flat plate.

The same material properties carry over for the test simulation as for the fixed array. The properties are listed in Table 4-V. A geometric evaluation of the test setup produced radiation view factors.

The array temperature predictions for the JPL test simulation are shown as a function of wind velocity in Figure 4-40. The effect of air circulation under the plywood platform is also shown. The morning and afternoon test data points at 800 W/m^2 are plotted at the average wind speed measured during those time periods. The predictions correlate reasonably well with the measured values. A more detailed evaluation would require further data on wind speeds and directions in the immediate vicinity of the test article. However, this comparison indicates that the thermal models used in the study have acceptable accuracy.



Notes: Enclosure radius: 45.7cm Array: 38.8 X 117cm
 Enclosure length: 229cm Area cells/area module = 0.679

Figure 4-39. Dome Test Setup

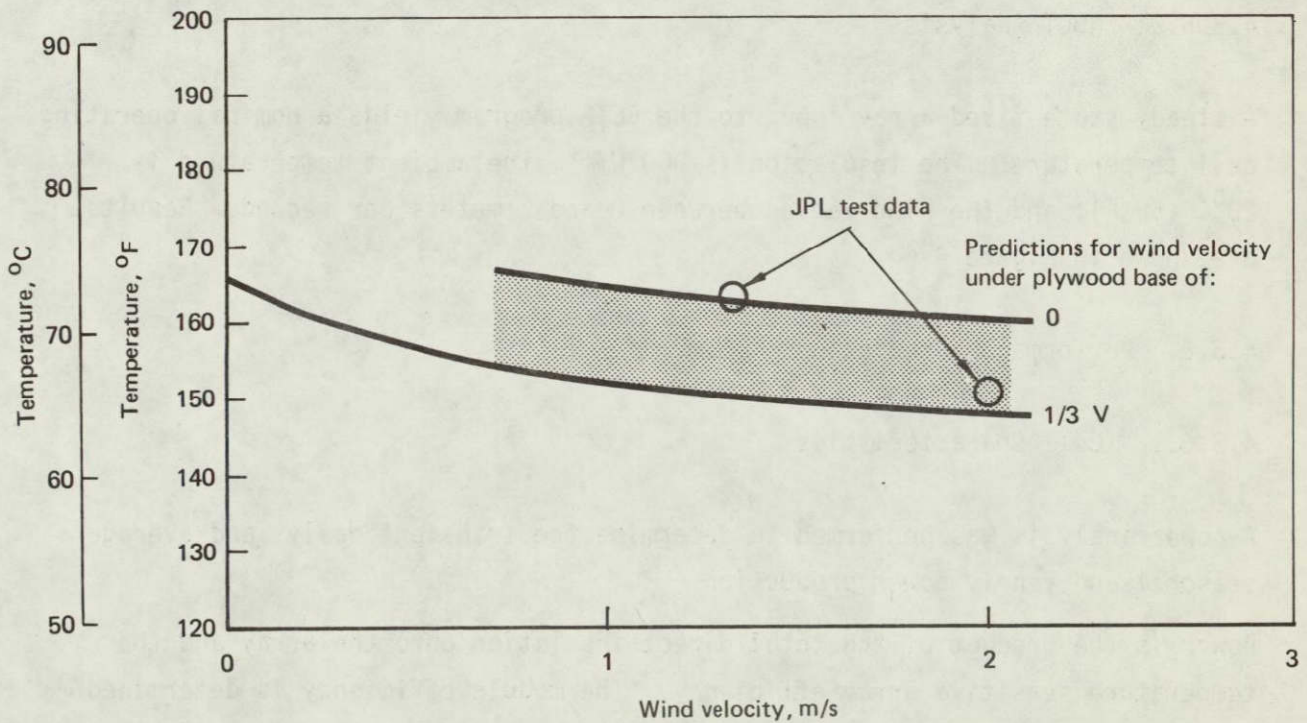


Figure 4-40. Comparison of Predictions and Measurements of Temperatures on JPL Subscale Model

4.3.5 Temperature Predictions

The results for the fixed array temperature predictions are shown in Figure 4-41. The highest array temperature is 72°C (162°F) at 1:00 PM in the summer. The corresponding enclosure temperature is about 48°C (118°F). The air inside the enclosure is 58°C (137°F) at 1:00 PM during the summer. The temperature profiles react quickly to the insolation and ambient temperature.

4.3.5.1 Extreme Temperature Analyses

The temperature curves for the hot and cold extreme temperature cases are shown in Figure 4-42. With an ambient temperature of 47°C (116°F), the array reaches 79°C (175°F). The cold extreme ambient temperature is -7°C (19°F). The array is -2°C (28°F) at the coldest part of the day. The enclosure air spaces gets as low as -5°C (23°F).

4.3.5.2 NOCT Analysis

A steady state fixed array input to the BETA program yields a nominal operating cell temperature. The insolation is 800 W/m^2 , the ambient temperature is 20°C (68°F), and the wind varies between 0 and 2 meters per second. Results are shown in Figure 4-43.

4.3.6 Performance Predictions

4.3.6.1 Cell Characteristics

A power analysis was performed to determine the transient daily, and average seasonal and yearly power production.

Power is the product of the total direct insolation onto the array and the temperature sensitive array efficiency. The module efficiency is determined

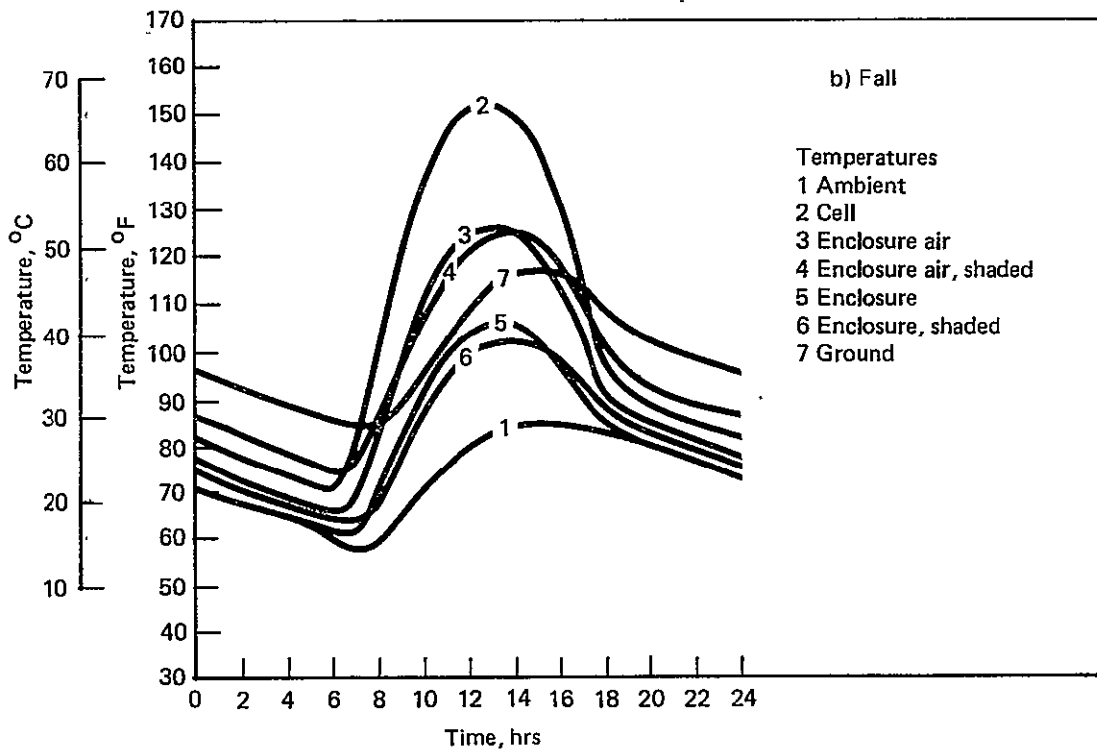
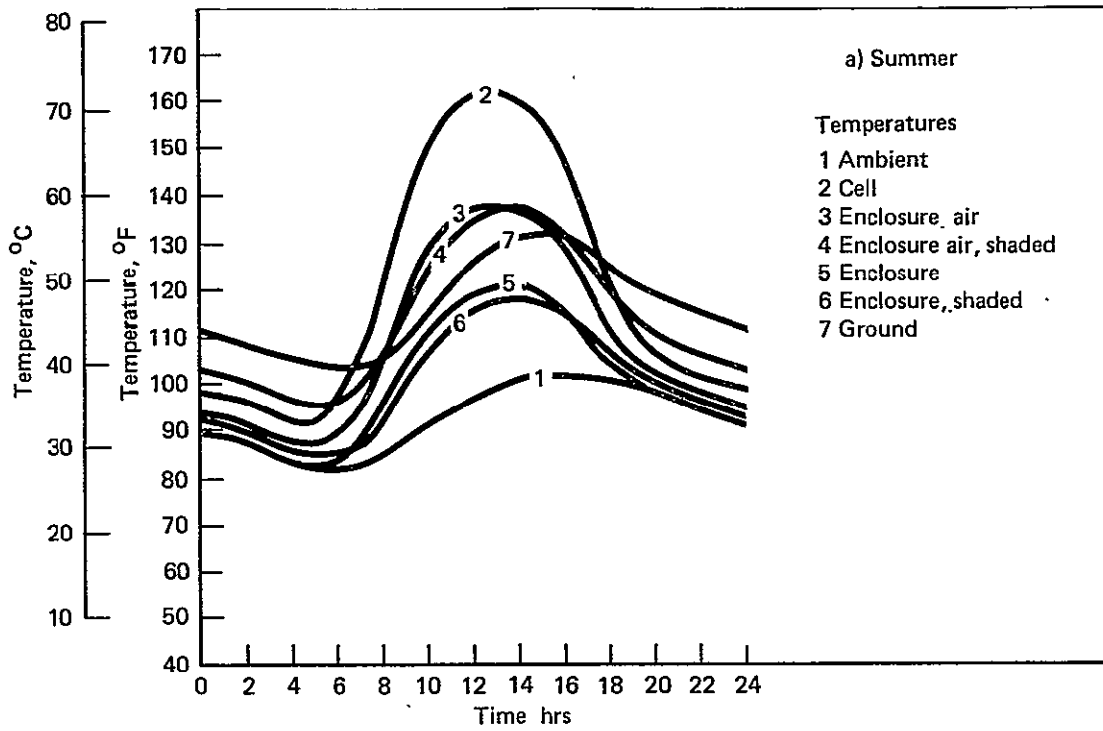


Figure 4-41. Fixed Array Temperature Predictions

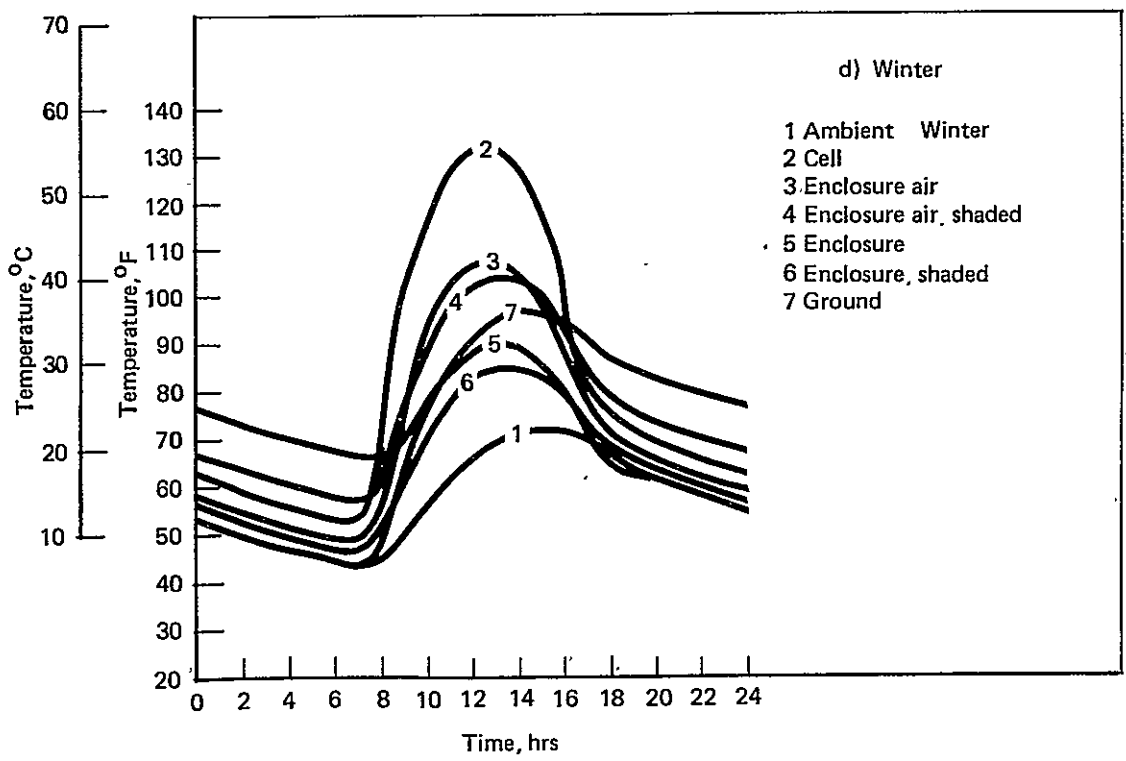
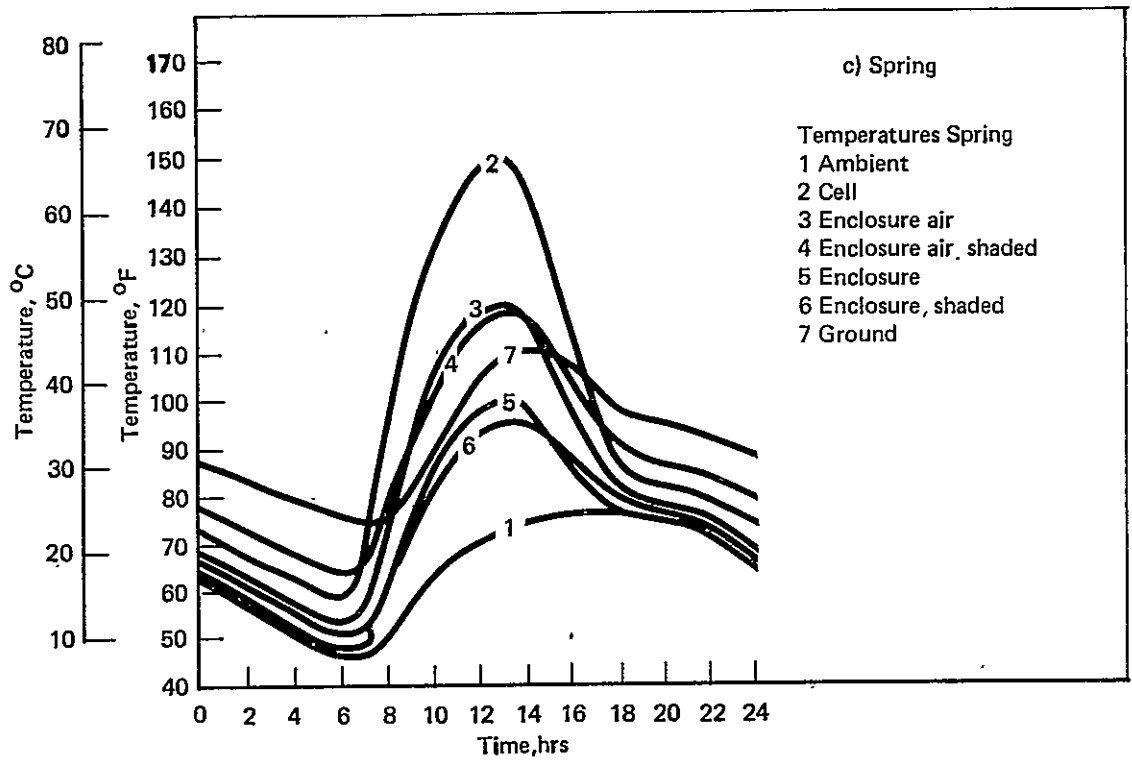


Figure 4-41 Fixed Array Temperature Predictions (Continued)

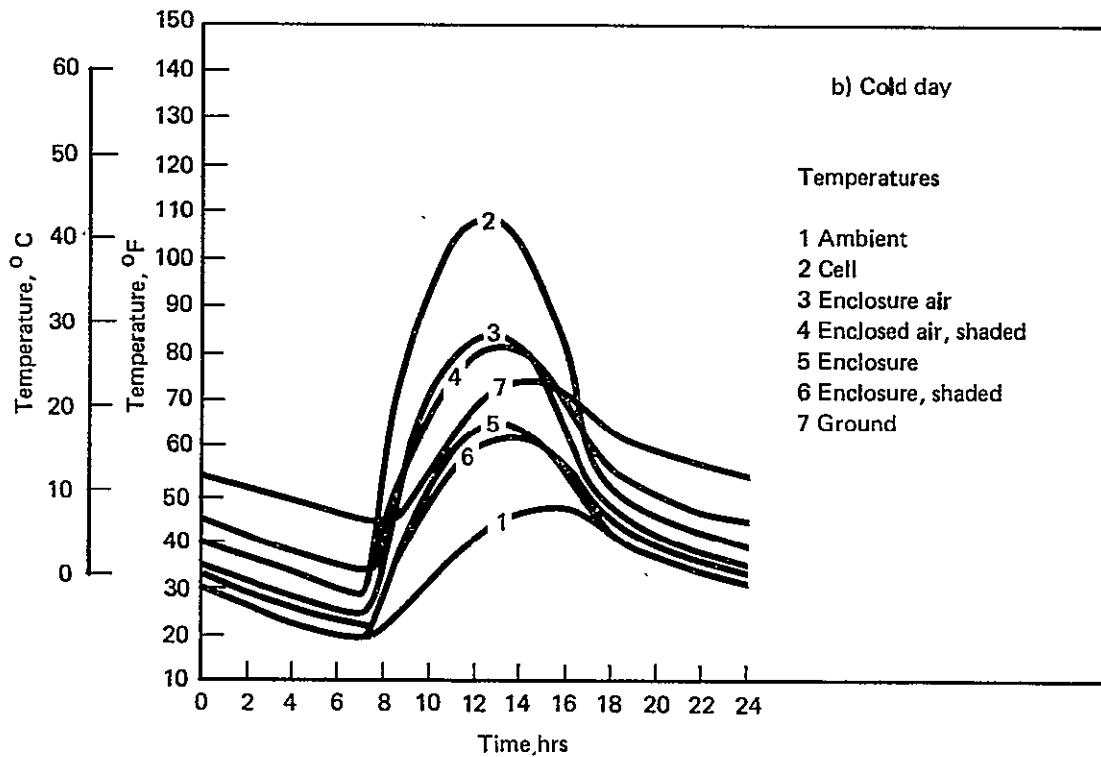
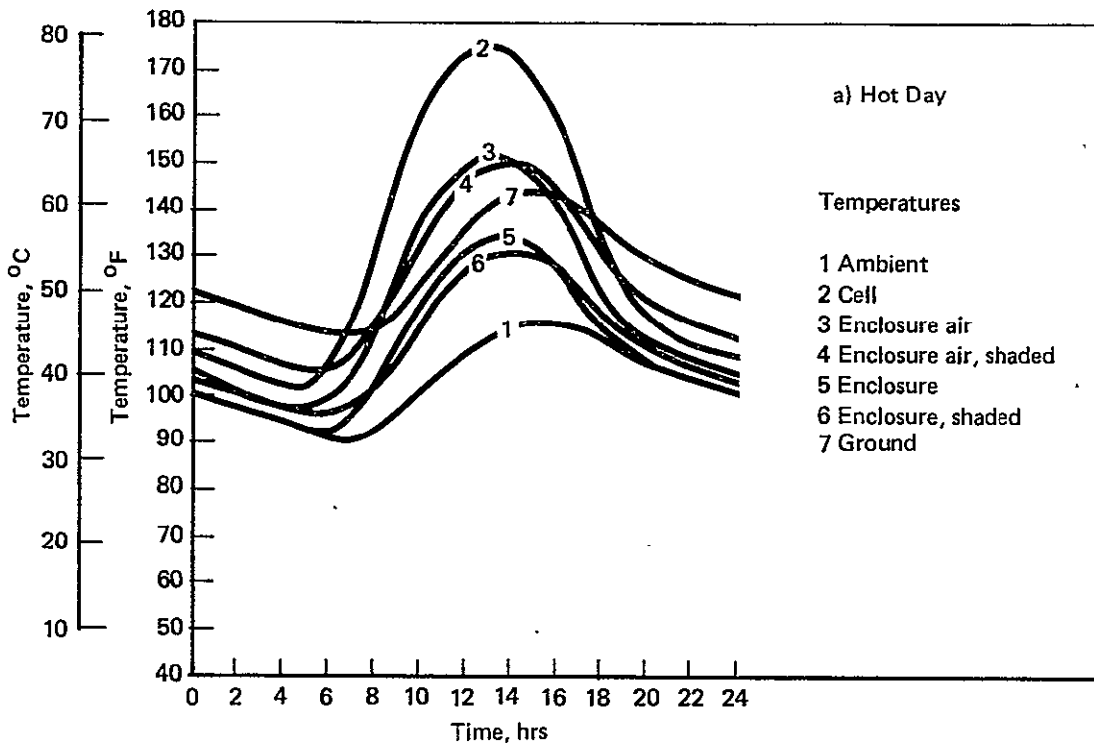


Figure 4-42. Fixed Array Temperature Predictions

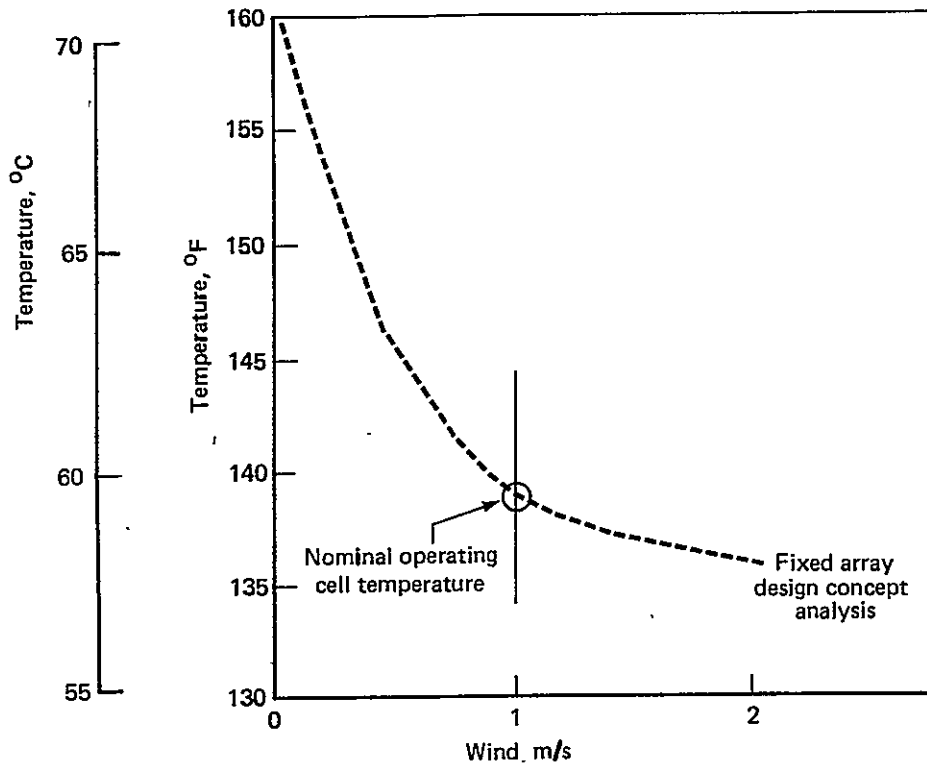


Figure 4-43. Effect of Wind on Fixed Array Cell Temperature

using the temperature sensitivity coefficients supplied by JPL, as listed in Section 3.2.1.1. The cell nesting efficiency is 93% and including borders, the module packing efficiency is 89.3%. The transmittance of the enclosure in the range of cell response was estimated to be 88.3%.

The module efficiency can then be described by:

$$\eta_{\text{module}} = .126 [1 - .00278 (T - 82.4)]$$

where: T is in $^{\circ}\text{F}$

Half-hourly values determined by the BETA program are integrated throughout the day to yield a daily power production value typical for the season. The seasonal values are then averaged to determine a yearly power production figure.

4.3.6.2 Seasonal Analysis

Power production and cell efficiency for an average day in each season is shown in Figure 4-44. For the fixed array, the power production is a sharp peak. Efficiency drops off a few percent with the higher temperatures during the middle of the day.

4.3.6.3 NOCT Analysis

The power production and efficiency for the steady state fixed array case is shown in Figure 4-45. The figure shows the power varying with wind velocity. The cooling provided by the wind increases array efficiency and power.

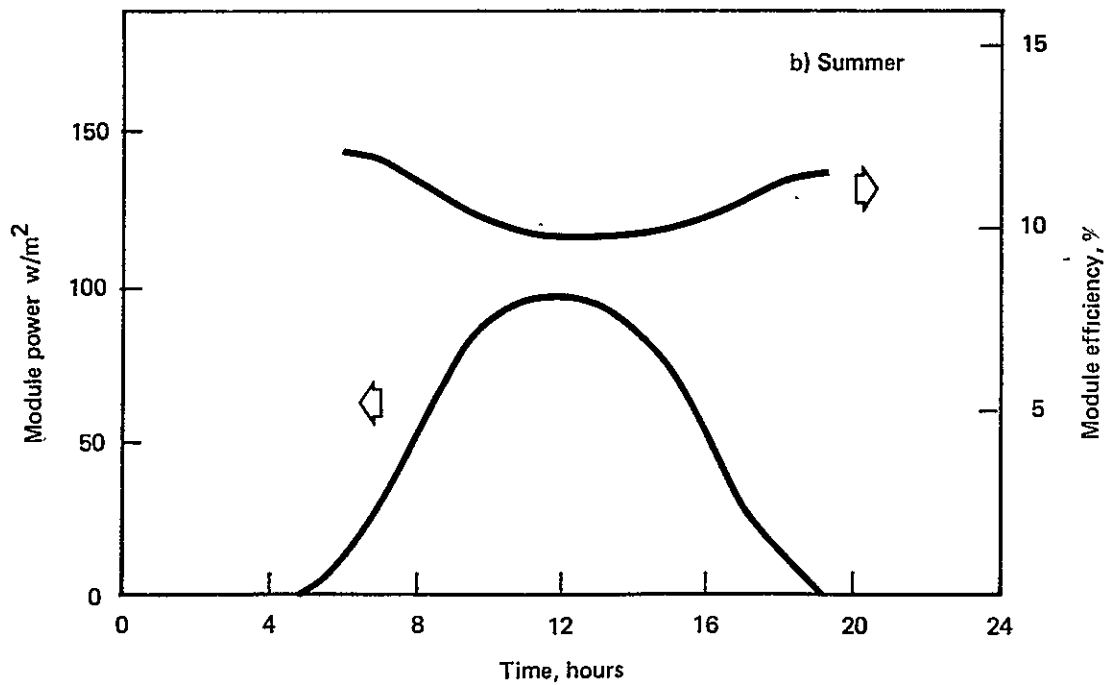
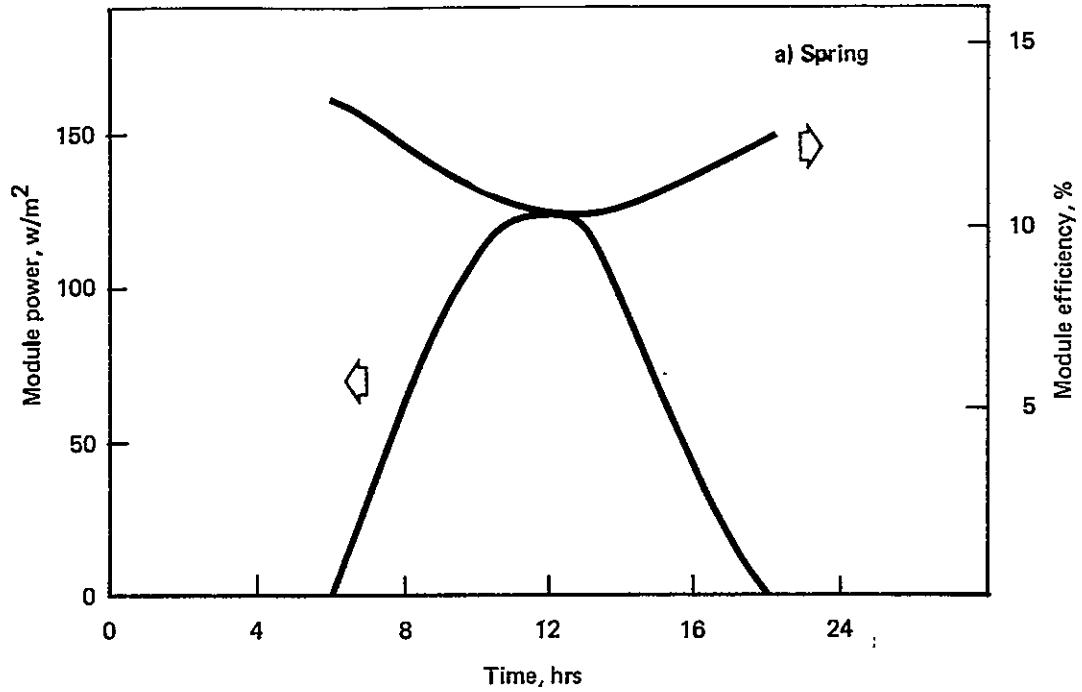


Figure 4-44. Fixed Tilt Array Transient Power Output

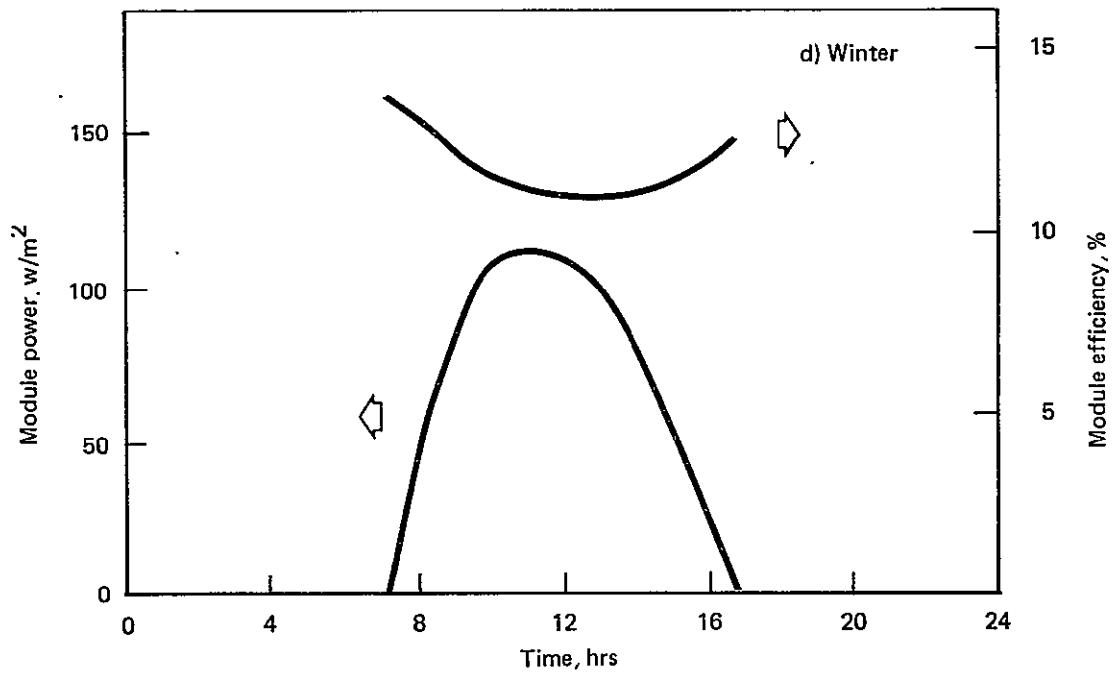
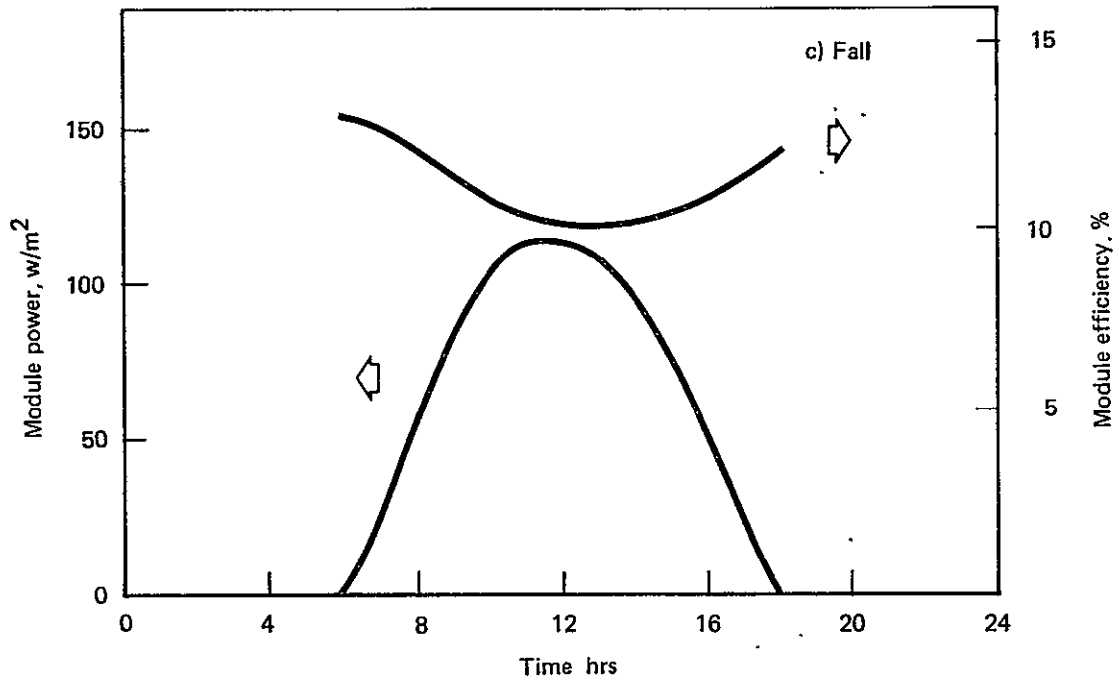


Figure 4-44. Fixed Tilt Array Transient Power Output (Continued)

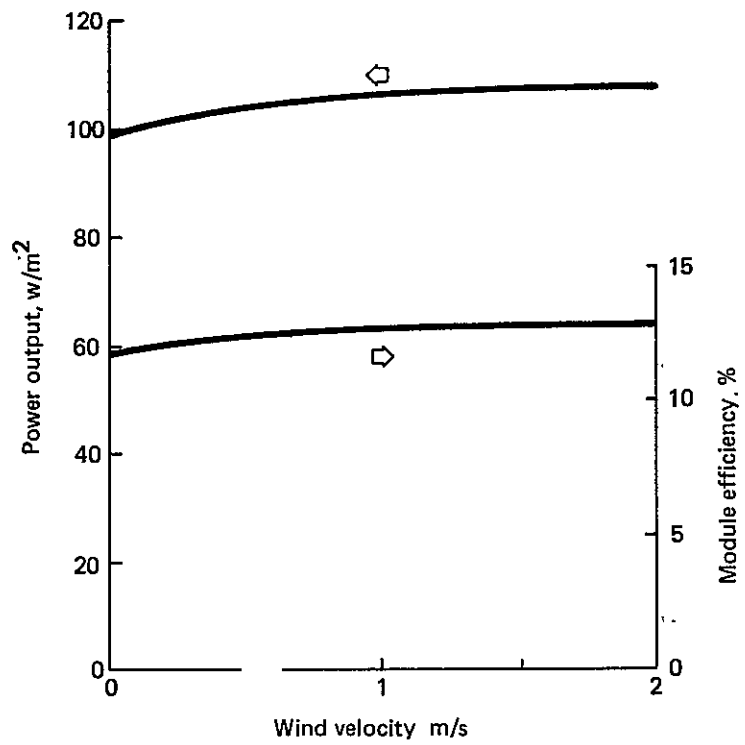


Figure 4-45. Fixed Array Output for NOCT Conditions

4.4 Manufacturing and Installation

This section describes an initial concept for manufacturing and installation of the enclosed fixed-tilted photovoltaic array. The manufacturing and installation plans provide a basis for the estimated costs presented at the end of the section.

4.4.1 Production Scenario

The plans and costs for this study are based on a continuing commercial production program supplying photovoltaic central power stations for electrical energy generation in the southwestern United States. The power stations are assumed to be located near population centers to assure local availability of manufacturing, assembly and site installation labor. However, specialized manufacturing activities, primarily module and panel fabrication, are performed at other locations and could supply components or assemblies to other power station sites as well. Off-site module/panel production facilities are considered to be permanent installations dedicated to fabricating a given module/panel design. The on-site facilities include an office and factory which is converted to the power station maintenance and control building. An adjacent warehouse for staging and storage of components is dismantled at the end of construction, and is charged entirely to the plant costs. Figure 4-46 shows where most of the production activities would occur.

The assumed production rate is one 200 MWe power station per year, seasonally phased so that workers can tolerate the average daily maximum temperatures within the enclosure. This permits a six month array installation period with the remainder of the year available for facility construction and disassembly, site cleanup, and array checkout.

Non-recurring costs other than facilities and equipment are not included in the cost estimates or plans. It is assumed that a pilot production program has provided a design and has proved the design performance and production processes.

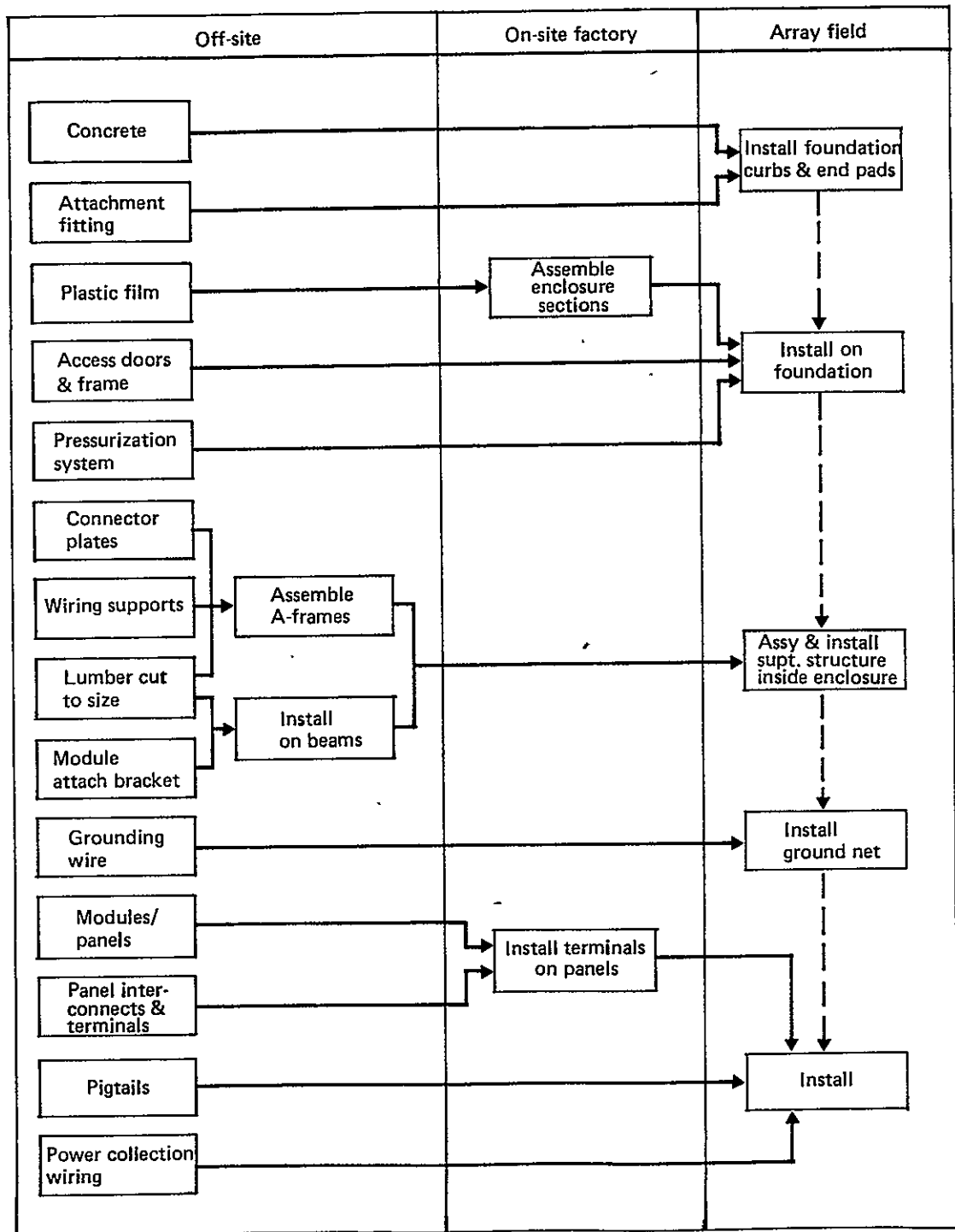


Figure 4-46. Array Production Flow

4.4.2 Module/Panel Fabrication

The module/panel fabrication facility is a 7430 m² (80,000 sq. ft.) building designed specifically for producing the panel design of Section 4.1.4. This plant annually produces all panels required for a 200 MWe power plant, or about 133,000 panels per year. Unlike the seasonal plant installation, panel production is year-round with a three shift, five day week.

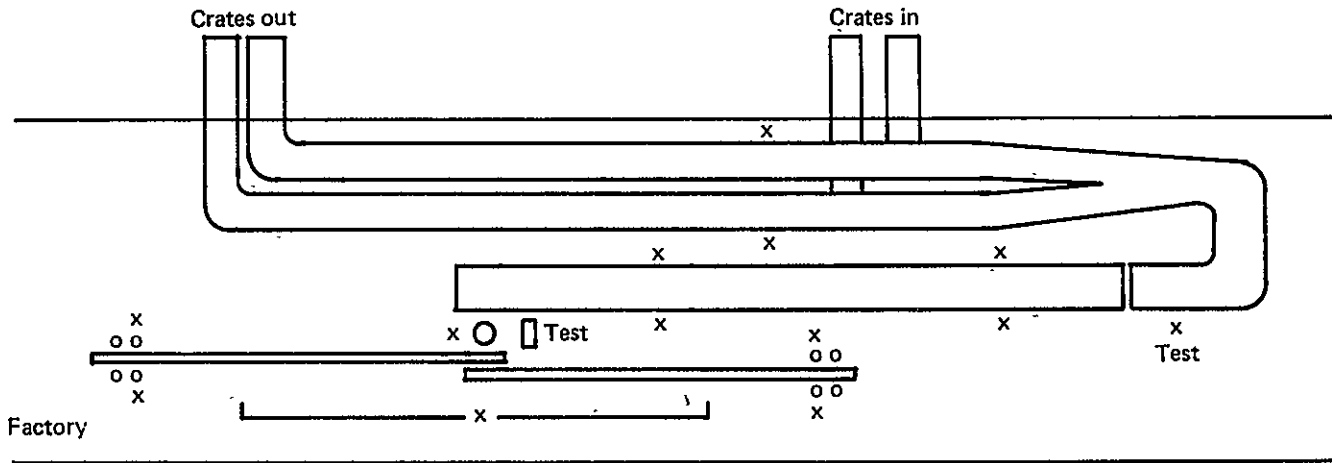
The plant layout shown in Figure 4-47 requires a 7430 m² (80,000 sq. ft.) building. The factory production line concept, Figure 4-48, has two fabrication lines feeding the panel assembly line. In the fabrication lines the cells (with tabs soldered to the top side) are fed face down from cassettes onto a carrier film, the interconnects are soldered, and a nylon net is bonded to the back side of the cells. This completes a 406 centimeter (16 inch) wide section of the three section module, which is then tested and transferred to the assembly area. Interconnects within the module and the panel wiring are added, and the polyester film substrate is bonded in place. Stripping the carrier film, folding and sealing the edges around the busses and the ropes at the supporting edges, and adding the support fitting extrusions completes the panels, which are then tested and packed. The production flow described above is shown in Figure 4-49. Equipment for the factory area is listed in Table 4-VI.

4.4.3 Structure Fabrication

The array structure is assembled on site from components fabricated elsewhere as shown in Figure 4-46. On site facilities are primarily for warehousing and staging for flow of material to the installation areas. Factory operations on site are simple assembly procedures that permit shipping to the site to be high density and within legal limits to minimize costs. The plastic film is received at the factory, then cut to length, bonded, edge ropes installed, and rolled on a dispensing reel for field installation. The panels are uncrated and placed on installation pallets. The terminals are installed

C-2

Warehouse, Receiving Shipping & Storage



89

Office and support

Figure 4-47. Solar Cell Array Feasibility Study - Module/Panel Manufacturing -Plant Layout

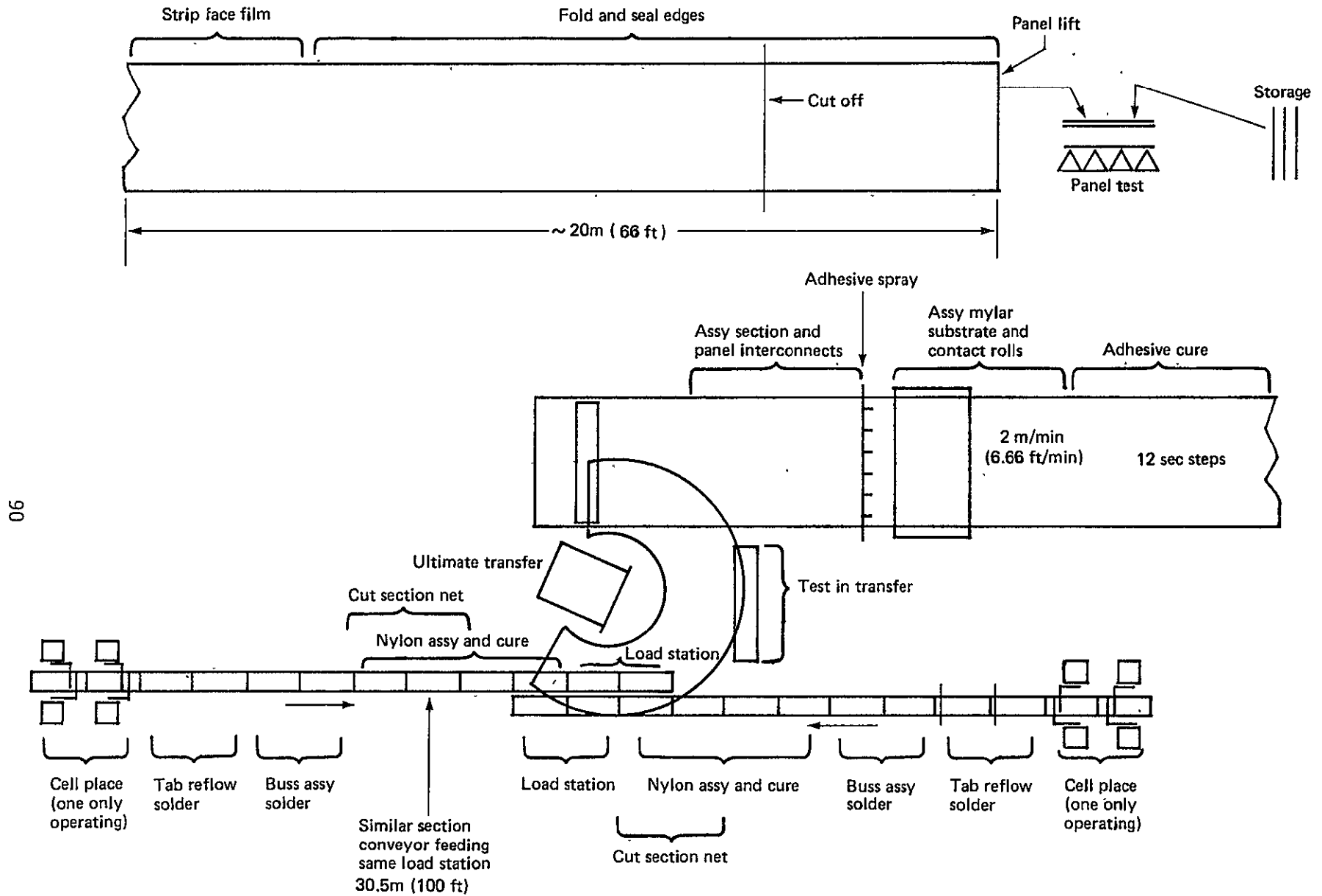


Figure 4-48. Panel Factory Production Line

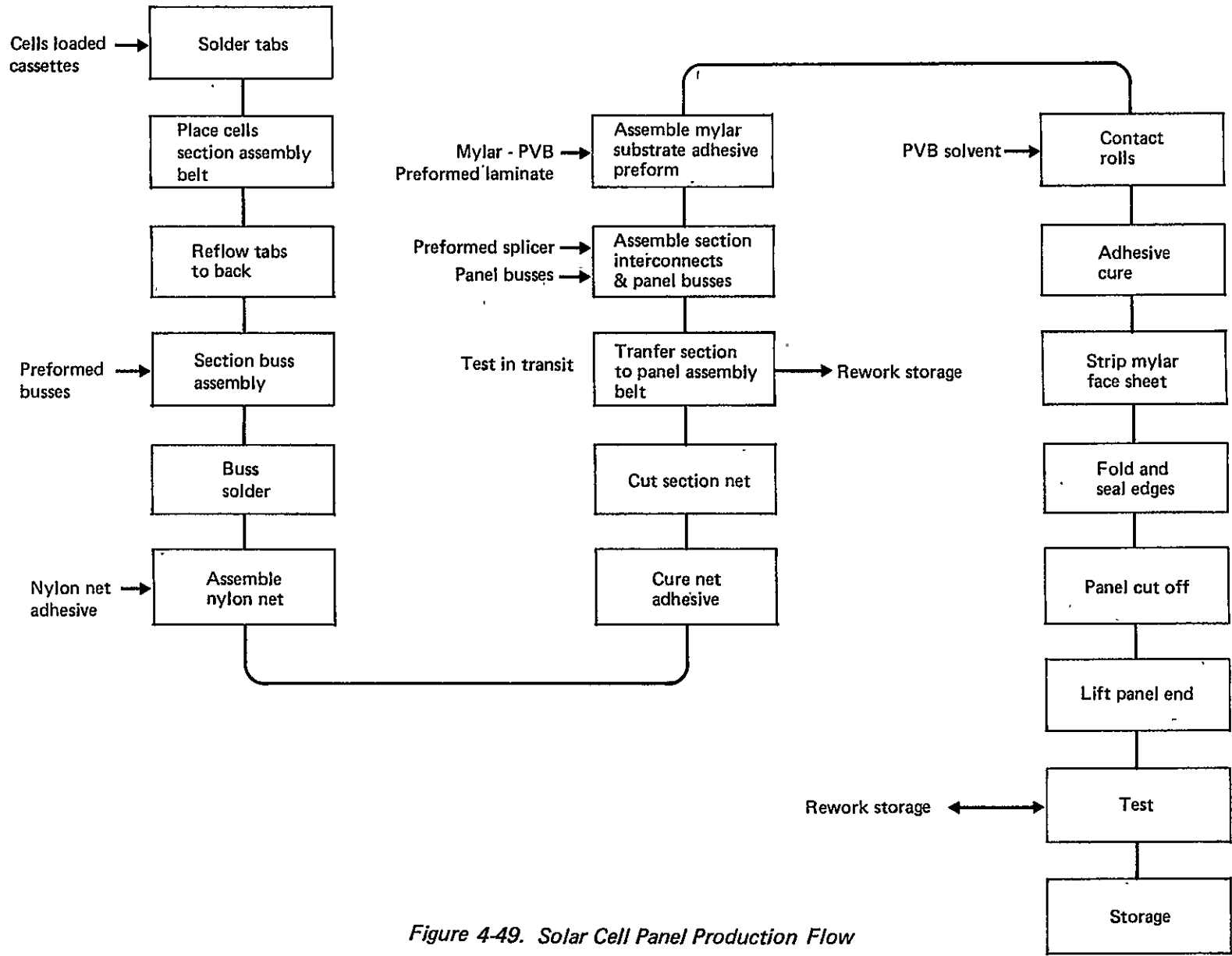


Figure 4-49. Solar Cell Panel Production Flow

TABLE 4-VI: SOLAR CELL ARRAY FEASIBILITY STUDY MODULE/PANEL
MANUFACTURING FACILITY EQUIPMENT LIST

ITEM	QUANTITY
Pickamatic (Cell Pick and Place)	8
Reflow Solder (Tab)	2
Buss Assembly Solder (Minor)	2
Nylon Assembly and Cure	2
Load Station	2
Conveyor 50 x 480 cm (20" x 96")	24
Unimate	1
Tester (Module)	1
Section and Buss Assembly (Major)	1
Spray (Solvent)	1
Assembly Mylar Roller and Adhesive Coater	1
Adhesive Cure (Infra-Red) 4.8 x 14.6 m (8' x 48')	1
Edge Seal	2
Panel Cut Off	1
Conveyor 4.8 x 213 m (8' x 700')	1
Panel Life (Handler)	1
Tester (Panel)	1
Solvent Storage Tank and Pump	1
Material Storage Racks	10
Fork Lifts	2
Fork Life Accessories	2
Packaging Equipment	2

on the upper attachment extrusion and the pallets are stacked on the panel installation vehicle.

The facilities required for these operations are estimated to be 4650 m² (50,000 sq. ft.) of factory and office floor area and 23,200 m² (250,000 sq. ft.) of warehouse storage area. Enclosure final assembly and panel final assembly and loading each occupy about one-fourth the factory floor area, and miscellaneous activities use the remainder. The warehouse area is used primarily for storage of panels with less area needed for plastic film and detail parts.

4.4.4 Installation

The arrays are installed in the 200 MWe power station field in the sequence shown in Figure 4-46. The area is leveled to a near final grade before array construction starts. Strips for the enclosure footings are graded to the desired contour with clear areas on each side for the curb-laying machine. The curb-laying machine is used to continuously slipform the foundation shapes shown in Figure 4-50. The machine shown with a foundation slipform is the Curbmaster Robot made by Curbmaster of America, Inc. This machine guides on a stringline to automatically control grade, slope, and steering of the machine. The form leaves a groove for inserting the attachment plate for the enclosure. An alternate approach would be to feed the attach strip into the slip form to automatically embed it in the concrete. Final grading places soil on each side of the foundations to lock the footing in place against side loads.

The enclosure is installed in a continuous operation by a moveable installation vehicle. The plastic film feeds from the dispensing reel over a half circle form close to the final cross section. A moveable dam separates the installed and inflated portion of the enclosure for the section being installed. Once the edges are attached to the foundation, the section is inflated and the dam moved forward to the installation vehicle. Field joints in adjoining enclosure sections are made on the installation vehicle after mounting a new roll of the plastic film.

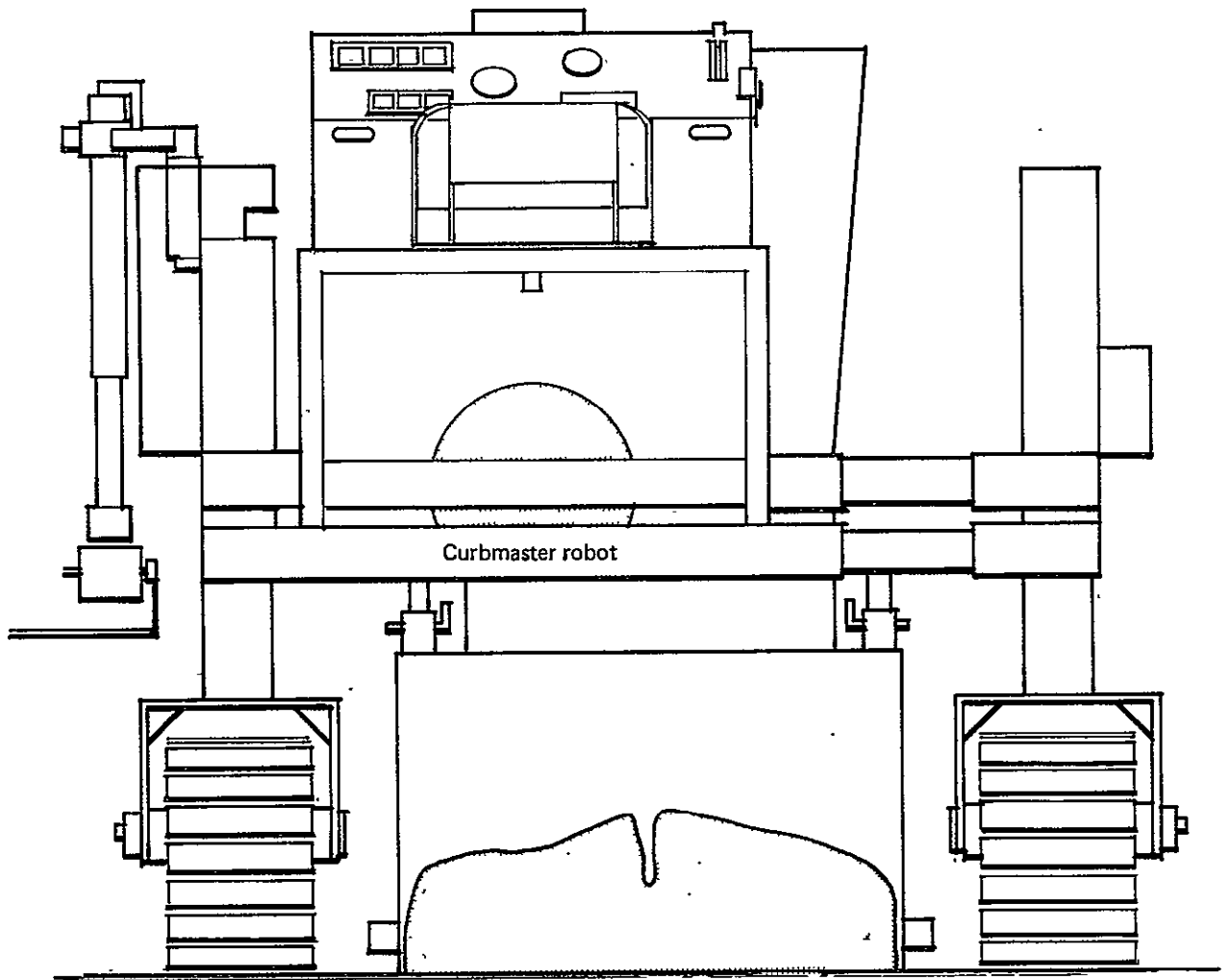


Figure 4-50. Curb Laying Machine

A temporary airlock is located at each end of the enclosure during the construction of the array inside the enclosure. A-frames, beams, and bracing members are brought into the enclosure and installed. Next, vehicles with the panels on the installation pallets enter. The pallets are slid from their racks onto special handling equipment where the pallets are rotated 90⁰, hooked to the lower bracket, lifted to the support beam and hooked to the upper bracket. Another vehicle reels out the power collection wiring; the wiring is attached to previously installed brackets on the A-frames, and the panel interconnects and pigtails are installed. The airlocks are moved to another enclosure after the array is completely installed and checked out.

4.5 Maintenance

The maintenance concept is adapted from the current enclosed heliostat maintenance plan. The major maintenance activities will be enclosure washing on a scheduled basis, replacement of the enclosures at about 18 years, pressurization system filter replacement, and panel repair and replacement.

Enclosures will be rinsed frequently (every few weeks) to remove particulate matter before it develops bonds with the plastic film. The enclosures will be washed semi-annually to provide a more thorough cleaning. Rinsing will be done by a spray from a truck driven between the arrays. Reclaiming the rinse water may be necessary; this can be accomplished by modifying the foundations to include a gutter and using the proper slopes and catch basins. The machine used for the semi-annual washings would straddle the enclosure and guide on the outer edge of the foundation. High pressure water would be sprayed from nozzles on a semi-circular pipe over the enclosure. The machine would be towed on both sides, with pressurized water supplied from one of the tow vehicles.

Enclosure replacement after 18 years is anticipated, in order to meet the 30 year structural life requirement. This will be more difficult than the original installation due to the presence of the array structure and panels. An enclosure replacement machine that straddles the array will be necessary and has been included in the costing. It is also assumed that the pressurization system will wear out and be replaced at the same time. The prefilters for the pressurization system will be replaced annually, based on the expected air flow into the enclosure. The main filters will probably last until replacement of the entire pressurization system.

Costs for repair and replacement of panels is based on a 1% per year replacement rate. This is assumed to occur at a uniform rate over the life of the plant, although infant mortality and wearout probably would bias the required replacement rate. Most failed panels should be reuseable after local repairs or replacement of modules. The panel repair would take place in the power station maintenance facility after their removal from the array and replacement by a spare panel.

4.6 Life Cycle Costs

The capital investment for fabrication and installation, estimated maintenance costs for 20 years operation, and the resulting cost of energy for the fixed tilted array is presented in this section.

4.6.1 Costing Assumptions

Many of the assumptions affecting the cost analysis were given as part of the production and maintenance descriptions. Additional assumptions are given below:

- 1) Life cycle costing is based on a 30 year plant life (structures, buildings, etc.), except for the modules/panels for which a 20 year life is used.
- 2) Interconnected solar cells cost \$40 per square meter of active module/panel area. Since the cost analysis included interconnecting

the cells, the cost of cells alone was assumed to be \$39.25 per square meter of active module/panel area.

- 3) The cost analysis was based on current (1978) dollars, and factored to 1975 dollars by dividing by 1.17.
- 4) Rates and factors are based on Ref. 24, the Low-Cost Solar Array Project interim price estimation guidelines. Specific items which deviate from this are the on-site temporary warehouse, and the overhead rates for non-factory labor. Material overhead was reduced from 30% to 2-10%, due to the large volumes involved.
- 5) Labor rates were derived from current (1st half 1978) base and overhead rates with an appropriate skill mix for the general category of task. On-site work is assumed to be manned entirely by craft labor using an average of electrician, carpenter and general site labor rates for the Phoenix area. Craft labor overhead has been reduced slightly based on the relatively long-term project. The rates used and the factors applied for overhead and quality control inspection (Q.C.) are as follows:

Type of Labor	<u>Hourly Rate</u>	<u>O/H Factor</u>	<u>Q.C. Factor</u>
On-site Fabrication, Assembly Labor	\$ 10.50	1.8	6%
Off-site Component Fabrication	7.00	2.1	6%
Module Fabrication	8.00	2.1	10%
Field Installation	10.50	1.8	6%
Alignment and Checkout	13.00	1.67	6%
Maintenance	10.50	1.8	6%

- 6) Costs were broken down according to the cost breakdown structure (CBS) shown in Table 4-VII. This CBS covers the entire power station but only the array field capital investment and operation and maintenance costs are included in the detailed cost analysis.

TABLE 4-VII: COST BREAKDOWN STRUCTURE

1.	ARRAY FIELD
1.1	Land Acquisition and Preparation
1.2	In-Field Service Roads
1.3	Security Fence
1.4	Lightning Protection
1.5	Field to PCU Wiring
1.6	Foundations
1.7	Enclosure
1.8	Support Structure
1.9	Panels
1.10	Controls and Instrumentation (AF)
2.	BALANCE OF PLANT
2.1	Power Conditioning (PCU's)
2.2	PCU to Switchyard Cabling
2.3	Switchyard (including main transformer)
2.4	Controls and Instrumentation (BOP)
2.5	Control Building
2.6	Maintenance Building
2.7	General Roads, Parking Lot, Landscaping
2.8	Facilities (e.g., pump, sewage, water tanks)
3.	DISTRIBUTABLES AND INDIRECTS
3.1	A/E
3.2	Construction
3.3	Plant Start-Up
3.4	Interest During Construction
3.5	Etc.
4.	OPERATION AND MAINTENANCE
4.1	Array Field
4.2	Balance of Plant

4.6.2 Costing Analysis Results

A cost summary for the fixed tilted array in terms of 1975 dollars is presented in Table 4-VIII. A detailed breakdown of the quantities, rates and factors, and overall costs is contained in Table 4-IX, as analyzed in first half 1978 dollars. A constant factor of 1.17 is used to reduce 1978 costs to 1975 dollars.

TABLE 4-VIII: FIXED-TILT ARRAY COST SUMMARY, 1975 DOLLARS

CBS NO.	TITLE	COST, \$/m ² OF MODULE/PANEL AREA					
		LABOR	MATERIAL	EQUIPMENT	FACILITIES	TRANSPORTATION	TOTAL
1.1	Land Acquisition and Preparation						1.90
1.2	In-field Service Roads						**
1.3	Security Fence						.13
1.4	Lightning Protection						**
1.5	Field to PCU Wiring	.19	5.31	.01			5.51
1.6	Foundations	.87	3.62	.03			4.52
1.7	Enclosures	1.03	3.48	.09			4.60
1.8	Support Structure	.27	1.02	.04			1.33
1.9	Modules/Panels	1.19	43.98	.77	.97	.30	49.21
1.0	Array Field*	3.56	57.41	.94	2.97	.30	67.20
3.2, 3.3	Distributables and Indirect*	.50			1.15		
	Initial Capital investment for items costed	4.06	57.41	.94	4.12	.30	68.85
4.1	Array Field Maintenance	1.26	12.21	1.50			14.97
	Capital and Maintenance Costs	5.32	69.62	2.44	4.12	.30	83.82

* Costs do not cover entire CBS item.

** Costs for this item not included.

TABLE 4-IX: FIXED TILT ARRAY DETAILED COSTS, 1978 DOLLARS

CBS No. 1.1 and 1.3

TITLE Land Acquisition and Preparation, Fence ELEMENT Labor and Materials

Item	Quantity Req'd	Unit Cost	Factors			Total Cost \$	Unit Cost \$/m ²
			Overhead	Quality Control	Prorate, Years		
Land Cost	1,260 acres	\$100.00/acre				126,000	.06
Coarse Grading	2,000,000 c.y.	\$ 1.25/c.y.				2,500,000	1.12
Fine Grading	6,080,000 s.y.	\$.38/s.y.				2,310,000	1.04
						CBS 1.1 TOTAL	\$ 2.22/m ²
(CBS 1.2, In-field Service Roads - not included)							
Security Fence	29,400 ft.	\$ 12.00/ft.				352,800	\$.15/m ²
						CBS 1.3 TOTAL	\$.15/m ²
(CBS 1.4, Lightning Protection - not included)							

101

TABLE 4-IX (Continued)

CBS No. 1.5 TITLE Field to PCU Wiring ELEMENT Labor, Materials and Equipment

Item	Quantity Req'd	Unit Cost	Factors			Total Cost \$	Unit Cost \$/m ²
			Overhead	Quality Control	Prorate, Years		
<u>Labor</u>							
Install Terminals	2,235 hrs.	\$10.50/hr.	1.8	1.06		44,800	.02
Install Module Interconnects	4,470 hrs.	\$10.50/hr.	1.8	1.06		89,600	.04
Install Cable Trays	11,100 hrs.	\$10.50/hr.	1.8	1.06		222,100	.10
Install Cables and Pigtails	5,027 hrs.	\$10.50/hr.	1.8	1.06		100,700	.05
Fabricate Pigtails	265 hrs.	\$ 7.00/hr.	2.1	1.06		4,100	--
						Labor Total	.22
<u>Materials</u>							
Insulated Cable	7,250,000 ft.	\$1.25/ft.	1.02			9,243,800	4.15
Cable Trays	1,064,000 ft.	\$4.00/ft.	1.02			4,343,000	1.95
Terminals	267,800 ea.	\$.75/ea.	1.02			204,900	.10
Compression Connectors	16,900 ea.	\$.20/ea.	1.02			3,500	--
T-compression Connectors	16,900 ea.	\$.90/ea.	1.02			15,500	.01
Pigtail Wire	101,400 ft.	\$.06/ft.	1.02			6,200	--
						Material Total	6.21
<u>Equipment</u>							
Cable Installation Vehicle	1 ea.	\$25,000 ea.			7	12,250	.01
						CBS 1.5 TOTAL	\$6.43/m ²

102

TABLE 4-IX (Continued)

CBS No. 1.6

TITLE Foundation

ELEMENT Labor, Material and Equipment

Item	Quantity Req'd	Unit Cost	Factors			Total Cost \$	Unit Cost \$/m ²
			Overhead	Quality Control	Prorate, Years		
<u>Labor</u>							
Concrete Footings	39,984 hrs.	\$10.50/hr.	1.8	1.06		801,000	.36
End Pad	1,517 hrs.	\$10.50/hr.	1.8	1.06		30,400	.01
End Attach Plates Prefab	600 hrs.	\$ 7.00/hr.	2.1	1.06		9,350	--
Attach Plates Prefab	92,022 hrs.	\$ 7.00/hr.	2.1	1.06		1,434,000	.64
						Labor Total	\$ 1.02/m ²
<u>Material</u>							
Concrete	165,700 c.y.	\$42.50 c.y.	1.02			7,183,100	3.23
3/16 Steel Plate	8,380,000 lb	\$.26 lb	1.02			2,222,000	1.00
Support Rods	165,000 lb	\$.26	1.02			43,600	.02
						Material Total	\$ 4.24/m ²
<u>Equipment</u>							
Curb Former Machine	2 ea.	\$30,000 ea.	1.05			63,000	.03
						CBS 1.6 TOTAL	\$ 5.29/m ²

103

TABLE 4-IX (Continued)

CBS No. 1.7 TITLE Enclosure ELEMENT Labor

Item	Quantity Req'd	Unit Cost	Factors			Total Cost \$	Unit Cost \$/m ²
			Overhead	Quality Control	Prorate, Years		
Enclosure Sections	19,992 hrs.	\$7.00/hr.	2.1	1.06		312,000	.14
Enclosure Ends	5,880 hrs.	\$7.00/hr.	2.1	1.06		92,000	.04
Attach Brackets	52,920 hrs.	\$7.00/hr.	2.1	1.06		825,000	.37
End Framework	491 hrs.	\$7.00/hr.	2.1	1.06		7,650	--
End Doors	544 hrs.	\$7.00/hr.	2.1	1.06		8,480	.01
Pressurization - details	759 hrs.	\$7.00/hr.	2.1	1.06		11,827	.01
" - install.	147 hrs.	\$10.50/hr.	1.8	1.06		2,950	--
Enclosure Installation	84,966 hrs.	\$10.50/hr.	1.8	1.06		1,459,000	.65
						Labor Total	1.21/m ²

TABLE 4-IX (Continued)

CBS No. 1.7

TITLE Enclosure

ELEMENT Material & Equipment

Item	Quantity Req'd	Unit Cost	Factors			Total Cost \$	Unit Cost \$/m ²
			Overhead	Quality Control	Prorate, Years		
<u>Material</u>							
Weatherized Polyester Film	53,600,000 ft ²	\$.10/ft ²	1.05			5,628,000	2.52
Adhesive	2,000 gal	\$ 50.00/gal.	1.02			102,000	.05
Blind Fasteners	8,600,000 ea.	\$.08/ea.	1.02			701,800	.31
Steel for Brackets	9,390,000 lb	\$.26/lb	1.02			2,489,800	1.12
Lumber for Doors	138 MBF	\$275.00/MBF	1.05			39,800	.02
Miscellaneous						108,000	.05
						Material Total	4.07/m ²
<u>Equipment</u>							
Enclosure Erection Equip.	4 ea.	\$ 80,000/ea.			7	156,800	.07
Miscellaneous	4 sets	\$ 20,000/set			1	80,000	.04
						Total Equipment	.11
						CBS 1.7 TOTAL	\$5.38/m ²

105

TABLE 4-IX (Continued)

CBS No. 1.8

TITLE Support Structure

ELEMENT Labor, Material & Equipment

Item	Quantity Req'd	Unit Cost	Factors			Total Cost \$	Unit Cost \$/m ²
			Overhead	Quality Control	Prorate, Years		
<u>Labor</u>							
A-Frames	8,820 hrs.	\$ 7.00/hr.	2.1	1.06		137,400	.06
Field Erection	15,582 hrs.	\$ 10.50/hr.	1.8	1.06		312,200	.14
Module Support Bracket	16,082 hrs.	\$ 7.00/hr.	2.1	1.06		250,600	.12
						Labor Total	.32
<u>Material</u>							
Dimension Lumber	3,825 MBF	\$430.00/MBF	1.05			1,727,000	.78
Connector Plates	572,000 ea.	\$.30/ea.	1.02			175,000	.08
Steel (support brackets)	1,395,000 lb	\$.26/lb	1.02			370,000	.16
Nails	22,000 kegs	\$ 17.40/keg	1.02			390,500	.17
						Material Total	1.19
<u>Equipment</u>							
Hauler-Workstand	4 ea.	\$25,000/ea.			7	49,000	.02
Miscellaneous	4 sets	\$15,000/set			1	60,000	.03
						Equipment Total	.05
						CBS 1.8 TOTAL	\$1.56/m ²

106

TABLE 4-IX (Continued)

CBS No. 1.9

TITLE Modules/Panels

ELEMENT Labor, Materials, Facility,
Equipment & Transportation

Item	Quantity Req'd	Unit Cost	Factors			Total Cost \$	Unit Cost \$/m ²
			Overhead	Quality Control	Prorate, Years		
<u>Labor</u>							
Fabrication & Assembly	150,900 hr.	\$ 8.00/hr.	2.1	1.10		2,788,000	1.26
Field Installation	15,141 hr.	\$ 10.50/hr.	1.8	1.06		303,300	.13
						Labor Total	1.39
<u>Materials</u>							
Solar Cells*	2,140,000 m ²	\$ 45.92/m ²	1.10			108,102,000	48.77
Miscellaneous Materials						6,000,000	2.69
						Materials Total	51.46
<u>Facility, Equipment & Transportation</u>							
Module Fabrication Factory	80,000 ft ²	\$ 97.00/ft ²	(unit cost based on 7 years life)		7	7,760,000	3.48
Automated Assy & Hdlg. Eqpt.	\$ 2,500,000				7	1,225,000	.55
Shipping/Handling Crates	6,000 ea.	\$250.00/ea.			7	735,000	.33
Installation Equipment	4 ea.	\$30,000/ea.			7	58,800	.03
Transportation to Site	4,281,000 c.f.	\$.18/c.f.	(1,000 miles)			771,000	.35
						Facilities, Equipment & Transportation Total	4.73
						CBS 1.9 TOTAL	\$ 57.58/m ²

* \$40/m² (1975 dollars) for interconnected cells per JPL.

\$.75/m² has been deducted for interconnecting, included under labor.

TABLE 4-IX (Continued)

CBS No. 3.2 & 3.3

TITLE Distributables & Indirect
(Construction and Plant Start-up Only)

ELEMENT _____

Item	Quantity Req'd	Unit Cost	Factors			Total Cost \$	Unit Cost \$/m ²
			Overhead	Quality Control	Prorate, Years		
Temporary Warehouse	250,000 ft ²	\$ 12.00/ft ²				3,000,000	1.34
Plant Start-up & Check-out	67,000 hrs	\$ 10.50/hr ²	1.67	1.06		1,245,000	.59
					CBS	3.2 & 3.3 TOTAL	\$ 1.93/m ²

TABLE 4-IX (Continued)

CBS No. 4.1

TITLE Maintenance (Array Field Only)

ELEMENT Parts & Equipment

Item	Quantity Req'd	Unit Cost	Factors			Total Cost \$	Unit Cost \$/m ²
			Overhead	Quality Control	Prorate, Years		
<u>Spare Parts</u>							
A-Frames & Beams	1%						.01
Enclosure & Pressurization	100%						2.76
Modules (1% per year)	20%	\$57.58/m ²					11.52
						Spare Parts Total	14.29
<u>Maintenance Equipment</u>							
Enclosure Washer	1 ea.	\$160,000 ea.			7	1,568,000*	.70
Enclosure Replacement Machine	1 ea.	\$200,000 ea.			7	1,960,000*	.88
Maintenance Truck	2 ea.	\$ 20,000 ea.			7	392,000*	.17
						Maintenance Equipment Total	1.76
* Total Cost = Annual Cost x 20 Years, Where Annual Cost = .49 x Purchase Cost For 7 year depreciation.							

109

TABLE 4-IX (Continued)

CBS No. 4.1

TITLE Maintenance (Array Field Only)

ELEMENT Labor

110

Item	Quantity Req'd	Unit Cost	Factors			Total Cost \$	Unit Cost \$/m ²
			Overhead	Quality Control	Prorate, Years		
<u>Scheduled Maintenance</u>							
Enclosure Replacement 	84,966 hrs.	\$ 10.50/hr.	1.8	1.06		1,702,200	.77
Enclosure Washing 	32,350 hrs.	\$ 10.50/hr.	1.8			648,100	.29
Filter Replacement 	17,600 hrs.	\$ 10.50/hr.	1.8			352,600	.15
Scheduled Maintenance Total							1.21
<u>Corrective Maintenance</u>							
Enclosure Repair	1,000 hrs.	\$ 10.50/hr.	1.8			20,000	.01
Pressurization Unit Repair	1,000 hrs.	\$ 10.50/hr.	1.8			20,000	.01
Module Repair/Replacement	26,700 hrs.	\$ 10.50/hr.	1.8	1.06		535,000	.24
Corrective Maintenance Total							.26
CBS 4.1 TOTAL							\$17.52/m ²
 Average at 18th year.	 Twice Annually	 Monthly					

4.6.3 Energy Cost Analysis

For the express purpose of comparing the two concepts - fixed and tracking - a dc bus bar energy cost (BBEC/dc) was developed for each concept. Indirect costs in Ref. 25 total 50% of the direct costs. These indirect costs account for contingencies and spares (25%), other indirect costs (15%), and interest during construction (10%). Since spares have been included as a direct cost under maintenance, the contingency allowance is reduced to 15%, giving a total indirect cost factor of 40%.

The initial capital investment is found from:

$$CI = (C_A \cdot A) (1 + IC)$$

where:

CI = Array Field Capital Investment, \$

C_A = Total Array Related Costs, \$/m²

A = Total Area, m²

IC = Indirect Costs

Substituting the numerical values:

$$CI = (68.85) (2.14 \times 10^6) (1 + 0.4) = \$206.3 \times 10^6$$

Bus bar energy costs based on the dc energy delivered to the power conditioning units are calculated from the initial capital investment, subsequent capital expenditures (scheduled module and/or enclosure replacement), and maintenance costs. Plant life affects the fixed charge rate and capital recovery factor used in the analysis. From Ref. 26, the equation for levelized bus bar energy cost is:

$$BBEC = \frac{FCR \cdot CI_{pv} + CRF(OP_{pv} + MNT_{pv} + FL_{pv})}{MWH_A}, \text{ mils/kW}\cdot\text{h}$$

where: FCR = fixed charge ratio

CI_{pv} = present value of the capital investment, \$

CRF = capital recovery factor

OP_{pv} = present value of operating costs, \$

MNT_{pv} = present value of maintenance costs, \$

FL_{pv} = present value of fuel costs, \$

MWH_A = expected annual energy output, MW·h

In this analysis, operating and fixed costs are assumed equal to zero. If the economic plant life is 20 years, same as the modules, the cost of the energy is (Ref. 26):

$$\begin{aligned} \text{BBEC (dc)} &= \frac{(.1589)(68.85 + 1.77) + (.1019)(9.46)}{.810 \times 365 \times .8 \times 10^{-3}} \\ &= 51.5 \text{ mills/kW}\cdot\text{h(dc)} \end{aligned}$$

The value 1.77 is the present value of the enclosure replacement at 19 years in $\$/\text{m}^2$. The denominator is the average annual energy production in $\text{mW}\cdot\text{h}$ using the previously computed average daily output and a 0.8 factor to account for cloudy days. With a 30 year plant life and module replacement at 20 years:

$$\begin{aligned} \text{BBEC (dc)} &= \frac{(.1483)(68.85 + 1.77 + 27.24) + (.0888)(15.82)}{.810 \times 365 \times .8 \times 10^{-3}} \\ &= 67.3 \text{ mills/kW}\cdot\text{h(dc)} \end{aligned}$$

The 27.24 entry is the present value of the cost of replacing the modules at 20 years. The results indicate that is not economical to replace modules (other than failed ones) to extend plant economic life.

5.0 TRACKING ARRAY DESIGN CONCEPT

The design goal for the tracking array was to use as much of the BEC prototype commercial heliostat configuration as possible, consistent with an effective photovoltaic system. The configuration size is controlled by using the heliostat 9.7 meter (31.8 foot) diameter spherical enclosure and base, and its foundation. Much less sensitivity to pointing errors permits a simplified drive and control system. Two approaches to the module and module support structure configuration were considered:

- 1) A design with minimum departure from the heliostat configuration is shown in Figure 5-1. This design uses a large one-piece panel for each array, which attaches to a circular ring supported from the gimbal mount by four arms. The ring and arms are essentially identical to the heliostat reflector support structure. The panel uses a plastic film substrate similar to the fixed-tilt array.
- 2) One disadvantage of the one-piece panel is the necessity of removing the enclosure to remove/replace the panel. A second configuration was designed to allow removal and replacement of smaller panels without disturbing the enclosure. This configuration shown in Figure 5-2 uses rhombic shapes for the modules which are then assembled into hexagonal-shaped panels, each composed of nine modules. One array utilizes seven panels. A hexagonal frame supports the seven panels which are attached to mounting plates on the six arms that radiate from the gimbal mount.

The one-piece panel configuration, Figure 5-1, is less complex and more fully utilizes the space within the enclosure. Hence, this design would be expected to produce energy at a somewhat lower cost compared to the small module configuration. However, maintenance requiring removal/replacement of a one-piece module also requires removal of the enclosure for access to the module. Enclosure replacement in the heliostat program will be accomplished with a mobile facility that straddles the enclosure, providing wind protection and overhead lifting capability, Ref. 8. The mobile facility is well suited to systematic removal and replacement of all units, but may be less cost effective for traveling throughout the array field to remote units with failed modules.

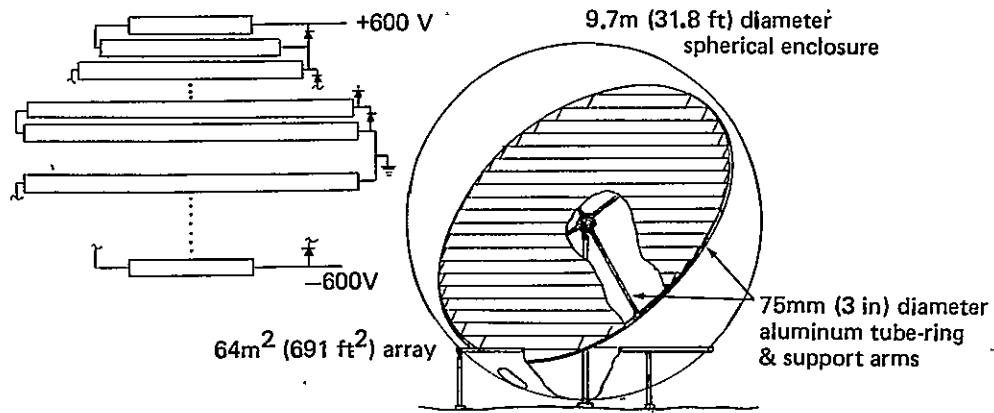


Figure 5-1. Large Panel Tracking Array

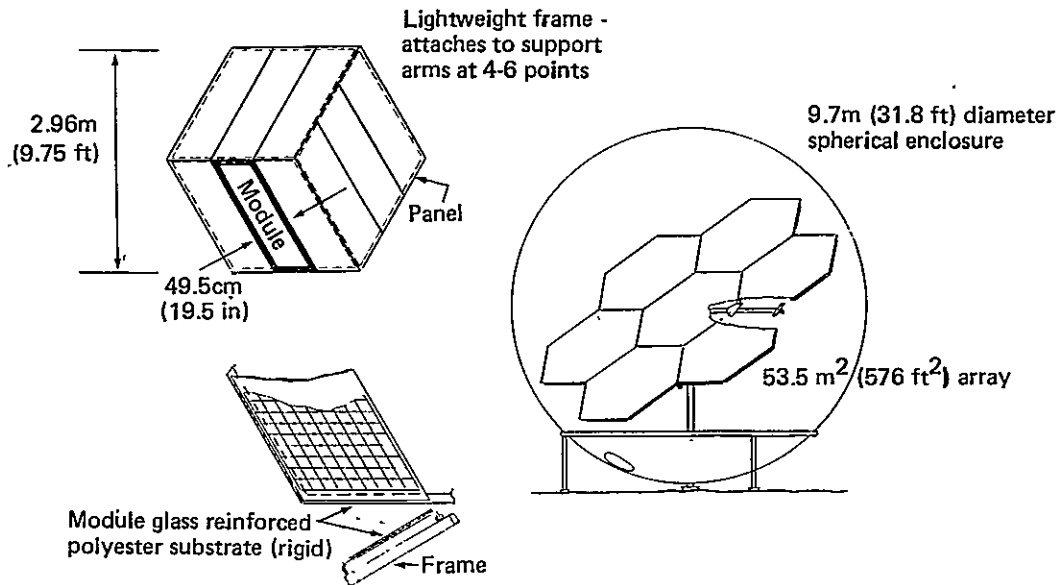


Figure 5-2. Small Panel Tracking Array

The best choice between the two configurations depends on the relative array performance and cost, module failure rates, and the relative maintenance costs. Time and available data were insufficient to permit a detailed evaluation of these parameters. Therefore, the small-module configuration was selected as the more conservative (but possibly less cost-effective) design concept.

The tracking array design relies very much on the heliostat design concept studies, Ref. 4 and Ref. 8. Design and supporting analyses from the heliostat program are covered only briefly here; further information can be found in the references.

5.1 Concept Description

While the dimensions of the fixed array depended to some extent on the total power station geometry, the tracking array size is completely independent of the overall array field. For the selected array size, using the baseline heliostat enclosure diameter of 9.7 meters (31.8 feet), each array produces about 4.9 kW. Using the 232.2 MW total array output from Section 4.0, the number of arrays required is 43,880. The spacing between arrays could be established by a trade of energy cost as affected by land and wiring cost, and array shadowing and wiring resistance losses. Costs in this study are based on an array spacing with the ratio of enclosure projected area to land equal to 4. This is representative of the similar heliostat field density. The arrays are spaced 17.1 meters (56 feet) center-to-center for this area ratio, which gives adequate clearance for equipment. Shadowing analysis with this array geometry is a complex problem and was not performed. A less dense array field may be optimum; even so, the selected tracking array field is 2-1/2 times the fixed array field area.

5.1.1 Protective Enclosure

The protective enclosure is a transparent weatherized polyester material thermoformed to a spherical shape. The spherical enclosure is truncated at

a 45° angle from the spherical center to interface with an attachment fitting at the base support ring. The enclosure is thermoformed from a 0.05 centimeter (0.020 inch) thick weatherized polyester film. The thermoforming results in a finished dome with a minimum film thickness of 0.008 centimeters (0.003 inches). The enclosure joins the base/foundation at a retention fitting which provides the tension load path and a positive air pressure seal.

5.1.2 Base/Foundation

The base/foundation consists of the above and below ground structure required to support and environmentally protect the array, tracking system and the transparent protective enclosure. The air supply system is considered part of the base/foundation. The above ground structure consists of a steel hemispherical dish segment welded to a circular steel pipe support ring. Loads are transferred from the transparent protective enclosure across the steel dish and into the support ring. Three steel pipe stanchions carry loads from the support ring to the subground structure. A steel pipe forms the pedestal mount for the array and gimbal. A diaphragm seal provides airtight penetration of the pedestal through the bottom of the steel dish. The subground structure used to support the stanchions and pedestal consists of four auger-cast concrete piles.

The access hatch located on the dish is elliptical in shape allowing complete removal of the hatch by rotating and tipping. Inside pressure augments the sealing force. The electronics package is mounted on the inside surface of the hatch, for convenient access.

Four components made up the pressurization system; a prefilter, a rotary vane compressor, a primary filter and a pressure relief valve. These components are located external to the heliostat in a sheet metal canister. The maximum power consumption of the air supply system is 10 watts. A positive internal pressure 690 Pa (0.1 psig) above external ambient pressure is required to maintain clearance between the enclosure and array.

5.1.3 Array Support Structure

The overall support structure configuration is shown in Figure 5-3 and its details are described in Figures 5-4 through 5-7. The basic approach with this design is to use available material forms with the minimum amount of further processing. The tracking array support structure assembly is counter-weighted as shown in Figure 5-7 to minimize torque loads on the drive system.

5.1.4 Tracking System

The elevation and azimuth drive concepts chosen for the tracking photovoltaic array system are shown in Figures 5-8 and 5-9. The design uses a gear motor and speed reduction system to rotate the array, and an inexpensive position potentiometer at each gimbal to sense array position.

The selected control system concept is based on microprocessor technology. microprocessor-based system provides capability for sun tracking and permits expansion of the basic system to include controlling or monitoring other components of the array, such as array output and temperatures. Primary components of the sun tracking control system are the system controller, array controller and interconnecting multiplexed serial data bus. One system controller for the array field and an array controller for each array are required.

The micro-programmable system controller, Figure 5-10, includes a central processing unit (CPU), random access memory (RAM), programmable read only memory (PROM), clock standard, and optional input/output capability for interfacing with a keyboard-printer terminal and a two-way serial data bus. Universal asynchronous receiver transmitters (UART's) may be used for keyboard printer and serial data bus communications in conjunction with a standard communication link, RS-232-C specification and differential voltage driver/receivers. All components of the system controller, with the exception of the driver/receivers, operate from a single 5 VDC power source. This approach provides increased reliability, reduced cost and a simplified battery backup capability.

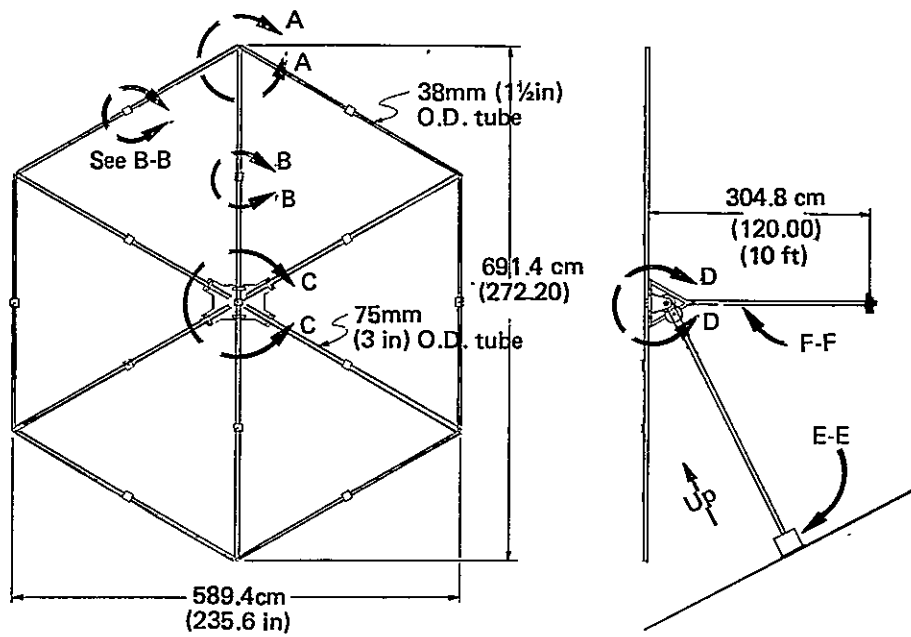


Figure 5-3. Tracking Array Support Structure Framework

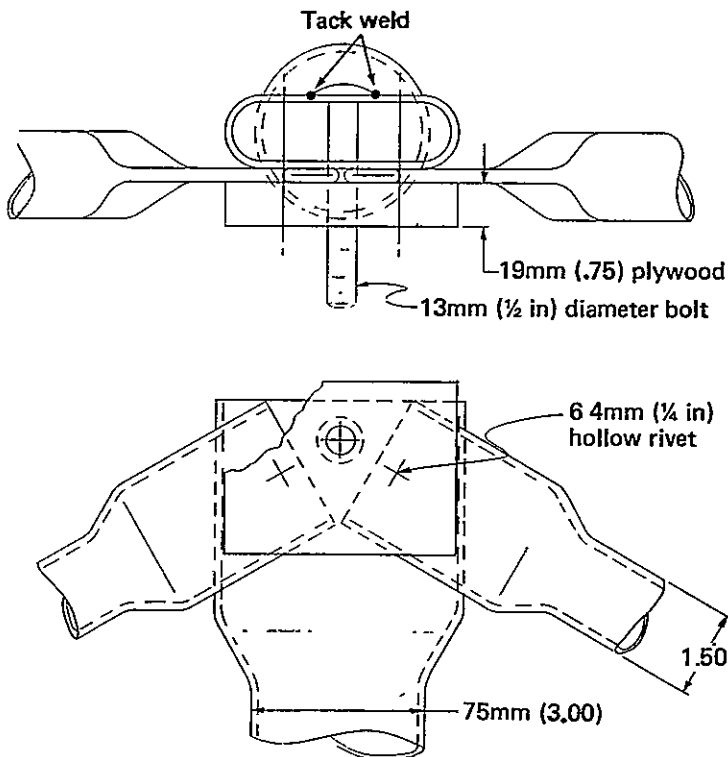


Figure 5-4. Tracking Array Outboard Support Arm Joint Detail (Sec A-A)

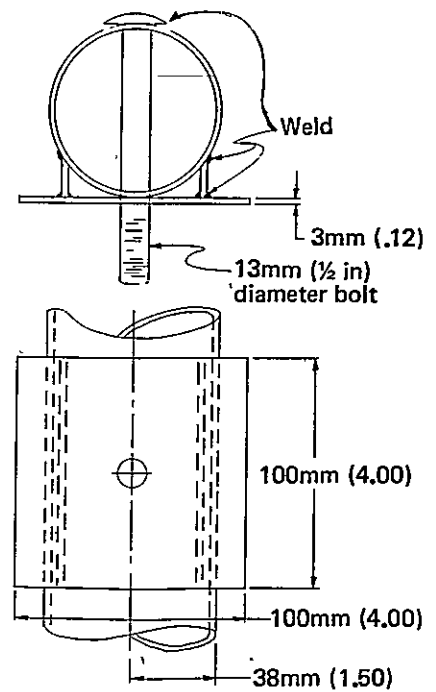


Figure 5-5. Tracking Array Midspan Support Point Detail (Sec B-B)

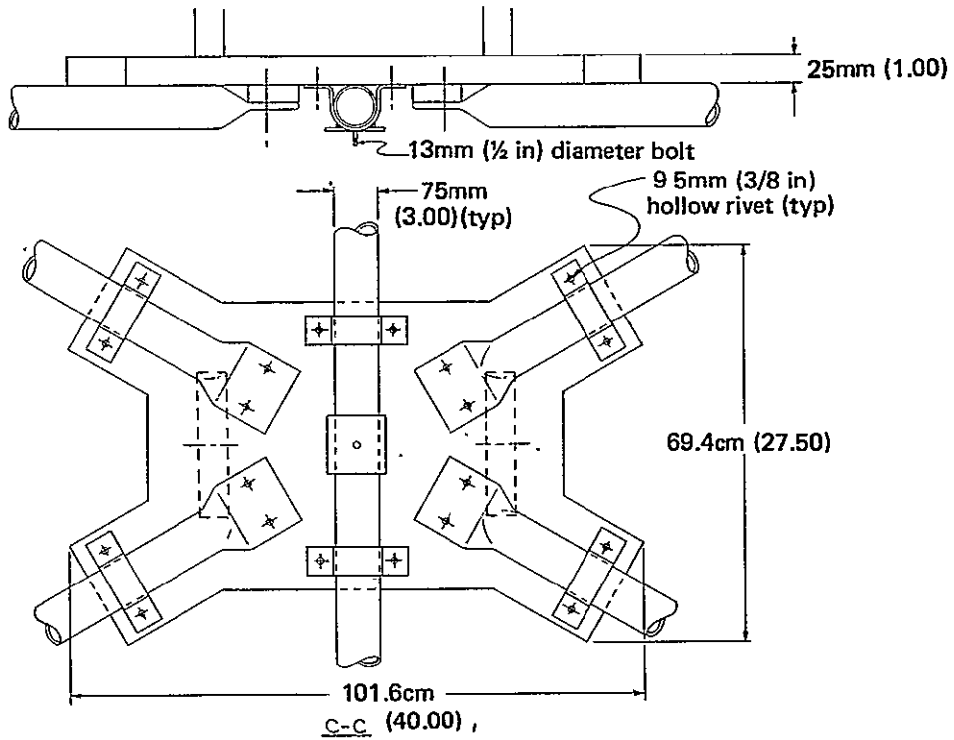


Figure 5-6. Tracking Array Inboard Support Arm Detail (Sec. C-C)

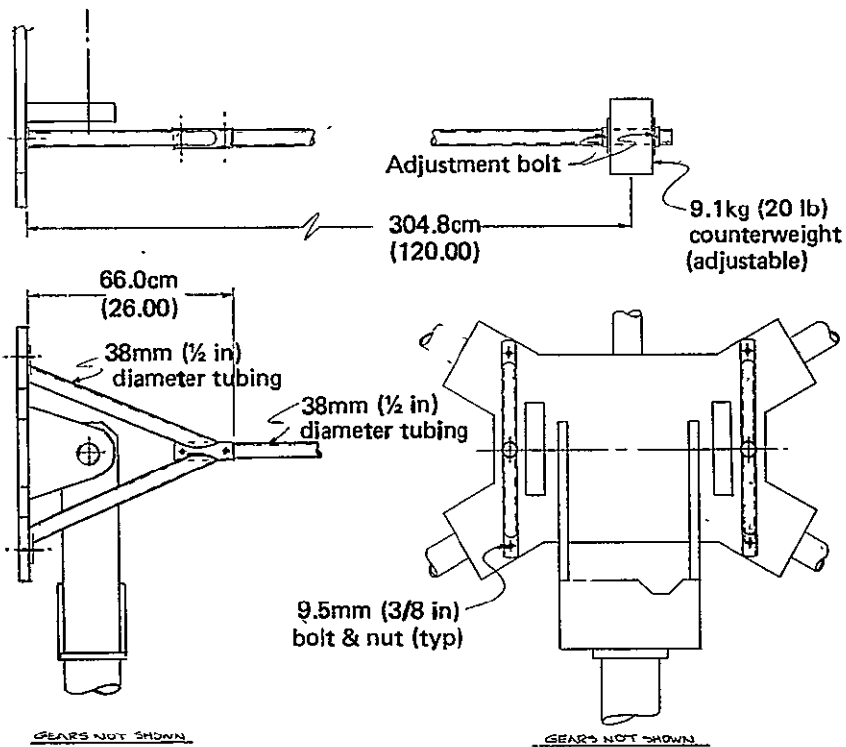


Figure 5-7. Tracking Array Gimbal Mount and Counterweight Detail (Sec. F-F)

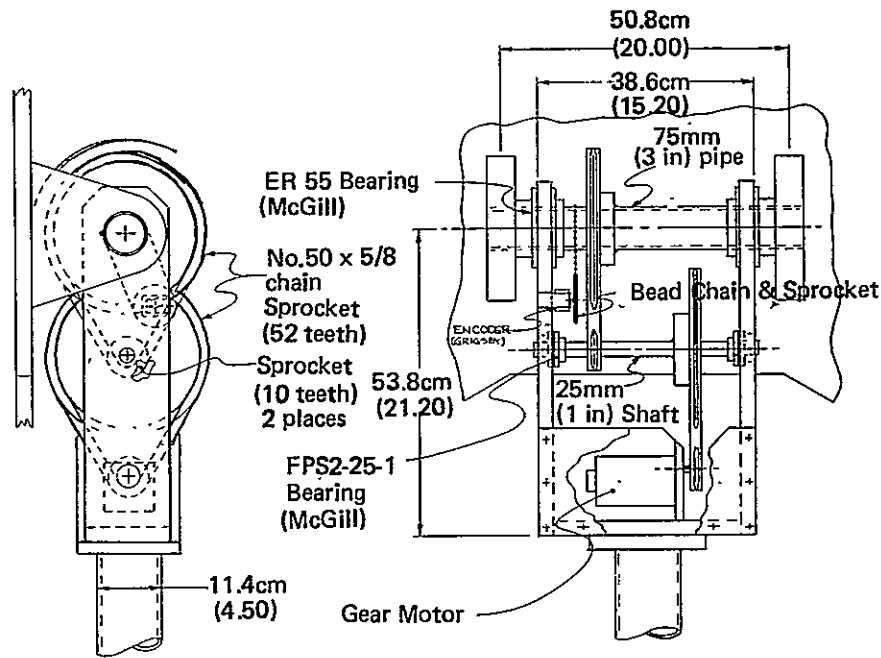


Figure 5-8. Tracking Array Elevation Drive Detail (Sec. D-D)

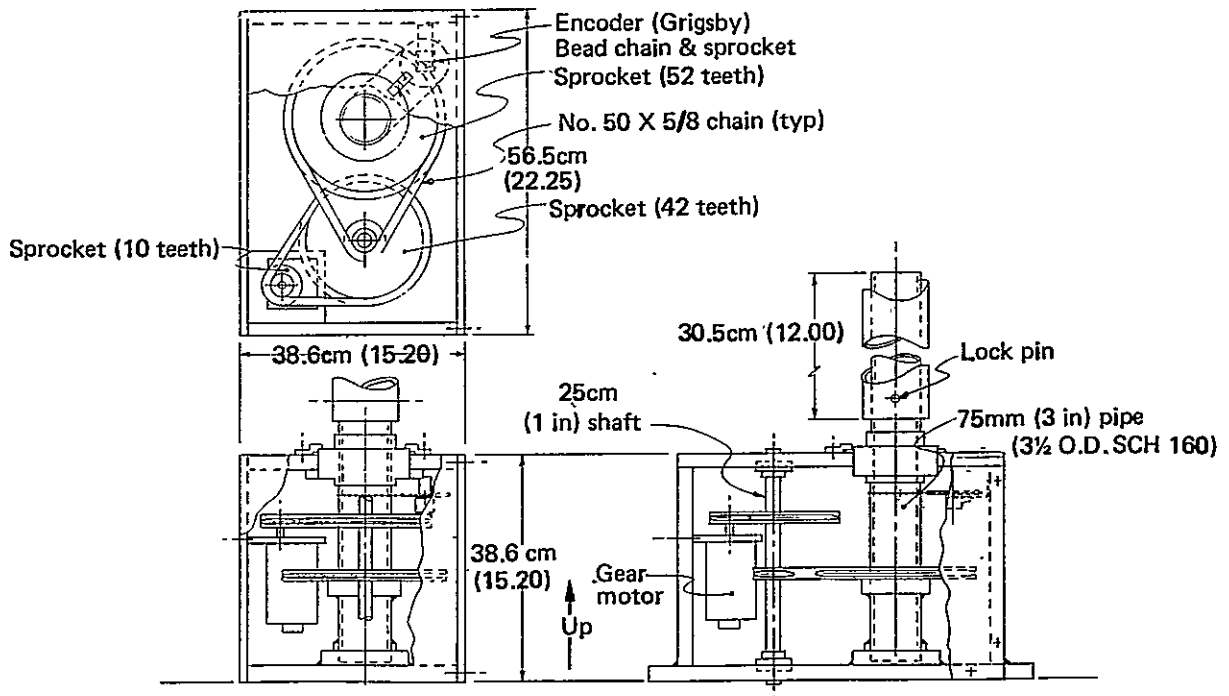


Figure 5-9. Tracking Array Azimuth Drive Detail (Sec. E-E)

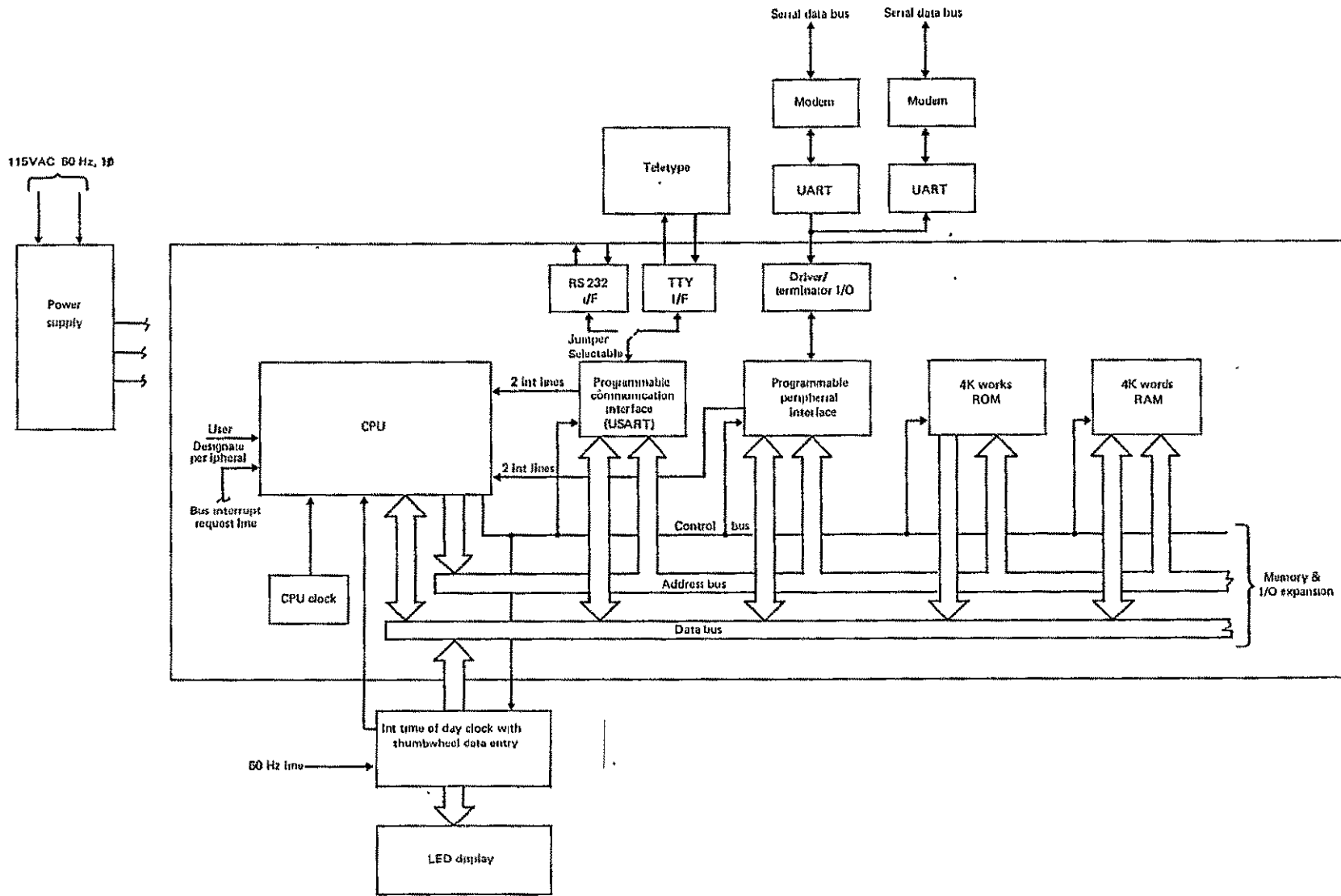


Figure 5-10. Tracking Array Field System Controller

The trigonometric calculations required for the proper positioning of each movable array, and the transmission of these data to the respective unit controllers once every thirty seconds, is the major computation requirement on the controller. PROM memory contains the necessary algorithms, instructions, and ephemeris data to calculate tracking parameters for a given day. These are read into RAM memory once each day before tracking begins. In addition, the system controller has provisions for interactive control from a keyboard for checkout and maintenance by an operator. The system controller could also perform functions such as array temperature evaluation, air pressure monitoring, alarm activation, unit controller loss-of-communications detection, array status data processing and storage, and data bus communications control.

A unit controller, Figure 5-11, located at each array contains a micro-computer which compares true position data from a position potentiometer mounted at each gimbal with desired position data as received over the multiplexed communications bus. Appropriate control signals activates solid-state switches in the motor control power supply unit which powers the gear motor in a forward or reverse direction, as required, to achieve the desired array position. The above components constitute a closed loop servo system to maintain array position within the required tracking tolerance.

A manual control panel on each tracking array contains necessary controls to turn off the automatic servo system and allow manual control of the array drive unit in forward or reverse, high or low speed modes.

Failure of the tracking system does not cause or make possible any catastrophic events, but it can result in degraded power output. If the system controller is inoperative, all arrays will remain in identical orientations, and the power output will be characteristic of a fixed array field. An inoperative system controller for more than a few hours would reduce daily power output by 30% or more for mid-day failures and would

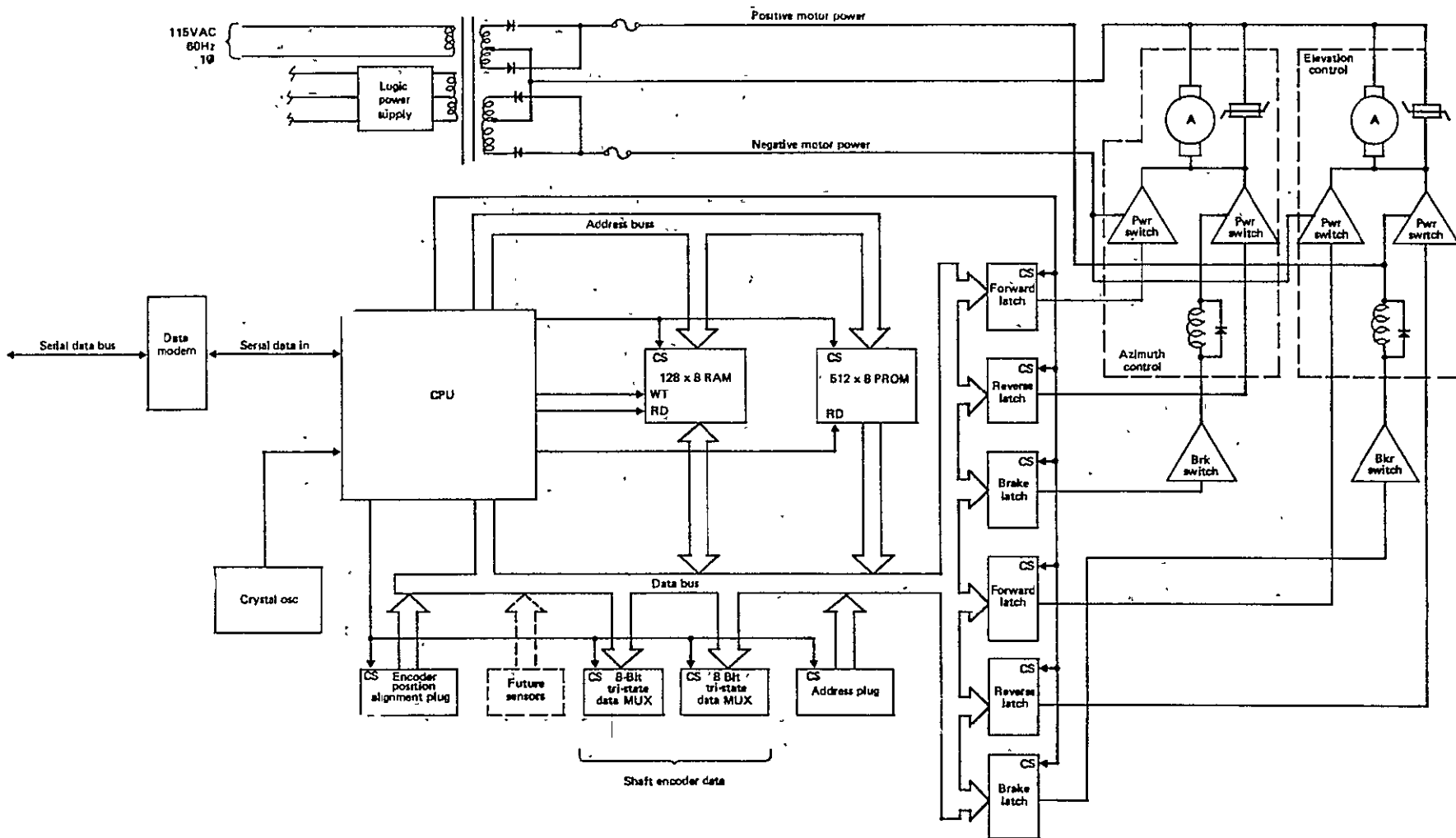


Figure 5-11. Tracking Array Controller

essentially shut down the power station if failures occurred early or late in the day. The system controller has a backup battery power supply in case power is interrupted. Redundant system controllers could be provided at a negligible increase in the bus bar energy cost. Failure of an individual array tracking system will degrade the panel's maximum current capability as the sun angle moves from the array normal. Eventually, the panel could be removed from the circuit by a panel bypass diode. The array controller can signal its failed condition, or the failure can be detected by a periodic visual check of relative array orientations.

5.1.5 Photovoltaic Modules

Configuration of the tracking array is shown in Figure 5-12. A total of 63 rhombic modules are mounted in the seven hexagonal frames. The frames are made of wood as shown in Figure 5-13 and attach to the support structure as shown in Figures 5-14 through 5-16. The module design concept is shown in Figure 17. A thin plywood substrate is used to provide bending rigidity. The modules are interconnected and provided with bypass and blocking diodes, as shown in Figure 5-18 and produce a nominal system voltage of about 800 volts dc and a maximum of about 1000 volts dc. If dictated by constraints on the power conditioning equipment or other reasons, the system could be limited to 600 volts by using 50% wider modules, with 42 modules per array. The cells shown in Figure 5-12 are the same as for the fixed-tilt array except for size. As previously discussed, the initial cell size considered was five centimeters square. This was slightly reduced for the fixed-tilt array to fit a previously selected panel size. The five centimeter cell size was retained for the tracking array. Although the substrate for the tracking array modules are rigid, compared to the flexible film used in the fixed-tilt array, and sizes are quite different, the basic production concept is the same. Rigid modules are used for the tracking array for convenience in removing and replacing modules for maintenance.

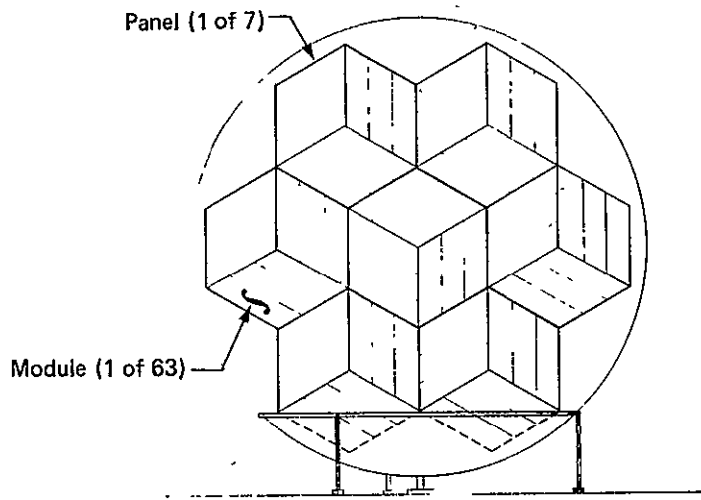


Figure 5-12. Tracking Array Panel and Module Configuration

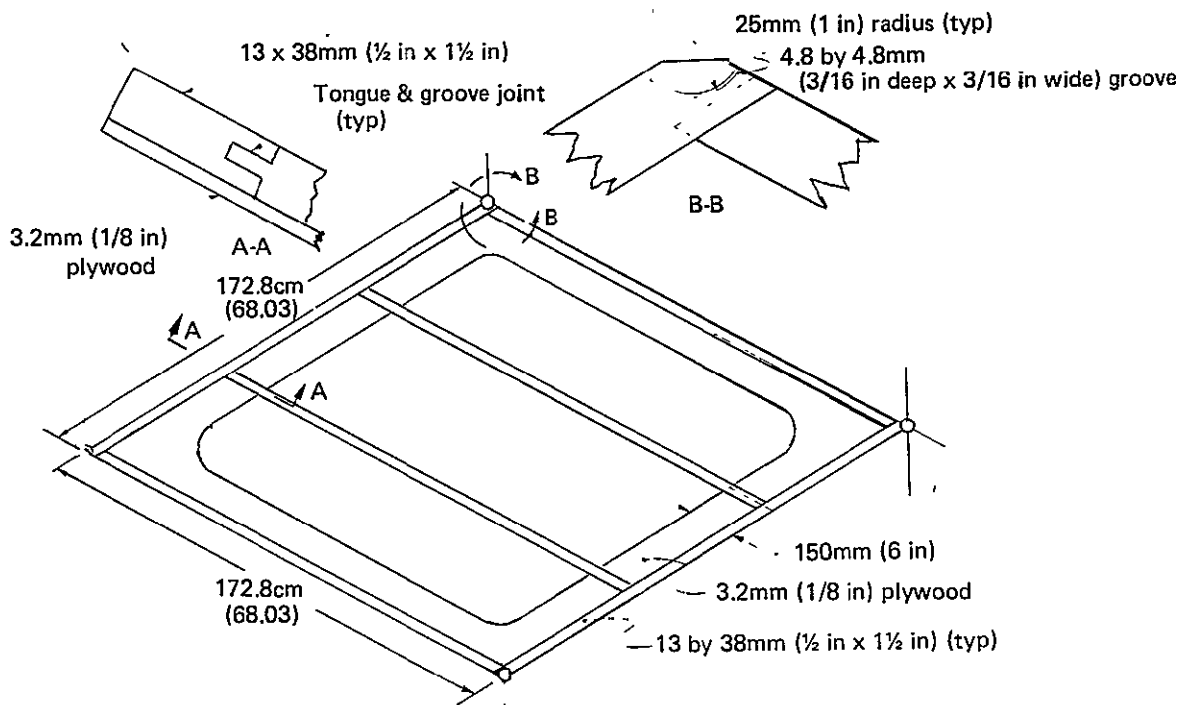


Figure 5-13. Module Mounting Frame (Three per Panel)

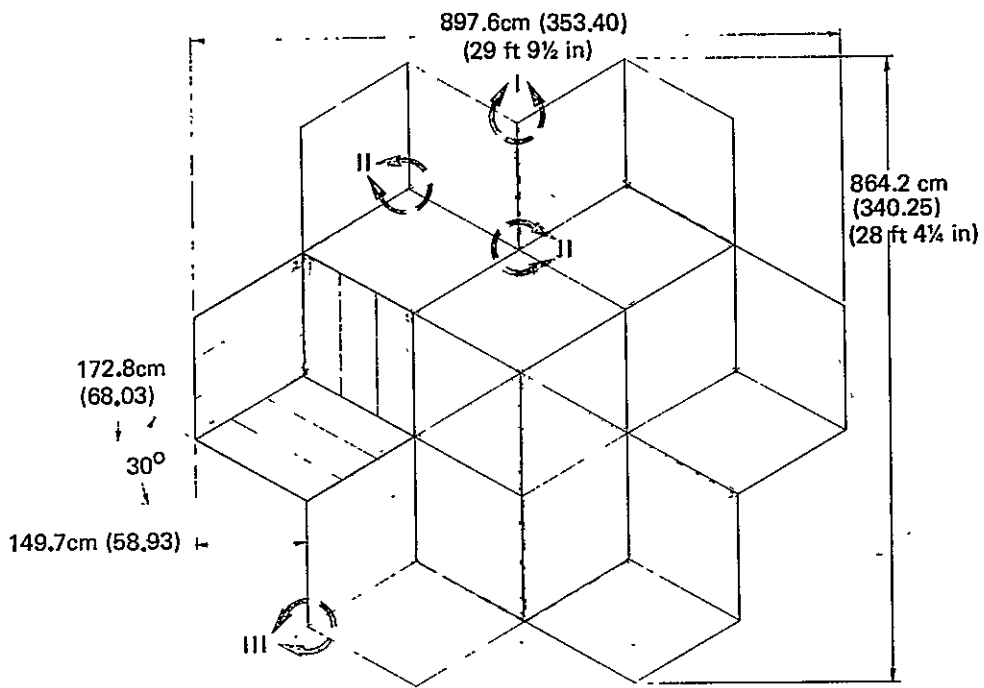


Figure 5-14. Tracking Array Panel Support Structure Configuration

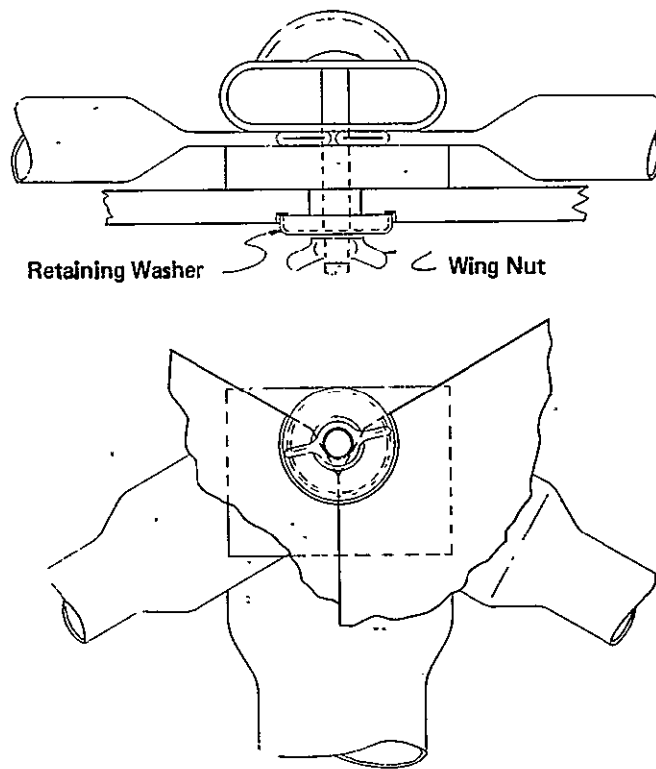


Figure 5-15. Tracking Array Panel Attachment (Detail I)

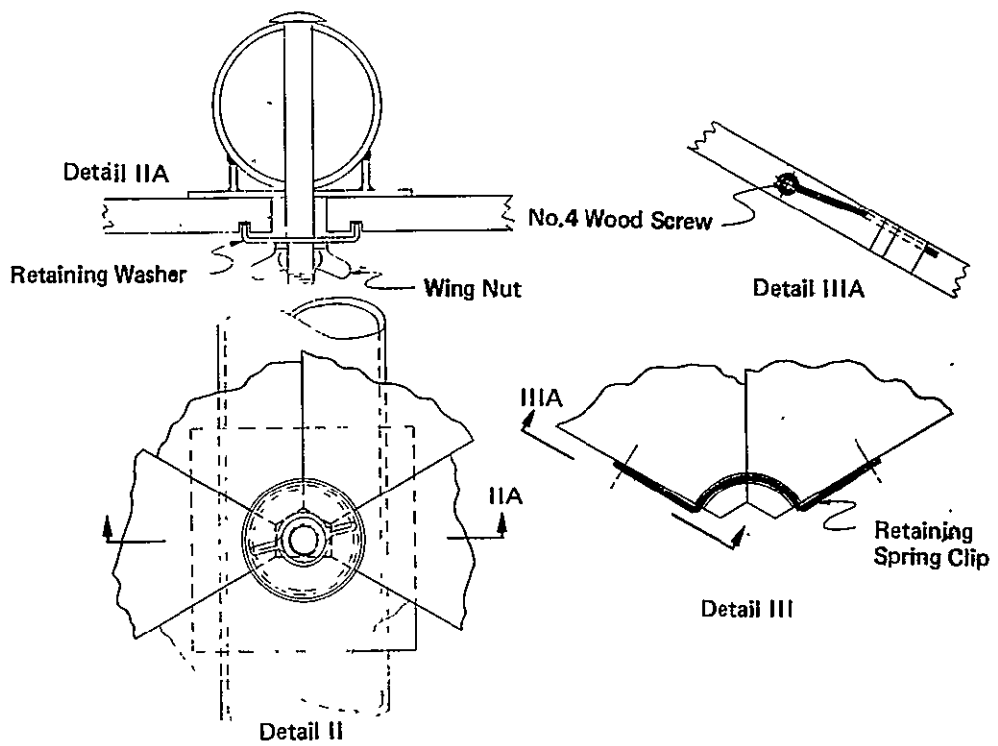


Figure 5-16. Tracking Array Panel Attachment (Details II & III)

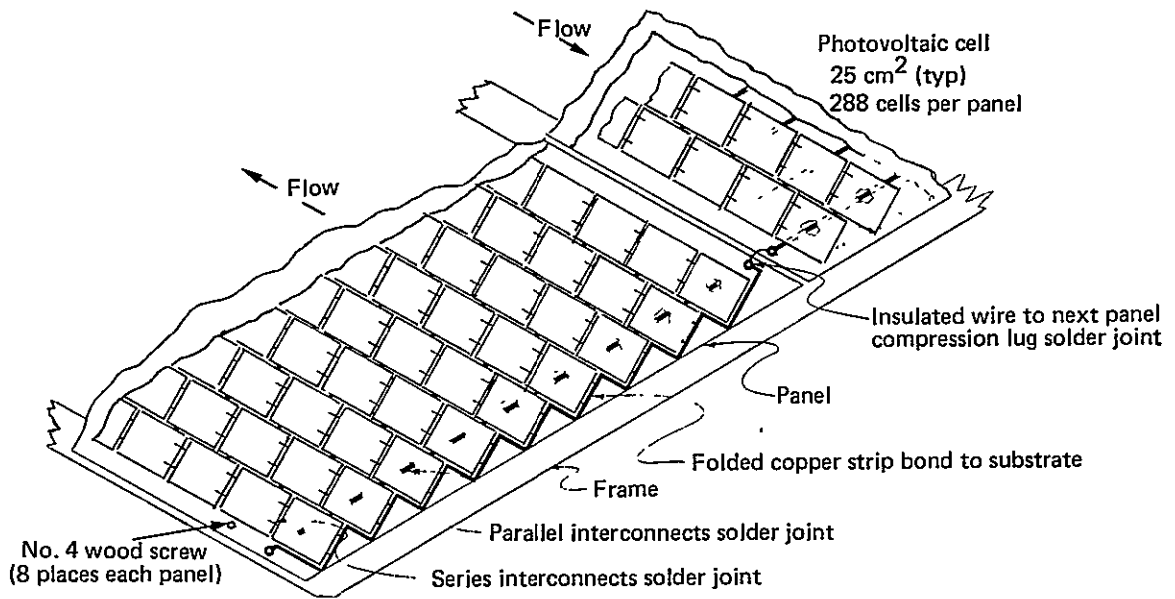


Figure 5-17. Detail of Tracking Array Photovoltaic Module/Panel

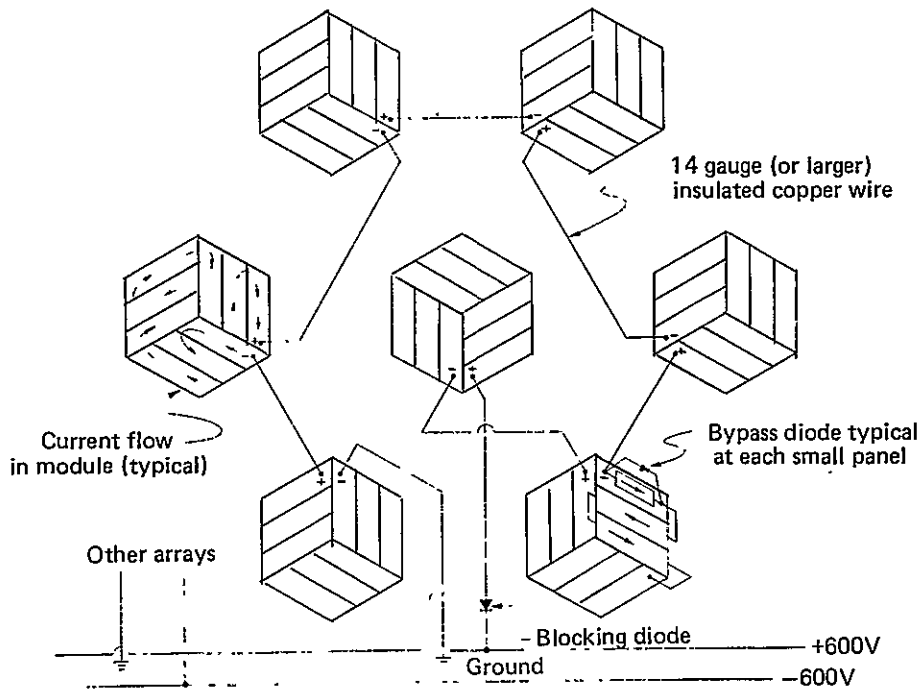


Figure 5-18. Tracking Array Module/Panel Interconnections

5.1.6 Power Collection Wiring

The wiring which gathers power within the array subfield does not have the protection provided by the enclosure as in the fixed array concept. Therefore, the wiring must be buried or placed in a covered trench. With the tracking arrays, the array subfield configuration can be more compact, with several shorter circuits collecting power.

5.2 Design Analysis

5.2.1 Environmental Loads

The discussion in Section 4.2.1 for the fixed array is generally applicable to the tracking array although specific details may differ. The following briefly covers the enclosure wind loads analysis. A more thorough discussion may be found in Ref. 4 and Ref. 8.

5.2.1.1 Enclosure Wind Loads Analysis

Transparent enclosure size is controlled by wind velocity and the allowable stress of the membrane material. A wind tunnel test program (Ref. 4) was performed to determine the pressure distribution on enclosures and the effect on pressure distribution of sheltering due to the density of the array and a peripheral fence. Tests ranged from single units to 60 enclosure models in square and diagonal patterns, at varying spacing densities. The design nomograph obtained from the heliostat wind tunnel test program, Figure 5-19, permits determination of the allowable enclosure size based on array density, enclosure configuration, and enclosure material allowable strength. For the selected field density (enclosure plan view projected area divided by ground area) of 0.25, the nomograph indicates an enclosure membrane load of 6.13 kN/m (35 lb/in) requiring a minimum polyester thickness of 0.08 millimeters (0.003 inch).

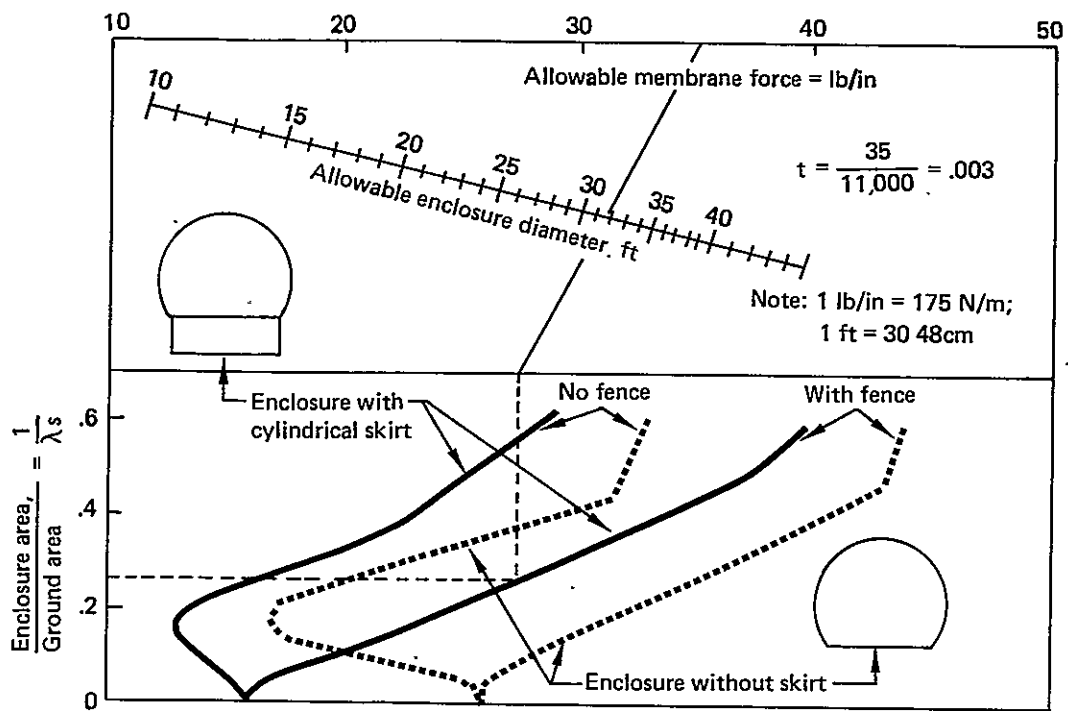


Figure 5-19. Allowable Enclosure Diameter from Wind Tunnel Test Results

The wind tunnel measurements also provided overall forces acting on the enclosure and base, and sized the concrete auger-cast piles supporting the base. The foundation for the central pedestal does not carry any of the wind loads due to a flexible boot seal between the pedestal and base.

5.2.2 Electrical Design

Detailed analysis of the array shadowing and failure effects were not performed for the tracking array. The shadowing geometry is very complex and could best be done with a computer analysis, which is beyond the scope of this study. Failure effects are expected to be comparable to the general behavior of the fixed array, so that the number of series and parallel elements and placement bypass and blocking diodes can be selected to give an acceptable design.

5.2.3 Tracking System

The maximum angular error is assumed to apply to both the elevation and azimuth axes. The angular error budget for each of the axes is given in Table 5-1. With the maximum error in each axis based on arithmetical addition of the errors, the peak angular error is approximately seven degrees. However, a more realistic root-sum-square combination indicates nominal pointing error of 3.2 degrees, or only about 0.2% performance loss due to pointing inaccuracies.

The maximum gimbal angular accelerations are 0.032 rad/sec^2 for the azimuth axis and 0.004 rad/sec^2 for the elevation axis. Torques due to acceleration are calculated to be $23.6 \text{ N}\cdot\text{m}$ ($17.4 \text{ lb}\cdot\text{ft}$) and $3.2 \text{ N}\cdot\text{m}$ ($2.3 \text{ lb}\cdot\text{ft}$) for the azimuth and elevation axes. With assumed values of static friction torque of $9.1 \text{ N}\cdot\text{m}$ ($6.7 \text{ lb}\cdot\text{ft}$) in the azimuth and $2.3 \text{ N}\cdot\text{m}$ ($1.7 \text{ lb}\cdot\text{ft}$) for elevation and $.3 \text{ N}\cdot\text{m}$ ($.2 \text{ lb}\cdot\text{ft}$) gear friction, the maximum torque loads are $49.4 \text{ N}\cdot\text{m}$ ($36.4 \text{ lb}\cdot\text{ft}$) and $8.4 \text{ N}\cdot\text{m}$ ($6.2 \text{ lb}\cdot\text{ft}$) about the azimuth and elevation axes, respectively.

Table 5-1 Angular Error Budget

(a)	Azimuth error budget	
	Position feedback device (accuracy and resolution)	+ 1.76 ^o
	Alignment accuracy	+ 0.50 ^o
	Overshoot and nonlinearity	+ 1.00 ^o
	Update rate error (30 sec)	+ 0.06 ^o
	Calculation error (single precision)	+ 0.05 ^o
	Structural deflection	+ 1.11 ^o
		<u>+ 4.93^o</u>
(b)	Elevation error budget	
	Position feedback	+ 1.22 ^o
	Alignment accuracy	+ 0.050 ^o
	Overshoot and nonlinearity	+ 1.00 ^o
	Update rate error (3 min)	+ 0.30 ^o
	Calculation error	+ 0.50 ^o
	Structural deflection	+ 1.11 ^o
		<u>+ 4.63^o</u>

Assuming a Bodine Model NSH-11D5 gear motor with drive model 535, the low end speed is $1.2^{\circ}/s$. The maximum tracking speed is $0.0555^{\circ}/s$, requiring a speed reduction between the motor and the azimuth gimbal shaft of 21.6:1. The gear ratio for the elevation axis must be 27:1. With these reduction ratios and a 30% reduction of efficiency due to the low speed through the worm gears, the torque capability is 67.8 N·m (50 lb·ft) in the azimuth and 85.4 N·m (63 lb·ft) for elevation, well above the requirements.

5.3 Thermal/Performance Analysis

5.3.1 Groundrules and Assumptions

The SOLMET tape data for Phoenix, Arizona, supplied insolation values for the tracking array analysis. Environmental conditions of wind and ambient ground temperatures are the same as for the fixed array transient thermal analyses. The tracking steady state environmental conditions are also the same as the fixed array case.

5.3.2 Ambient Environment

A small computer calculation program provided the necessary changes in insolation data. The total horizontal surface insolation had to be transformed into total insolation onto the tracking array, Ref. 14. The same ambient temperature-time relationships were used for the tracking array as for the fixed array.

5.3.3 Thermal Performance Model Description

The main part of the nodal network used in the BETA program to describe the tracking array is shown in Figure 5-20. Allowing for changes in geometry, the heat transfer relationships between the nodes of the tracking array are the same as the relationships used for the fixed array.

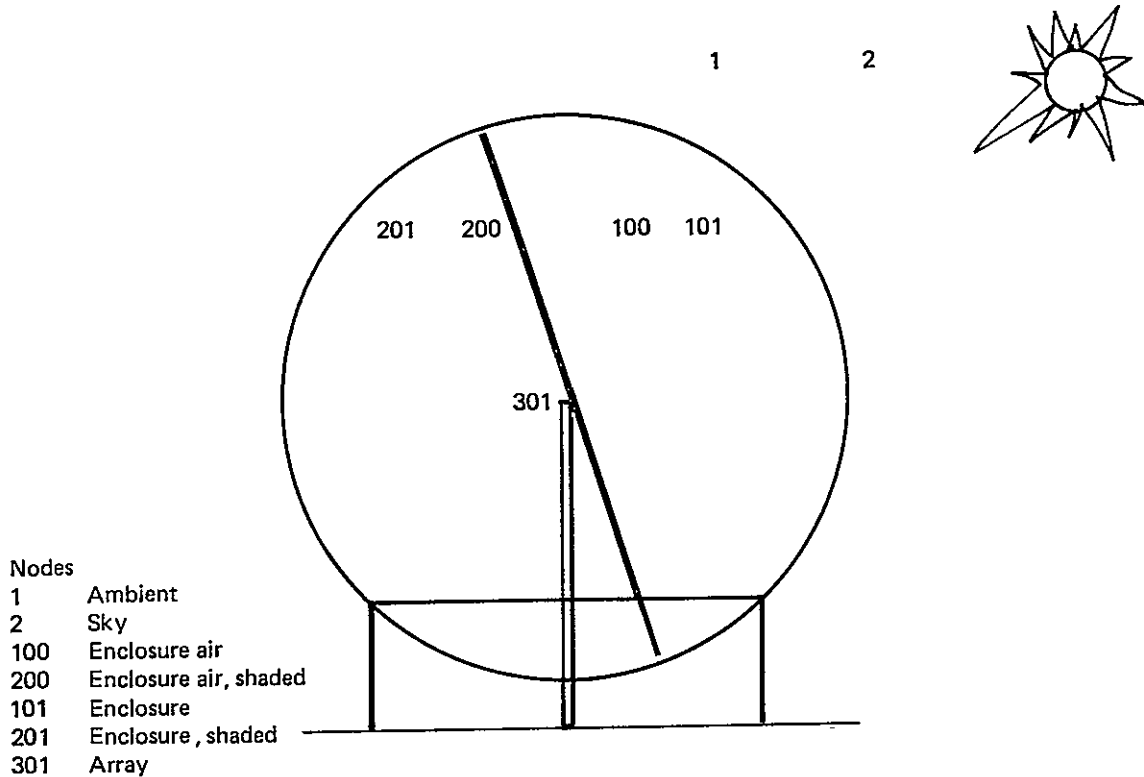


Figure 5-20. Nodal Network for Tracking Array

5.3.4 Temperature Predictions

5.3.4.1 Seasonal Analyses

Temperature predictions for the four seasons are shown in Figure 5-21. The highest array temperature is 78°C (173°F) at 3:00 PM in the summer. The corresponding enclosure temperature and enclosure ambient temperature are 48°C (118°F) and 58°C (136°F) respectively. The component temperatures react quickly to insolation and ambient temperature input.

5.3.4.2 Extreme Temperature Analysis

The extreme temperature time relationships created for the fixed array were also used for the tracking array. The results are shown in Figure 5-22. The array peaks at 86°C (186°F).

The array extreme temperatures are similar for the tracking and fixed arrays. The tracking array is 6.1°C (11°F) hotter than the fixed array because it has more incident insolation. The cold extremes are practically the same.

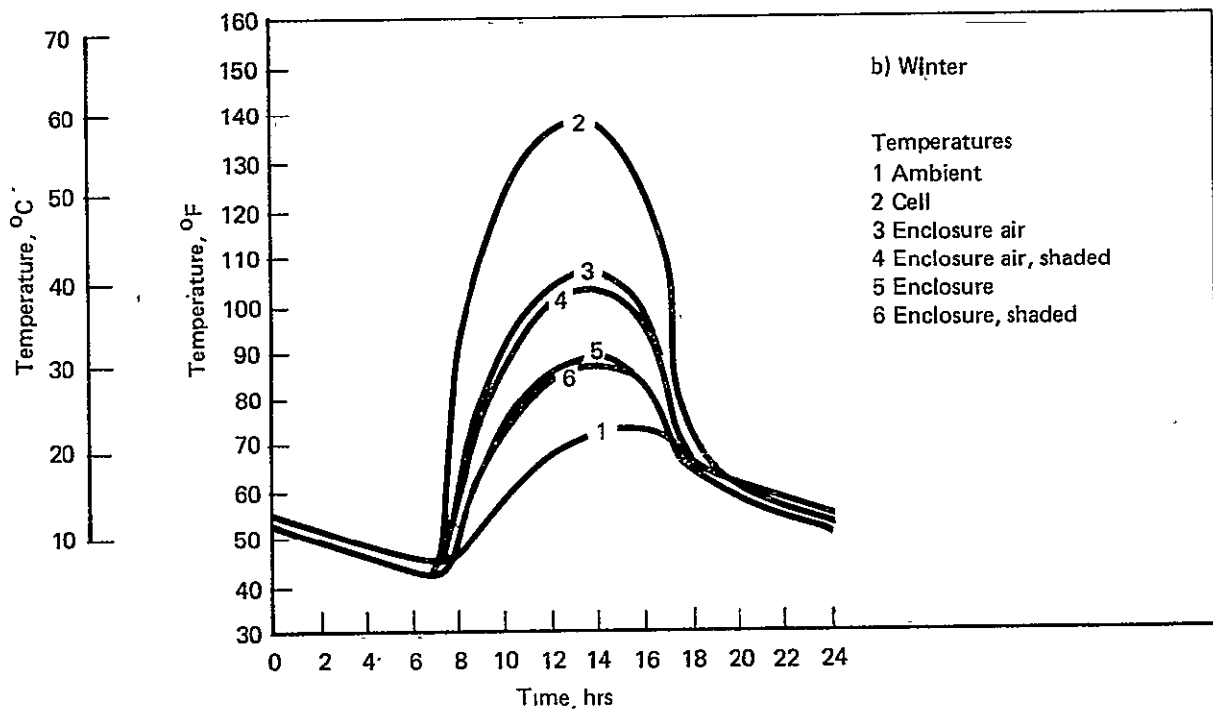
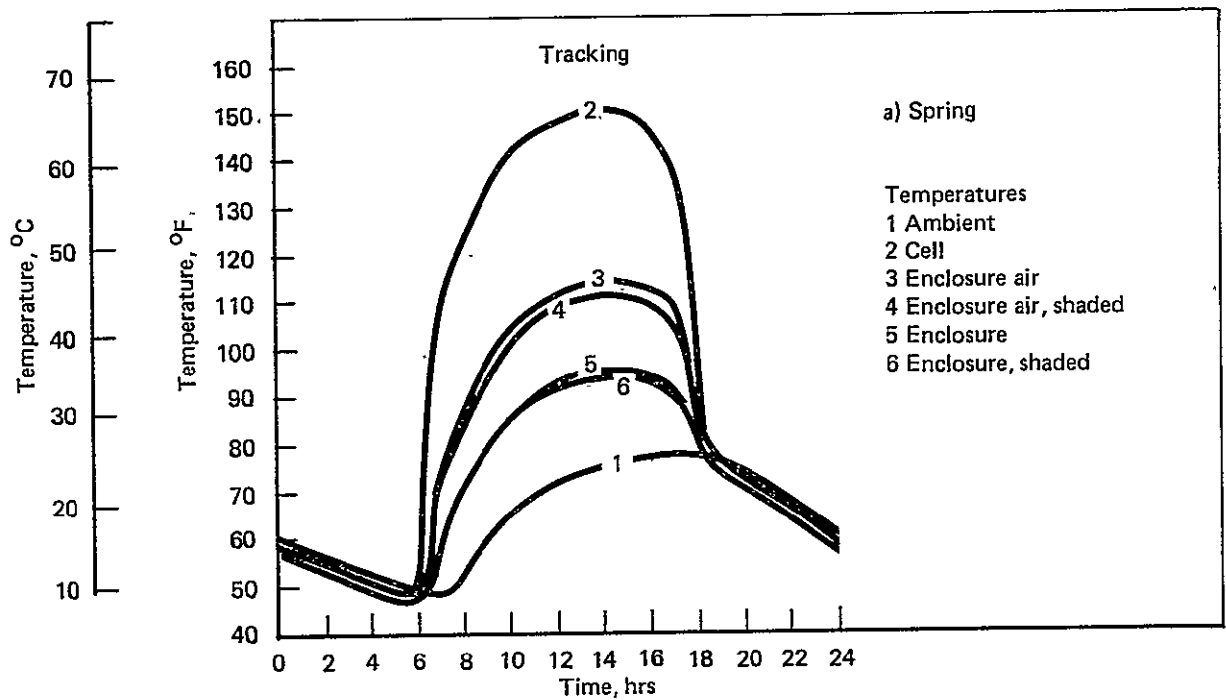


Figure 5-21. Temperature Predictions for Tracking Array

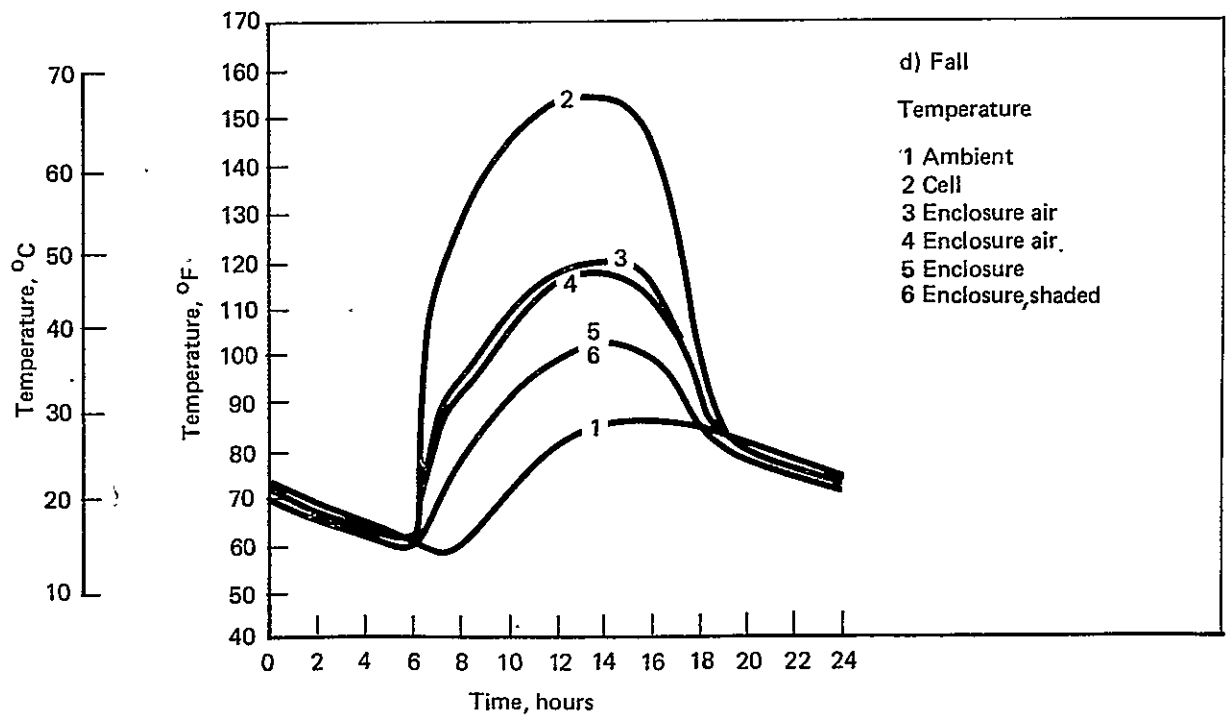
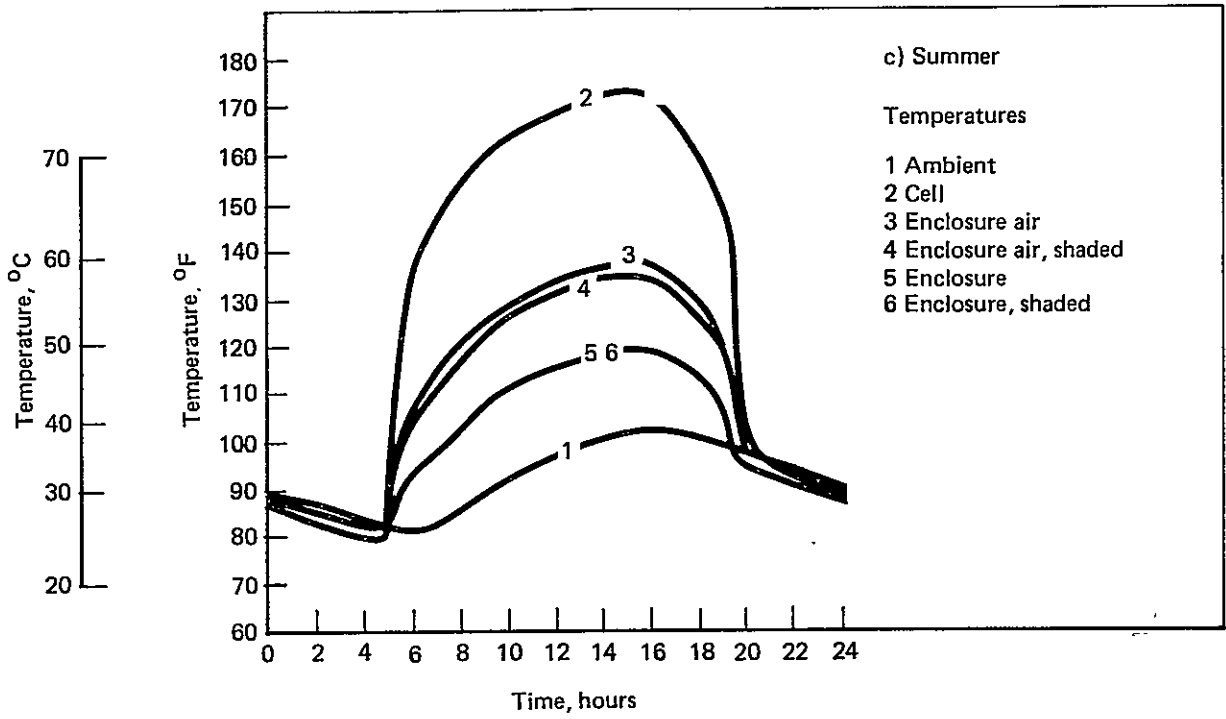


Figure 5-21. Temperature Predictions for Tracking Array (Continued)

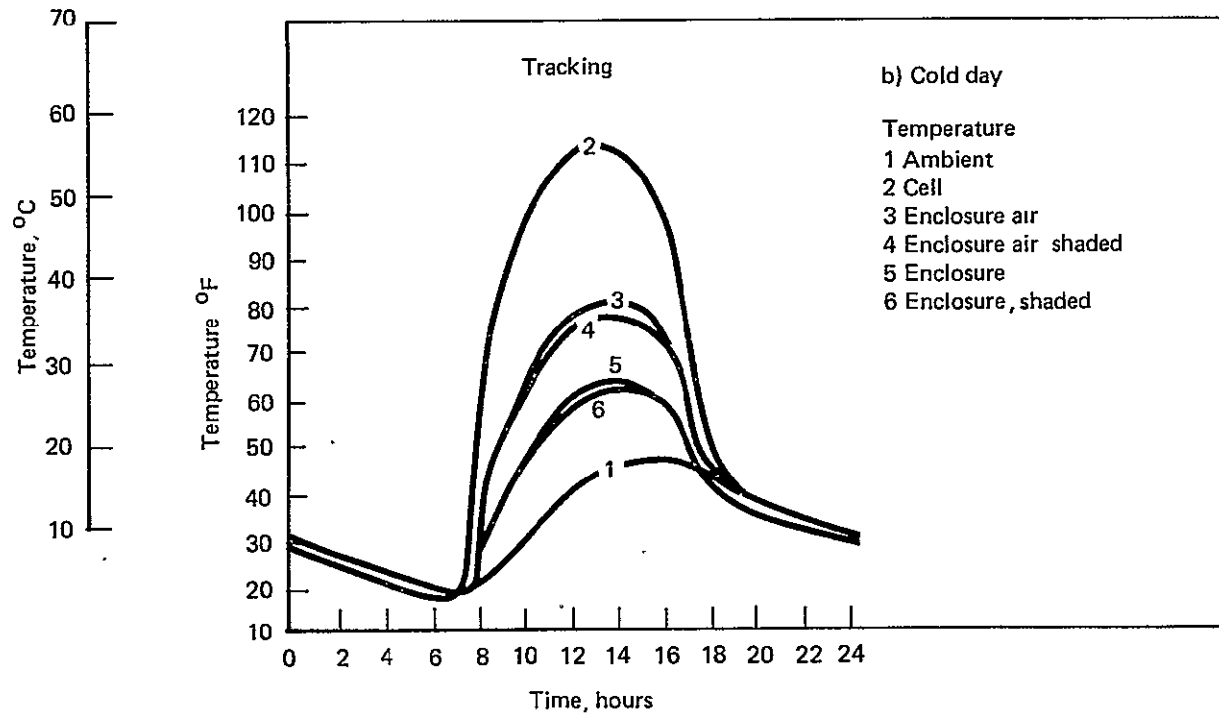
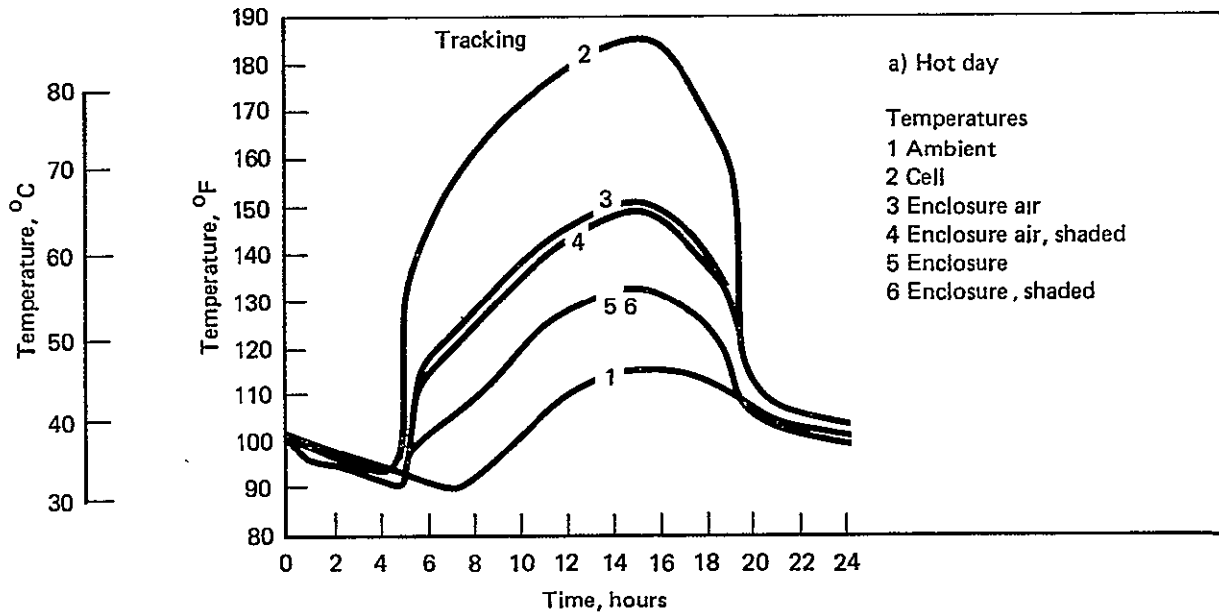


Figure 5-22. Temperature Predictions for Tracking Array

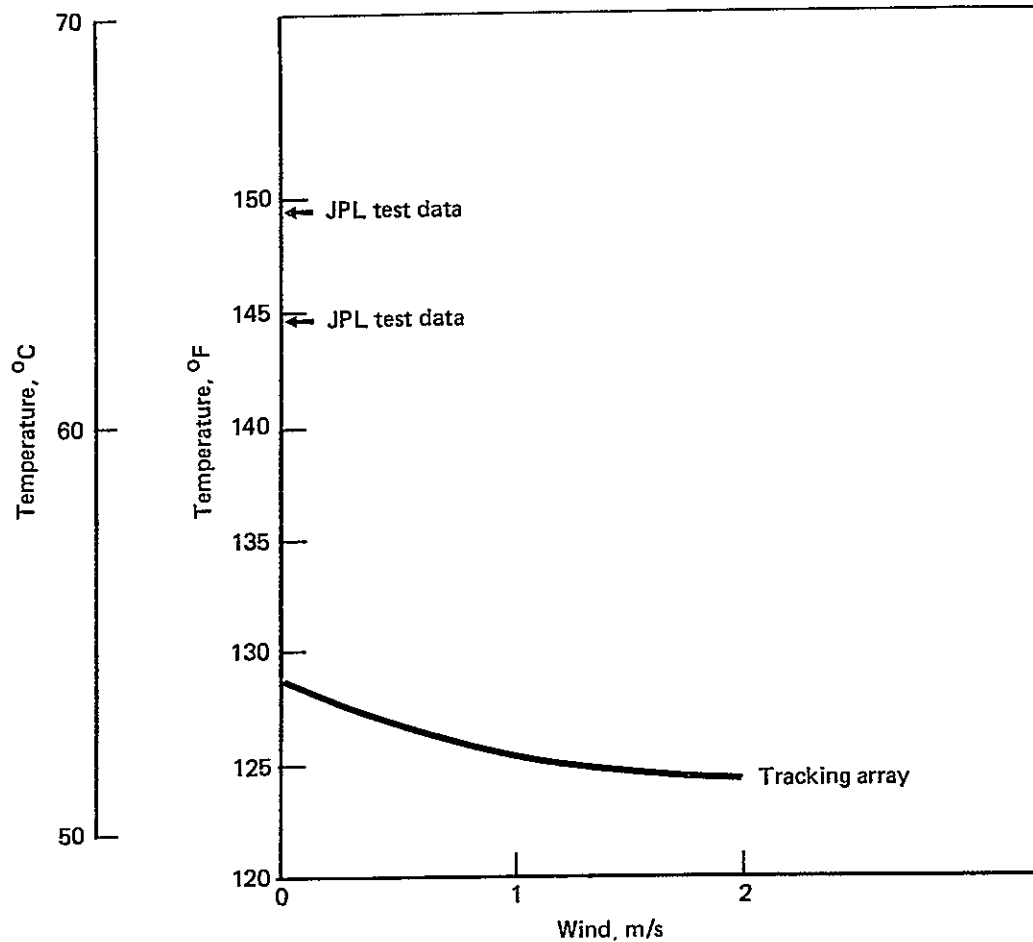


Figure 5-23. Effect of Wind on Tracking Array Cell Temperature

5.3.4.3 Thermal Analysis at NOCT Conditions

The nominal operating cell temperature (NOCT) as influenced by the wind velocity is shown in Figure 5-23. The tracking array NOCT is lower than the fixed value for any wind speed. Because of its greater enclosure surface area, the tracking array loses more heat by free and forced convection than the fixed array, which reduces the cell operating temperature.

5.3.5 Performance Predictions

5.3.5.1 Seasonal Analysis

Power production for each of the seasons is shown in Figure 5-24. The curves tend to be more rounded than their fixed array counterparts, because of the tracking. The efficiency is only slightly higher than the average fixed array efficiency.

The daily power production values for the tracking and fixed array are compared in Figure 5-25. Although the tracking array has higher annual average, the fixed array has a more consistent seasonal power output.

5.3.5.2 Power Analysis at NOCT Conditions

The steady-state analysis simulated varying wind velocities. The slight change of power production with wind velocity is shown in Figure 5-26. With a large enclosure the free convection probably accounts for the majority of the heat transfer. Little is gained by increasing the forced convection, because the free convection is operating at the maximum efficiency.

5.4 Manufacturing and Installation

Similar to the fixed array production plan, modules and panels are produced at a dedicated factory located off-site. The smaller components and detail parts which are readily shipped are also procured from off-site sources. The large components such as the base dish will undergo final assembly on-site. The entire array, including the enclosure and base, is assembled in the on-site factory, transported to the field, and attached to the pilings. The more extensive on-site factory fabrication requires an estimated $16,700 \text{ m}^2$ (180,000 square feet) of floor area compared to only 3720 m^2 (40,000 square feet) for the fixed array. The excess area is assumed to be chargeable to the arrays.

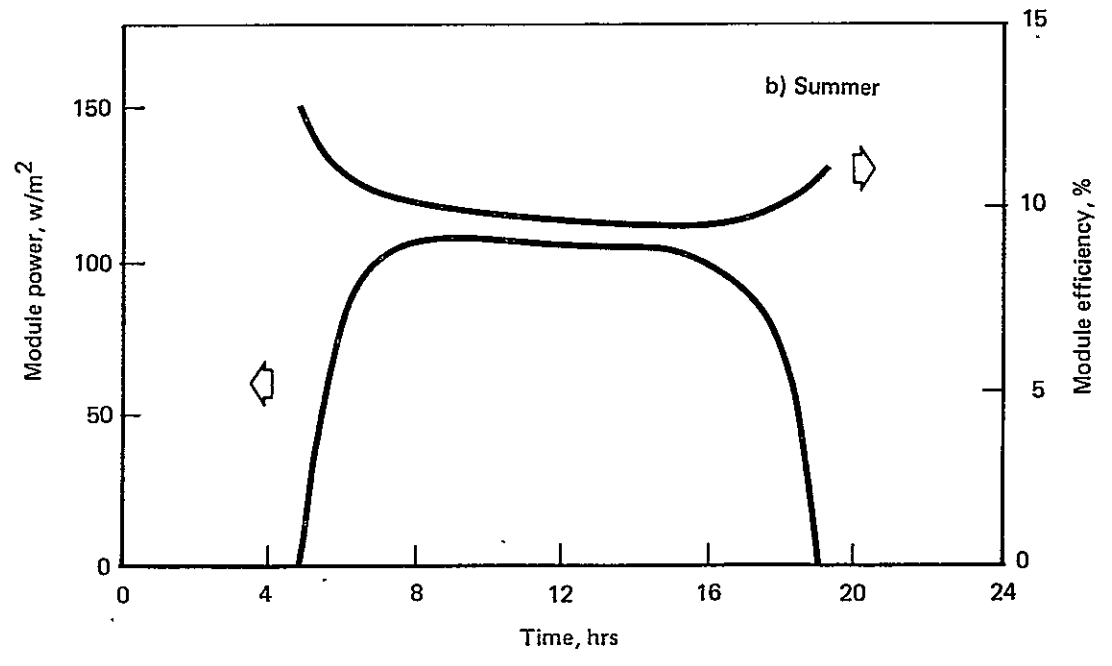
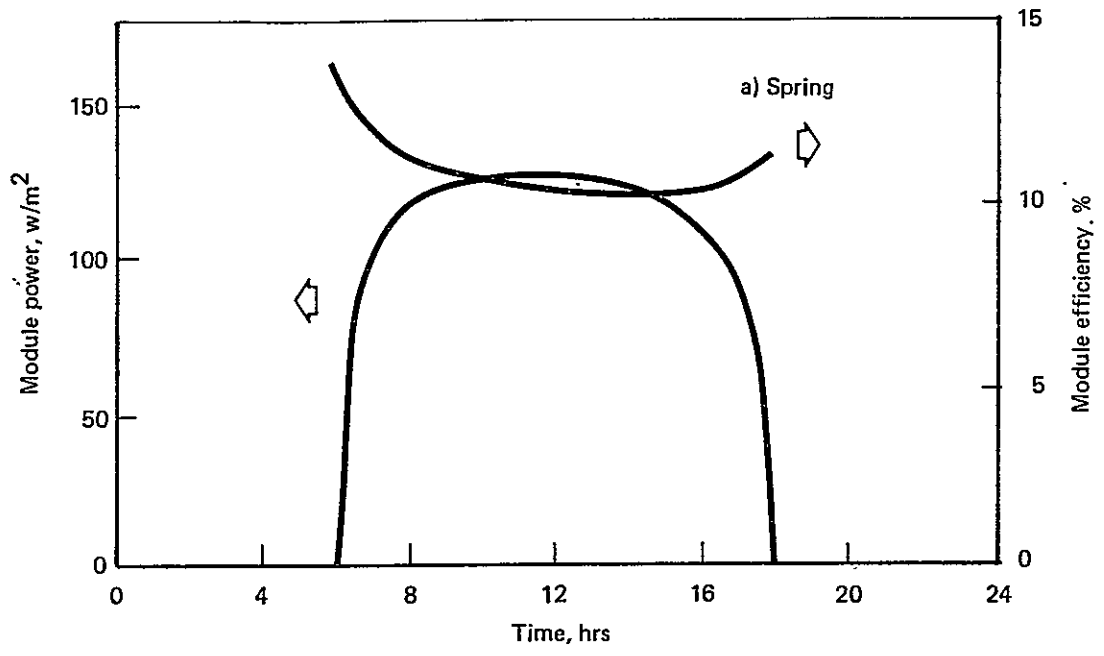


Figure 5-24. Tracking Array Transient Power Output

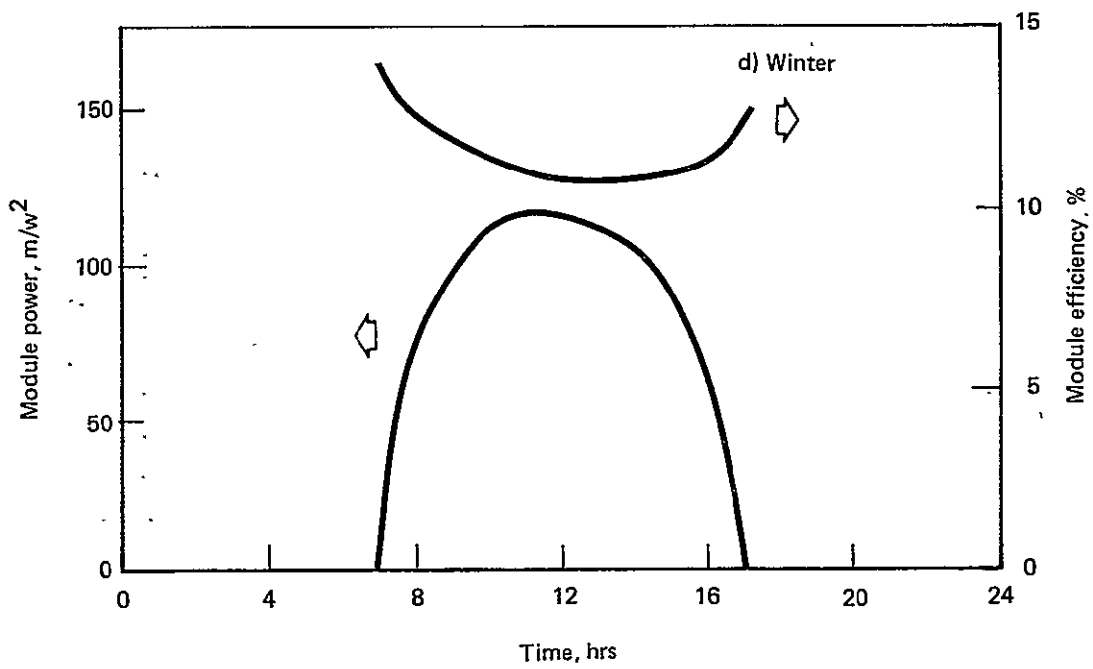
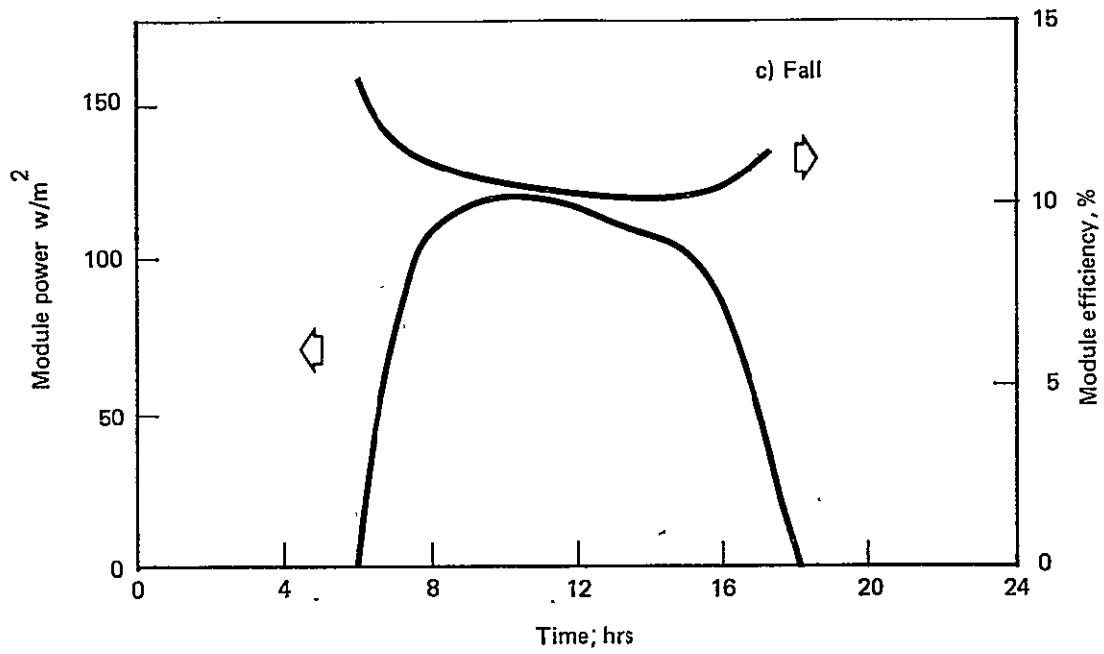


Figure 5-24. Tracking Array Transient Power Output (Continued)

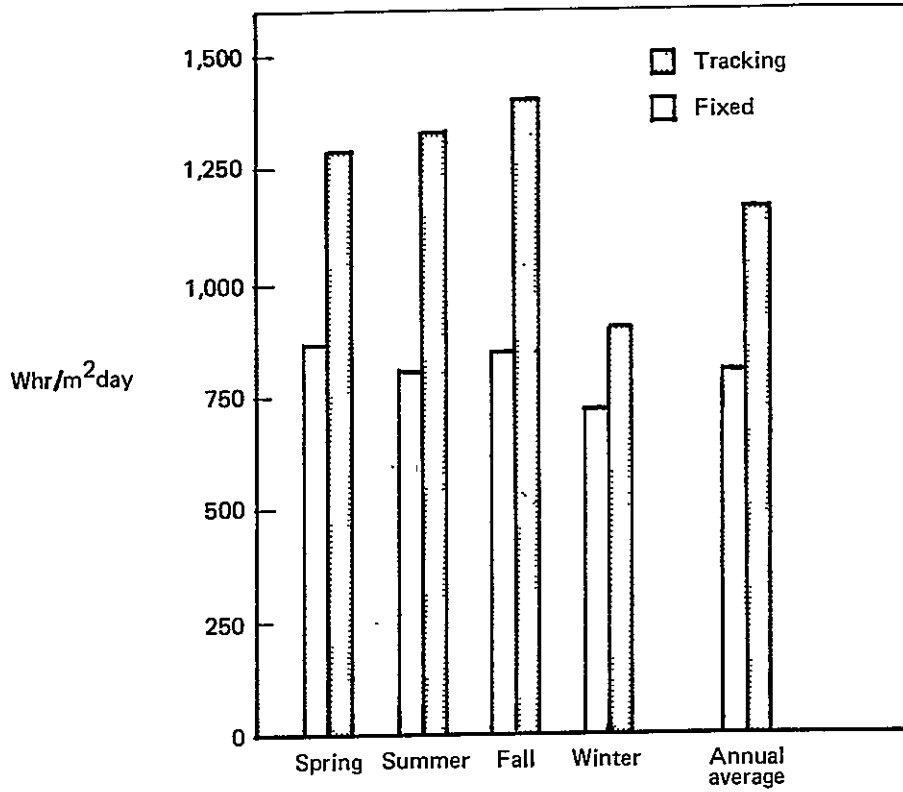


Figure 5-25. Comparison of Seasonal and Annual Average for Fixed and Tracking Arrays

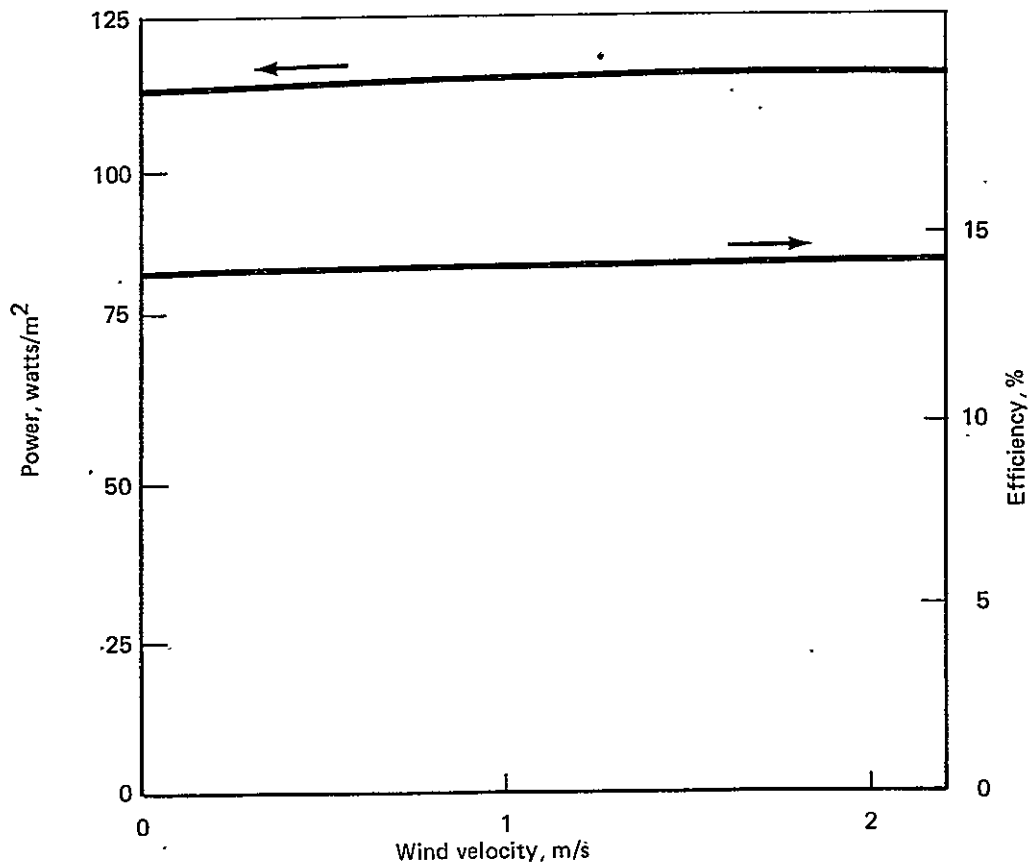


Figure 5-26. Tracking Array

The incoming procured components and the raw material stock for the "make" components flow through receiving/inspection stores adjacent to the production assembly lines. The parts handling equipment and the manufacturing assembly tooling will be highly automated to achieve the production rates.

Three basic assembly lines feed to the final assembly area: support structure, reflector assembly, and enclosure fabrication. The final assembly position installs and pressurizes the enclosure. The completed array is then attached to a transporter and delivered to the array field.

Array foundations are installed at the surveyed locations in the field. The foundations consist of the reinforced augercast concrete piling. Three pilings anchor the base stanchions and a center piling anchors the pedestal. The power and signal wiring connections are made to the tracking controller, the ground connection made, and the array is ready for functional checkout and alignment processes.

Details of the on-site manufacturing and installation process common to the heliostat concept design may be found in Ref. 8.

5.5 Maintenance

The maintenance concept and costs are identical to the heliostat plan, Ref. 8, except for the panels. Panel/module maintenance will be performed by first removing and replacing it with a new panel or module; repair is then performed in the power station maintenance facility.

Access to a module or panel to be replaced is gained by using manual controls to orient the array in the desired position, connecting a special maintenance van to the access hatch, and extending a ladder to the panel location as shown in Figure 5-27. The microprocessor-based tracking system offers a convenient means to monitor status of the array performance, and perhaps to pinpoint malfunctioning modules or panels within the array. Additional sensors and instrumentation wiring would be required for this purpose and these have not been included in the cost analysis.

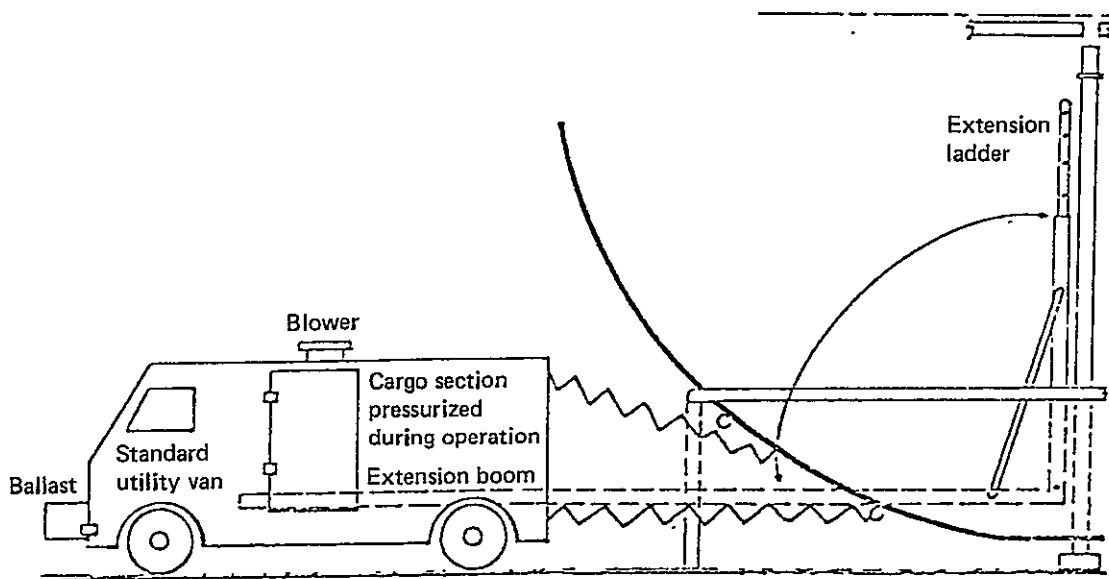


Figure 5-27. Tracking Array Maintenance Vehicle

5.6 Life Cycle Costs

Assumptions used in the tracking array cost analysis are the same as those in Section 4.6.1, except that the CBS contains an additional item for the tracking system.

5.6.1 Costing Analysis Results

The cost summary for the tracking array is shown in Table 5-II. Details are given in Table 5-III. Further breakdown of the costs of items common to the heliostat design is contained in Ref. 27.

5.6.2 Energy Cost Analysis

Energy cost is estimated with the same equations and assumptions used for the fixed-tilt array given in Section 4.6.3. The capital investment for the array field is:

$$CI = (107.38) (2.26 \times 10^6) (1 + 0.4) = \$340.0 \times 10^6$$

For a 20 year plant life, the dc bus bar energy cost is:

$$\begin{aligned} BBEC(dc) &= \frac{(.1589)(107.38 + 1.93) + (.1019)(15.04)}{1.149 \times 365 \times .8 \times 10^{-3}} \\ &= 56.3 \text{ mills/kW}\cdot\text{h(dc)} \end{aligned}$$

The values 107.38 and 1.93 are the present values of the initial capital investment and the enclosure replacement, respectively, in $\$/\text{m}^2$. The maintenance cost (present value is $\$15.04/\text{m}^2$).

With a 30 year plant life and module replacement at 20 years:

$$\begin{aligned} BBEC(dc) &= \frac{(.1483)(107.38 + 1.93 + 32.63) + (.0888)(20.61)}{1.149 \times 365 \times .8 \times 10^{-3}} \\ &= 68.2 \text{ mills/kW}\cdot\text{h(dc)} \end{aligned}$$

The additional entry, 33.63, is the present value of the module replacement cost, and the maintenance cost reflects the ten additional years of operation. As with the fixed array analysis, the results indicate the 20 year life without module replacement is more economic.

TABLE 5-II: TRACKING ARRAY COST SUMMARY, 1975 DOLLARS

CBS-No.	TITLE	COST, \$m ² of Array					
		LABOR	MATERIAL	EQUIPMENT	FACIL-ITIES	TRANSPOR-TATION	TOTAL
1.1	Land Acquisition and Preparation						4.71
1.2	Infield Service Roads						**
1.3	Security Fence						.21
1.4	Lightning Protection						**
1.5	Field to PCU Wiring	1.41	6.38				7.79
1.6	Foundations						5.56
1.7	Enclosures	.40	3.60	.01			4.01
1.8	Support Structure	2.74	20.16	.09			22.99
1.9	Modules/Panels	1.61	43.25	.67	2.93	.29	48.74
1.10	Tracking System	.27	8.92				9.19
1.0	Array Field*	6.44	82.31	.76	2.93	.29	103.21
3.2, 3.3	Distributables and Indirect*	.50			3.68		4.18
	Initial Capital Investment for Items Casted	6.94	82.31	.76	6.61	.29	107.38
4.1	Array Field Maintenance	6.06	14.66	.70			21.42
	Capital and Maintenance Costs	13.00	96.97	1.46	6.61	.29	128.80

* Costs do not cover entire CBS item.

** Costs for this item not included.

TABLE 5-III: TRACKING ARRAY DETAILED COSTS, 1978 DOLLARS

CBS No. 1.1 and 1.3 TITLE Land Acquisition and Preparation, Fence ELEMENT Labor and Materials

Item	Quantity Req'd	Unit Cost	Factors			Total Cost \$	Unit Cost \$/m ²
			Overhead	Quality Control	Prorate, Years		
Land Cost	3205 Acres	\$ 100.00/acre				320,500	.14
Coarse Grading	5,000,000 c.y.	\$ 1.25/c.y.				6,250,000	2.76
Fine Grading	15,500,000 s.y.	\$.38/s.y.				5,895,000	2.61
(CBS 1.1 TOTAL)							\$ 5.51/m ²
(CBS 1.2, In-field Service Roads - not included)							
Security Fence	47,660 ft.	\$ 12.00/ft				571,900	.25
(CBS 1.3 TOTAL)							\$.25/m ²
(CBS 1.4, Lightning Protection - not included)							

TABLE 5-III. (Continued)

CBS No. 1.5

TITLE Field to PCU Wiring

ELEMENT Labor and Materials

148

Item	Quantity Req'd	Unit Cost	Factors			Total Cost \$	Unit Cost \$/m ²
			Overhead	Quality Control	Prorate, Years		
<u>Labor</u>							
Fabricate Pigtails	7,313 hrs	\$ 7.00/hr.	2.1	1.06		113,950	.05
Fabricate Connector Wiring	21,940 hrs	\$ 7.00/hr.	2.1	1.06		341,900	.15
Excavate Trench	154,800 c.y.	\$.89/c.y.	--	--		137,800	.06
Install Concrete	45,870 hrs	\$10.50/hr.	1.8	1.06		919,00	.41
Install Array Wiring	21,940 hrs	\$10.50/hr.	1.8	1.06		439,500	.19
Install Inter-array Wiring	117,950 hrs	\$10.50/hr.	1.8	1.06		2,363,000	1.04
						Labor Total	1.65
<u>Materials</u>							
Array Wire and Connectors	43,880 sets	\$32.00/set	1.02			1,432,000	.63
Insulated Wire	3,686,000 ft.	\$ 1.25/ft.	1.02			4,700,000	2.08
Conduit	2,457,000 ft.	\$.44/ft.	1.02			1,102,800	.49
Trench Covers	2,457,000 ft	\$.70/ft.	1.02			1,754,000	.78
Concrete	182,000 c.y.	\$42.50/c.y.	1.02			7,891,000	3.49
						Material Total	7.46
						CBS 1.5 TOTAL	\$9.11/m ²

TABLE 5-III (Continued)

CBS No. 1.6 and 1.7

TITLE Foundation and Enclosure

ELEMENT Labor, Materials and Equipment

Item	Quantity Req'd	Unit Cost	Factors			Total Cost \$	Unit Cost \$/m ²
			Overhead	Quality Control	Prorate, Years		
Foundation (Common to Heliostat Design)	43,880 ea.	\$ 335.00/ea.				14,700,000	6.50
						CBS 1.6 TOTAL	\$6.50/m ²
Protective Enclosure							
Labor	43,880 sets	\$ 24.41/set				1,071,000	.47
Materials	43,880 sets	\$ 217.00/set				9,522,000	4.21
Tooling	43,880 sets	\$.37/set				16,235	.01
						CBS 1.7 TOTAL	\$4.69/m ²

149

TABLE 5-III (Continued)

CBS No. 1.8

TITLE Support Structure

ELEMENT Labor and Materials

150

Item	Quantity Req'd	Unit Cost	Factors			Total Cost \$	Unit Cost \$/m ²
			Overhead	Quality Control	Prorate, Years		
<u>Labor</u>							
Items Common to Heliostat Design:							
Onsite	43,800 sets	\$ 96.15/set				4,219,000	1.87
Offsite	43,880 sets	\$ 47.65/set				2,091,000	.98
Module Support Frame Fabrication	41,770 hrs.	\$ 7.00/hr.	2.1	1.06		650,000	.29
Support Frame Storage and Handling	10,000 hrs.	\$ 7.00/hr.	2.1	1.06		156,000	.07
						Labor Total	\$3.21/m ²
<u>Materials</u>							
Aluminum Plate	4,914,000 lb	\$.78/lb	1.05			4,025,000	1.78
Tubing, 3 in. O.D.	3,291,000 ft.	\$ 1.60/ft.	1.02			5,371,000	2.37
1½ in. O.D.	3,159,000 ft.	\$.75/ft.	1.02			2,417,000	1.07
Items Common to Heliostat						41,533,000	18.37
						Materials Total	\$23.59/m ²
Tooling	43,880 Arrays	\$ 4.79/array				210,000	.10
						CBS 1.8 TOTAL	\$26.90/m ²

TABLE 5-III (Continued)

CBS No. 1.9

TITLE Modules/Panels

ELEMENT Labor, Materials, Facilities,
Equipment & Transportation.

Item	Quantity Req'd	Unit Cost	Factors			Total Cost \$	Unit Cost \$/m ²
			Overhead	Quality Control	Prorate, Years		
<u>Labor</u>							
Fabrication and Assembly	186,400 hrs.	\$ 8.00/hr.	2.1	1.10		3,445,000	1.52
On-site Installation	40,624 hrs.	\$ 10.50/hr.	1.8	1.06		813,900	.36
						Labor Total	1.88
<u>Materials</u>							
Solar Cells	2,140,000 m ²	\$ 45.92/m ²	1.10			108,102,000	47.80
Miscellaneous Materials						6,000,000	2.80
						Materials Total	50.60
<u>Facilities, Equipment & Transportation</u>							
Module Fabrication Factory	80,000 ft ²	\$ 97.00/ft ²			7	7,760,000	3.43
Automated Handling Equipment	\$2,090,000				7	1,024,000	.45
Shipping/Handling Crates	6,000 ea.	\$ 250.00/ea.			7	735,000	.33
Transportation to Site	4,281,000 c.f.	\$.18/c.f.	(1000 miles)			771,000	.34
						Facilities, Equipment, Transportation Total	4.55
						CBS 1.9 TOTAL	\$57.03/m ²

151

TABLE 5-III (Continued)

CBS No. 1.10

TITLE Tracking System

ELEMENT Labor and Materials

Item	Quantity Req'd	Unit Cost	Factors			Total Cost \$	Unit Cost \$/m ²
			Overhead	Quality Control	Prorate, Years		
<u>Labor</u>							
Controller Final Assembly and Installation	7,300 hrs	\$ 10.50/hr.	1.8	1.06		146,250	.06
Drive Unit Final Assembly and Installation	29,250 hrs	\$ 10.50/hr.	1.8	1.06		586,000	.26
						Labor Total	.32
<u>Materials</u>							
Unit Controller	43,880 ea.	\$ 242.00/ea.	1.02	1.06		11,481,000	5.08
System Controller	731 ea.	\$1,510.00/ea.	1.02	1.06		1,193,000	.53
Gearmotors	87,760 ea.	\$ 40.00/ea.	1.02	1.06		3,795,400	1.68
Reduction Gears and Pulleys	87,760 ea.	\$ 75.00/ea.	1.02	1.06		7,116,500	3.15
						Materials Total	10.44
						CBS 1.10 TOTAL	\$10.76/m ²

TABLE 5-III (Continued)

CBS No. 3.2 and 3.3

TITLE Distributables and Indirect Construction and Plant Startup only.

ELEMENT _____

Item	Quantity Req'd	Unit Cost	Factors			Total Cost \$	Unit Cost \$/m ²
			Overhead	Quality Control	Prorate, Years		
Warehouse	250,000 ft ²	\$ 12.00/ft ²				3,000,000	1.33
Temporary Factory	140,000 ft ²	\$ 48.00/ft ²				6,720,000	2.97
Plant Startup and Checkout	67,000 hr.	\$ 10.50/hr.	1.8	1.06		1,342,300	.59
						CBS 3.2 and 3.3 TOTAL	\$4.89/m ²

153

TABLE 5-III (Concluded)

CBS No. 4.1

TITLE Maintenance (Array Field Only)

ELEMENT Labor, Materials, Equipment[†]

Item	Quantity Req'd	Unit Cost	Factors			Total Cost \$	Unit Cost \$/m ²
			Overhead	Quality Control	Prorate, Years		
<u>Labor</u>							
Items Common to Heliostat Design	43,800 ea.	\$ 345.95/ea.				15,180,300	6.71
Module Replacement	1% year						.38
						Labor Total	7.09
<u>Materials</u>							
Items Common to Heliostat Design	43,800 ea.	\$ 295.95/ea.				12,986,300	5.74
Modules	1% year						11.41
						Materials Total	17.15
<u>Equipment</u>							
Items Common to Heliostat Design							.82
						CBS 4.1 TOTAL	\$25.06/m ²

154

6.0 EVALUATION OF RESULTS

This section of the report discusses the results presented in Sections 4.0 and 5.0 and compares the two design concepts with each other and to a conventional flat-plate array. Areas where improvements in the design concepts are possible are suggested.

6.1 Summary of Results

The two array concepts described in Sections 4.0 and 5.0 are very different design solutions, but with the same basic premise of protecting flat plate photovoltaics arrays in inflated plastic enclosures. The following comparisons between the two concepts can be made:

The spherical enclosure of the tracking array has greater heat rejection area than the fixed array enclosure, for the same amount of incident insolation. Therefore, the tracking array is cooler than the fixed array for the same environmental conditions. However, the tracking array may reach higher temperatures in mid-afternoon when the ambient temperature reaches its maximum. The tracking array is still normal to the sun at this time, while the fixed array is no longer directly facing the sun.

Peak power output of the two concepts is about the same:

Array Concept	Peak Power W/m^2	
	NOCT Conditions	Transient Analysis (Spring)
Fixed-Tilt	106.0	123.4
Tracking	109.4	125.1

However, additional power produced by the tracking array in morning and afternoon hours, because the array is maintained normal to the sun, results in 42% more energy per unit area from the tracking array. The more uniform power produced by the tracking array may be more convenient and, hence, of higher value to an electric utility than

the sharply peaking power from the fixed-tilt array. Further study would be required to determine how the different daily power profiles are used in the utility power grid, the effect of energy storage, and their impact on the economic evaluation.

- . The fixed array is based on simpler technology. It should be easier to develop, and more reliable in service than the tracking array.
- . A structural failure in the fixed array would affect more array area compared to the relatively insulated tracking arrays.
- . The fixed array is generally more accessible and convenient for installation and maintenance than the tracking array. Less on-site fabrication is required.

In summary, each array concept has design features of value and potentially deserves further investigation based on design considerations. Costs of the two concepts must also be considered, which is discussed in the next section.

As shown in Table 6-I, the fixed-tilt array requires a one-third lower capital investment for a given peak power rating and has a 10% lower bus bar energy cost. Thus, strictly based on costs, the fixed-tilt type of enclosed array would appear to be the best choice. It should be noted that the tracking array is based in part on design features common to the heliostat development program. An effort is being directed to reduce costs on the heliostats which would be of benefit to the tracking array designs, also.

In view of the above, further development could emphasize items common to the two approaches, further evaluate areas where data is lacking (as in the question of wind loads), and maintain surveillance of cost trends for each array concept.

6.2 Comparison to Conventional Array

A conventional flat plate photovoltaic array can be defined as one using glass panels to support and protect the solar cells. The module, consisting

TABLE 6-I: SUMMARY CAPITAL AND MAINTENANCE COSTS
FOR ENCLOSED ARRAYS

ITEM	COST - \$/m ² EXCEPT AS NOTED	
	FIXED ARRAY	TRACKING ARRAY
Land and Fence	2.03	4.84
Field to PCU Wiring	5.51	7.79
Foundations	4.52	5.56
Enclosures	4.60	4.01
Support Structure	1.33	22.99
Module/Panels	49.21	48.74
Tracking System	--	9.19
Array Field Total	67.20	103.21
Distributables and Indirect	1.65	4.18
Capital Cost	68.85	107.38
(Cost at NOCT Output, \$/W)	(.65)	(.98)
Maintenance Cost	14.97	21.42
Total Cost	83.82	128.80
(Total Cost, at NOCT Output, \$/W)	(.79)	(1.18)
Direct Current Bus Bar Energy Cost, Mills/kW-H(dc) (1975 Dollars)	51.5	56.3

of the glass, solar cells, circuits and encapsulants, are supported by a metal framework, or panel structure, which is mounted onto a post and beam or similar support structure. The array is anchored to the ground with concrete foundations. Bechtel National, Inc. has recently completed a study of conventional arrays (Ref. 31) under essentially the same groundrules as those used in this study. Thus, a direct comparison with their results can be made. Bechtel studied a large number of flat plate array configurations; comparisons are made here with the least-cost configuration reported in Ref. 31. This configuration - array case 7, panel type J as listed in Table 7-1 of Ref. 31 - is characterized by the following:

- . Four modules, each 1.2 x 2.4 m (4 ft by 8 ft), are mounted in a 2.4 x 4.8 m (8 ft by 16 ft) panel frame.
The panel frame, with the short dimension horizontal, is supported at the lower corners and the upper quarter points.
- . Support structure is beams mounted on posts at 4.8 m (16 ft) intervals.
- . Concrete sleepers support the posts and anchor the entire array to the ground.

Costs in the Bechtel study were performed parametrically as a function of the design wind loading acting normal to the panel surface. The costs used for the comparisons are for the lightest loading that Bechtel investigated - 1.7 kPa (35 PSF).

Since the Bechtel study did not include field to PCU wiring, land, maintenance, or indirect costs, the comparison is made for only those items where a direct equivalence is available. The comparison, Table 6-II, shows that the fixed-tilt array capital cost is substantially (38%) less expensive than the conventional array and its costs per peak power output at NOCT conditions is 26% less than the conventional array. The latter difference is less because the enclosed array efficiency is somewhat less than the conventional array, due to transmission loss through the enclosure and higher temperatures inside the enclosure. Reduced costs are due partly to lower module costs but primarily to much lower costs for the remainder of the array.

TABLE 6-II: NORMALIZED COST SUMMARY
(1975 DOLLARS)

ITEM	\$/m ²		\$/w _p AT NOCT	
	AIR ENCLOSURE	CONVENTIONAL* ARRAY (BECHTEL)	AIR ENCLOSURE (10.6% AT NOCT)	CONVENTIONAL ARRAY (BECHTEL) (12.7% AT NOCT)
Modules	49.21	60.00	0.46	0.47
Structures				
Air-Enclosure	4.60	--	0.04+	--
Panel Structure	--	14.70	--	0.11
Support Structure	1.33	7.40	0.01	0.06
Foundations	<u>4.52</u>	<u>14.90</u>	<u>0.04+</u>	<u>0.12</u>
Structure Total	10.45	37.00	0.10	0.29
Array Total	59.66	97.00	0.56	0.76

*Ref. 31, Table 7-1 (page 154), Array Case 7, Panel Type J

The tracking cost is near the cost of the conventional array: 7% lower capital costs and 9% higher costs per peak watt. Of course, the tracking array produces more energy than a fixed-array for a given peak power rating. Thus, the cost of energy would be expected to be lower than the conventional array. Energy costs cannot be compared without additional data.

From the above comparisons, it is evident that the air supported enclosure protection can result in substantially lower cost photovoltaic arrays and less expensive power in a central power station application.

7.0 CONCLUSIONS

This study has evaluated the benefits that might be derived from enclosing photovoltaic arrays in a transparent, air-supported structure. Two enclosed design concepts were formulated and analyzed: one using a cylindrical enclosure covering fixed latitude-tilt arrays, and the other using spherical enclosures for tracking arrays. These were evaluated for a large central power station application.

The design concepts and supporting analyses show that air-supported enclosures:

1. Efficiently carry external environmental loads, resulting in an array with minimal material usage.
2. Increase array nominal operating cell temperatures (NOCT) by approximately 16°C (fixed array only) with an attendant reduction in efficiency.
3. Protect the modules from hail impact and potential damage.
4. Provide a dry environment, simplifying wiring and connector design.

The costing analyses show that initial capital cost of the enclosed fixed array will be 38% less than for the conventional array. With higher temperatures in the enclosure and an enclosure transmission loss slightly higher than the conventional array glass absorption, the cost per peak watt for the enclosed array is 26% lower than its conventional counterpart. Analyses of the tracking array show capital costs and costs per peak watt roughly equivalent to the conventional array. However, the tracking array does provide a more uniform power output through the sunlit hours and greater energy for a given peak power rating. It is likely that some areas may require the more uniform power production of the tracking array than the strongly peaking output of the fixed arrays. It is concluded that the enclosed fixed array definitely has an economic advantage over the conventional design, and that the tracking array possibly has some economic merit.

8.0 RECOMMENDATIONS

Because air supported enclosure protection of photovoltaic arrays offers a significant reduction in array and power cost, further development of the concept is recommended. The potential tasks fall into three basic categories: (1) resolution of uncertainties in the present study, (2) refinement and cost reduction of the design concept, and (3) prototype fabrication and test. The following effort is suggested in each of these areas:

Resolution of Uncertainties

- Wind loads on the conventional array structure and the cylindrical enclosures are not well defined, particularly where these structures are within the array field. A program is currently underway to define wind loads on the conventional array. In light of the economic attractiveness of the fixed tilt array, a similar wind loads program for the cylindrical enclosure should be considered.
- The SOLMET data tape for Phoenix was used in the transient analysis, which required transforming total insolation on a horizontal plate to the insolation on the arrays. This transformation resulted in normal insolation values (about 1200 W/m^2) that are well above the expected values ($1000\text{-}1100 \text{ W/m}^2$) for desert locations. It is recommended that a standard practice for using the SOLMET data or alternate climatic data be investigated. This uncertainty affects the calculated transient temperature and dc bus bar energy costs used to compare the fixed and tracking arrays. It does not affect the comparison to conventional arrays, which is based on NOCT conditions.
- The additional value, if any, of the more uniform power production from the tracking array should be determined.

Design Concept Refinement and Cost Reduction

- Sizes of both the fixed tilt array and the tracking array were selected arbitrarily based on past work, accessibility, and handling considerations. The effect of array size on energy cost should be explored also, to determine an optimal configuration.

- . Design improvements should be investigated which could further reduce costs. In particular, modules with higher packing efficiency than those obtained should have a direct impact on array cost. The packing efficiencies used - 88 and 89% - include generous allowances for edge margins. Another factor directly affecting array area required and cost is the enclosure film transmittance. Investigation of other films with potentially higher transmittance values would be desirable.
- . The production concept should be planned in further detail to allow costs to be refined and other areas of potential cost reduction to be identified.
- . The tracking array should be re-evaluated following current cost reduction efforts on the related heliostat program.

Prototype Fabrications and Test

- . Prototype modules using the fixed-tilt array design concept should be fabricated and tested to evaluate assembly techniques, handling problems, and performance under qualification and real-time environmental conditions.

9.0 NEW TECHNOLOGY

No reportable items of new technology have been identified by Boeing during the contract of this work.

10.0 REFERENCES

1. A. B. Meinel and M. P. Meinel, Applied Solar Energy, An Introduction, Addison-Wesley Publishing Company, Reading, Ma., 1976.
2. National Photovoltaic Program, Program Plan, February 3, 1978, U.S. Department of Energy Division of Solar Technology.
3. "American National Standard Building Code Requirements for Minimum Design Loads in Buildings and Other Structures", ANSI A58.1-1972, American National Standards Institute, Inc., New York, 1972.
4. "Central Receiver Solar Thermal Power System, Collector Subsystem Final Report", SNA 1111-76-7, Boeing Engineering and Construction, August 15, 1977.
5. H. J. Niemann, "Zur Windbelastung von Tragluftbauten", Konstruktiver Ingenierbau Berichte, November 13, 1972.
6. T. W. Singell, "Wind Forces on Structures: Forces on Enclosed Structures", Journal of the Structural Division, Proceedings of the American Society of Civil Engineers, July 1958.
7. E. W. Ross, Jr., "Large Deflections of an Inflated Cylindrical Tent", Journal of Applied Mechanics, Transactions of the ASME, December 1969.
8. "Solar Central Receiver Prototype Heliostat, Volume 1 Final Technical Report", SAN/1604-1, Boeing Engineering and Construction, 30 June 1978.
9. "Environmental Hail Model for Assessing Risk to Solar Collectors", LSSA Project Internal Report 5101-45, Jet Propulsion Laboratory, December 6, 1977.
10. M. D. Pope, "Solar Photovoltaic Field Tests and Applications Project", Proceedings of the Semi-Annual Review Meeting, Silicon Technology Programs - March 7-9, 1978, Solar Energy Research Institute, Golden Co.
11. R. B. Pettit, "Transmittance Properties of Unexposed and Weathered Tedlar", Sandia Laboratories, Albuquerque, NM, January 14, 1977.

12. G. Gurfinkel, Wood Engineering, Southern Forest Products Association, New Orleans, 1973.
13. H. S. Rauschenbach, Solar Cell Array Design Handbook, Volume I, NASA CR-149364, October 1976 (The method used is from this document's reference 9.3-9: J. R. Barton, "Power Output Analysis of Array Incorporating Shadow Diodes", Engineering Report No. 7062-6-011, TRW Systems Group, December 1966).
14. Bugler, J. W., "The Determination of Hourly Insolation on an Inclined Plane Using a Diffuse Irradiance Model Based on Hourly Measured Global Horizontal Insolation", Solar Energy, Vol. 19 pp. 477-491, 1977.
15. Ruffner, J. A. and F. E. Bair, The Weather Almanac, Gale Research Co., 1977.
16. Duffie, J. A. and W. A. Beckman, Solar Energy Thermal Processes, John Wiley & Sons, 1974.
17. "Thermal Performance Testing and Analysis of Photovoltaic Modules in Natural Sunlight", LSA Project Internal Report 5101-31, Jet Propulsion Laboratory, July 29, 1977.
18. Close, D. J., "The Performance of Solar Water Heaters with Natural Circulation", Solar Energy, Vol. 6, pp. 33-44, 1962.
19. Baker, L. H., "Film Heat Transfer Coefficients in Solar Collector in Solar Collector Tubes at Low Reynolds Numbers", Solar Energy, Vol. 11 No. 2, 1967, p. 78.
20. Newell, M. E. and F. W. Schmidt, "Heat Transfer by Laminar Natural Convection within Rectangular Enclosures", Journal of Heat Transfer, February 1970, p. 159.
21. Arnold, J. N.; I. Cotton, and D. K. Edwards, "Experimental Investigation of Natural Convections in Inclined Rectangular Regions of Differing Aspect Ratios", Journal of Heat Transfer, February 1976, p. 67.
22. ASHRAE Handbook of Fundamentals, American Society of Heating, Refrigerating and Air-Conditioning Engineers, Inc., 1972.

23. Parker, J. D., J. H. Boggs, and E. F. Blick, Introduction to Fluid Mechanics and Heat Transfer, Addison-Wesley Publishing Co., 1974.
24. "Interim Price Estimation Guidelines: A Precursor and an Adjunct to Samis III Version One", LSA Project Internal Report 5101-33, Jet Propulsion Laboratory, September 10, 1977.
25. E. A. DeMeo and P. B. Bos, "Perspectives on Utility Central Station Photovoltaic Applications", Report No. ER-589-SR, Electric Power Research Institute, January 1978.
26. J. W. Doane, et. al., "The Cost of Energy from Utility-Owned Solar-Electric Systems", Report No. JPL 5040-29, Jet Propulsion Laboratory, June 1976.
27. "Solar Central Receiver Prototype Heliostat, Vol. III Cost Estimates", SAN/1604-3, Boeing Engineering and Construction, June 30, 1978.
28. W. J. Stolte, "Central Power Station Module Design", in Proceedings: 8th Project Integration Meeting, LSA Project Report 5101-52, Jet Propulsion Laboratory, December 7-8, 1977.
29. "Fluid Forces and Moments on Flat Plates", Engineering-Sciences Data, Item No. 70015, Engineering Sciences Data Unit, The Royal Aeronautical Society, London, October 1972.
30. G. G. Meyerhof and J. I. Adams, "The Ultimate Uplift Capacity of Foundations", Canadian Geotechnical Journal, Vol. V, No. 4, pp. 225-244, November 1968.
31. "Module/Array Interface Study", DOE/JPL No. 954698-78/1, Bechtel National, Inc., August 1978.
32. Simon Ostrach, "Natural Convection in Enclosures", Advances in Heat Transfer, Volume 8, 1972, Academic Press, New York.
33. J. W. Stultz, "Thermal and Other Tests of Photovoltaic Modules Performed in Natural Sunlight", LSA Project Internal Report 5101-76, Jet Propulsion Laboratory, July 31, 1978.